UiT The Arctic University of Norway

Faculty of Biosciences, Fisheries and Economics, Department of Arctic and Marine Biology

Characterization of the biological clock in Svalbard ptarmigan (*Lagopus muta hyperborea*)

Anna Malena Hofinger

Master's thesis in Biology, BIO-3950, May 2021

UiT The Arctic University of Norway

Faculty of Biosciences, Fisheries and Economics, Department of Arctic and Marine Biology

Characterization of the biological clock in Svalbard ptarmigan (*Lagopus muta hyperborea*)

Anna Malena Hofinger

Master's thesis in Biology, BIO-3950, May 2021

Supervisor:

David Hazlerigg, UiT - The Arctic University of Norway

Co-supervisor:

Alexander West, UiT - The Arctic University of Norway

Cover photo:

Male Svalbard ptarmigan (*Lagopus muta hyperborea*)

Photo by Vebjørn J. Melum / Norwegian Polar Institute

Acknowledgements

I would like to thank my supervisor David Hazlerigg for giving me the opportunity to work on this highly interesting project, for your helpful advice and feedback.

A huge thank you goes to my co-supervisor Alexander West. You gave me the security I needed to work on this project. Thank you for helping me in the lab, with the analyses, for all your helpful advice, your thorough feedback and for teaching me so much. Your enthusiasm, knowledge, pedagogical skills and patience were a true inspiration to me. Thank you for always taking time for me throughout this project.

I would also like to thank Daniel Appenroth for performing the surgeries on the birds and for helping me with everything around the birds.

Thanks to Kenneth Bowitz Larsen for help with the transfections and microscopy.

Thank you, my fellow students Linn and Fayiri, for all the hangouts and for your friendship.

Thanks to all members of the Arctic Chronobiology and Physiology research group for your support and helpful input. Thank you Vebjørn for lending me the rights to the beautiful picture on the cover page. Thanks to the institute technicians Renate Thorvaldsen, Hans Arne Solvang and Hans Lian for the valuable help with animal care.

Finally, I would like to thank my friends and family for your support, especially my sister Marie - mia ghern zam!

Anna Malena Hofinger

Tromsø, May 2021

Abstract

Svalbard ptarmigan (*Lagopus muta hyperborea*), permanent inhabitants of the High Arctic, lose daily behavioral rhythmicity during polar day and night, and rhythms in core body temperature (T_b) weaken after prolonged exposure to constant photic conditions. A weak circadian system has been suggested in Svalbard ptarmigan, however, the molecular clockwork in Svalbard ptarmigan has not been investigated yet. Here, we studied activity and T_b in Svalbard ptarmigan after controlled changes in light conditions and examined the molecular dynamics of the clock.

We show that daily rhythms in locomotor and feeding activity in Svalbard ptarmigan stop after a transition from external light-dark cycles (LD) to constant dark (DD)/constant light (LL), while rhythms in T_b persisted for at least 10 days in all experimental birds. Approximately four days after a transition from DD to LD birds showed a rise in T_b in anticipation of light onset. These findings suggest an endogenous timing system in control of T_b under LD that weakens under constant conditions. A sustained ultradian rhythmicity was present during the entire experimental design, however, the underlying mechanisms driving ultradian rhythms in Svalbard ptarmigan remain unclear.

To investigate the molecular dynamics of the clock we performed luciferase promoter reporter assays and qPCRs with Svalbard ptarmigan skin fibroblasts. We observed daily oscillations in *Per2* and *Bmal1* transcription, however, no rhythmicity in clock gene expression was measured by qPCRs. This discrepancy may reflect the high temperature sensitivity of our promoter reporters to small temperature fluctuations we detected in our equipment. Finally, we show that ptarmigan fibroblasts cycle with simulated body temperature cycles with *Per1* and *Bmal1* transcription being in phase, indicating a response to temperature cycles rather than to an endogenous clock. Taken together, these findings argue for a weak circadian system in Svalbard ptarmigan.

Keywords: Svalbard ptarmigan, circadian, ultradian, activity, feeding, core body temperature, fibroblasts.

Table of Contents

List if Tables

List of Figures

List of Equations

List of Abbreviations

ATP: adenosine triphosphate

BMAL1: brain and muscle arnt-like 1

cDNA: complementary DNA

Clock: circadian locomotor output cycles kaput

Cry: cryptochrome

DD: constant dark

DMSO: dimethyl sulfoxide

DMEM: Dulbecco's modified eagle's medium

DNA: deoxyribonucleic acid

DUO: dopaminergic ultradian oscillator

FBS: fetal bovine serum

LD: light-dark cycle

LL: constant light

MBH: mediobasal hypothalamus

NE: norepinephrine

PBS: phosphate buffered saline

Per: period

Ppib: peptidyl-prolyl isomerase B

PT: pars tuberalis

qPCR: quantitative polymerase chain reaction

RHT: retinohypothalamic tract

RNA: ribonucleic acid

SCN: suprachiasmatic nucleus

SD: standard deviation

SEM: standard error of the mean

T_b: core body temperature

TSH: thyroid stimulating hormone

TTFL: transcription – translation feedback loop

1 Introduction

1.1 Biological rhythms

Organisms living on our planet experience a highly rhythmic environment. The Earth's rotation around its own axis every 24 hours creates day and night, and its yearly orbit around the Sun with an axis tilt of about 23.5° results in the seasons (**Figure 1**). Cycles of environmental conditions caused by the Earth's movement are complemented by organisms which have rhythms in physiology and behaviour, called biological rhythms. A strong evolutionary selection pressure results in most organisms possessing endogenous biological rhythms. They allow organisms to anticipate regular changes in the environment, adjust their physiology and behaviour to keep in synchrony with rhythmic changes in nature and are hypothesized to thereby increase fitness and survival. Biological rhythms can have different period lengths (eg. yearly, lunar, tidal), and this study focuses on circadian rhythms.

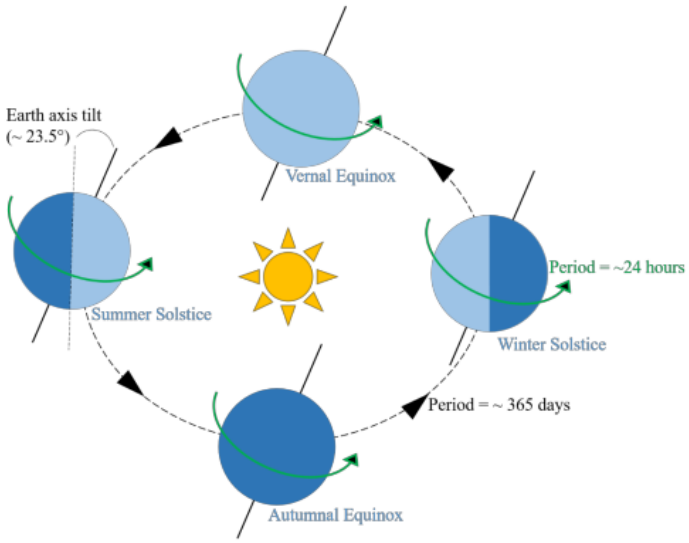

Figure 1 The Earth's orbit around the sun. Every ~ 365 days it completes one orbit with an axis tilt of ~ 23.5°, creating the seasons. Its rotation around its own axis creates day and night. The axis tilt is also responsible for greater differences in light and dark over the year at higher latitudes. Adapted from (Appenroth, 2016).

1.1.1 Circadian rhythms

The term ‘circadian’ derives from the Latin words ‘circa’ (about) and ‘diēm’ (day) and means ‘about a day’. Circadian rhythms have a period of about 24 hours and are driven by an endogenous molecular mechanism called circadian clock. Circadian clocks must satisfy three criteria:

1) **A circadian rhythm must be entrainable to the environment.** The circadian clock receives input from the environment and can use different external cues to stay entrained to a rhythmic environment. External cues that entrain the circadian clock are called zeitgebers (German for time givers). The environmental light-dark cycle is the most important zeitgeber, however, many external cues occurring in daily cycles (eg. ambient temperature, food availability) can be used as a zeitgeber.

2) **A circadian rhythm must persist under constant environmental conditions.** In the absence of external cues, a circadian rhythm is no longer entrained to the environment, but persists with a period close to 24 hours, called free-running rhythm. Persisting in constant conditions and thus being endogenous, circadian rhythms can be clearly distinguished from 24-hour rhythms that are exogenously driven and do not persist without external cues from the environment.

3) **Circadian rhythms must be temperature compensated** to maintain a constant period unaffected by ambient temperature fluctuations (over the range of temperatures at which the timer mechanism operates).

1.1.2 The circadian clock

In mammals, the circadian clock is based on biochemical processes within the cell, where the production and degradation of clock proteins drive a negative feedback loop (**Figure 2**), in which clock genes are regulated by their own products (Partch et al., 2014). This transcription-translation feedback loop (TTFL) makes up a cell autonomous molecular clock producing ~ 24-hour rhythms of gene expression and is composed of two major feedback loops. The primary feedback loop begins with the transcription factors CLOCK:BMAL1 bindings to E-box (a transcription factor binding site) elements in the promotor region of the repressor genes *Period* (*Per1,2,3*) and *Cryptochrome* (*Cry1,2*), which then are expressed. The protein products PER and CRY accumulate in the cytoplasm, heterodimerize and translocate to the nucleus where

they interact with CLOCK:BMAL1 to inhibit activation of transcription. Over time the repressive PER and CRY proteins are phosphorylated, which leads to their ubiquitination and ultimately to their degradation, at which point CLOCK:BMAL1 is able to transactivate at E-box elements once more, starting the cycle again. The time required to complete one cycle is approximately 24 hours. This primary feedback loop is supported by a secondary loop, which is regulated mainly by the induction of the receptors REV-ERBα and RORα through CLOCK:BMAL1. REV-ERBα represses the transcription of *Bmal1* while RORα induces *Bmal1* transcription (Preitner et al., 2002). In this loop the rhythmic transcription of *Bmal1* expresses a phase opposite to that of *Per* and *Cry*. The secondary loop is involved in the stabilisation of the primary feedback loop. The described core clockwork, a molecular oscillator, regulates temporal cycles in various physiological processes.

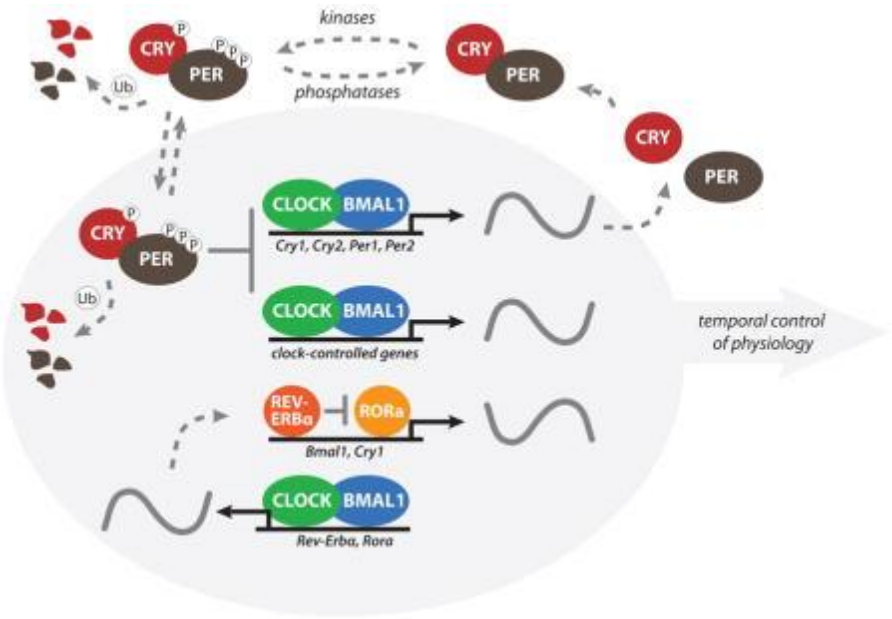

Figure 2 The transcription translation feedback loop in mammals. In this primary negative feedback loop the clock genes *Per* and *Cry* are regulated by their own protein products, and it takes ~ 24 hours to complete one cycle. Kinases and phosphatases control the degradation of clock proteins by the ubiquitin- (Ub) proteosome pathway. A secondary loop, regulated by REV-ERBα and RORα, contributes to the stabilisation of the primary feedback loop. This molecular clockwork regulates temporal organization many physiological processes. Adapted from (Partch et al., 2014).

In mammals, core clock genes are rhythmically expressed in most cells of the body (Cuninkova and Brown, 2008). Circadian gene expression has been found in peripheral tissues in multiple animals, including *Drosophila* (Plautz et al., 1997), zebrafish (Whitmore et al., 1998), and rats (Yamazaki et al., 2000). Balsabore et al. (1998) showed that the treatment of cultured rat-1 fibroblasts with high concentrations of serum induced the circadian expression of several genes that are also rhythmically expressed *in vivo*, including rat *Per1* and *Per2*, and showed that cultured rat-1 fibroblasts contain a clock that is capable of measuring time with high precision (Balsalobre et al., 1998).

In order to create a coherent rhythm, the clocks have to be synchronized. This is done by a 'master pacemaker', the suprachiasmatic nucleus (SCN) in the brain (Yamazaki et al., 2000, Yoo et al., 2004). The SCN consists of two small, paired structures in the anterior hypothalamus, located right above the optic chiasm. It contains about 20 000 neurons exhibiting a high degree of intercellular coupling (Reppert and Weaver, 2001). In this neuronal network the phase of clocks is not disturbed by systemic changes (Buhr et al., 2010). However, the phase of peripheral clocks can be influenced by the SCN through, for instance, circulating hormones, and by systemic changes including body temperature (Brown et al., 2002). It has been shown that circadian gene expression can be synchronized by simulated body temperature cycles with only 1 °C and 3 °C daily differences in mice and human fibroblast cultures (Saini et al., 2012). Thus, peripheral clocks are sensitive to changes within the body, whereas the SCN is not affected by systemic changes and is in control of the overall rhythm in the animal.

The external light-dark cycle is the most important zeitgeber, and in mammals the eyes are necessary for the detection of light to keep the SCN entrained with the solar cycle (Yamazaki et al., 1999). Light is detected in the retina, and the SCN receives lighting information via the retinohypothalamic tract (RHT) (Morin, 1994). The synchronized SCN controls multiple entrainment signals and consequently synchronizes peripheral clocks throughout the body and creates a coherent rhythm in the organism.

1.1.3 Avian circadian organization

Unlike mammals, birds possess several central pacemakers that together control overt circadian organization. The pineal gland, the retina and the SCN interact to sustain circadian rhythmicity in birds (Binkley et al., 1980, Ebihara et al., 1984, Gaston and Menaker, 1968, Takahashi and Menaker, 1982, Underwood et al., 1990, Zimmerman and Menaker, 1979).

The pineal gland produces and releases the hormone melatonin in a rhythmic fashion. Melatonin is the chemical signal for darkness, and it is involved in synchronizing the circadian

rhythm. The avian pineal gland contains both photoreceptors and an autonomous circadian oscillator (Natesan et al., 2002). Thus, daily patterns of melatonin synthesis can be directly entrained to the external light-dark cycle. In a study on house sparrows (*Passer domesticus*), surgical removal of the pineal gland (pinealectomy) resulted in the birds becoming arrhythmic in constant darkness (DD) (Gaston and Menaker, 1968). However, rhythmicity could be restored in pinealectomized house sparrows within one day after transplantation of pineal glands into the anterior chambers of the eye (Zimmerman and Menaker, 1979). These experiments show that the pineal gland is necessary and sufficient for the maintenance of circadian rhythmicity in house sparrows. Pinealectomy in Japanese quail (*Coturnix japonica*), on the other hand, did not alter free-running circadian rhythms (Simpson and Follett, 1981), which shows that there are species specific differences in birds.

In many bird species photoreceptors in the retina synthesize and release melatonin as well. The retina in Japanese quail and domestic pigeon (*Columba livia domestica*) produce nearly as much melatonin as the pineal gland (Ebihara et al., 1997). Experiments with Japanese quail also suggest that the ocular melatonin rhythm is driven by a clock located in the eye itself (Underwood et al., 1990).

The avian SCN contains two structures, the medial SCN (mSCN) and the visual SCN (vSCN) (Cantwell and Cassone, 2006, Cassone and Moore, 1987), which are connected through neuronal projections. The vSCN expresses metabolic rhythmicity and electrical activity and receives input from the RHT (Cantwell and Cassone, 2002, Cantwell and Cassone, 2006, Cassone and Moore, 1987, Juss et al., 1994, Lu and Cassone, 1993). Furthermore, it contains melatonin receptors (Cassone et al., 1995, RIVKEES et al., 1989). The mSCN does not possess these properties. It does, however, express clock gene rhythmicity (Yasuo et al., 2002, Yoshimura et al., 2000).

There are two complementary theories describing how the pineal gland, the SCN and the retina are connected to each other. The “neuroendocrine loop model” (**Figure 3**) suggests that inhibitory actions between the three pacemakers determine the overall output of the clock (Cassone and Menaker, 1984). Light passing through the skull of birds acts through photoreceptors in the pineal gland and inhibits the output of this pacemaker. At the same time, light causes an activation of the SCN output. During the night, the pineal gland secretes melatonin and thereby influences various downstream structures and processes, including the vSCN, which is inhibited by melatonin. The production of melatonin declines when dawn approaches, and its inhibition of the SCN output ends. During the day, the SCN are active and influence various downstream processes, including inhibition of the production of melatonin in

the pineal gland through the secretion of norepinephrine (NE). The retina has a similar function as the pineal gland, producing melatonin during the night. During the day, light information from the retina is transduced to the SCN via the RHT. In this way, stable phase relationships are maintained, and each pacemaker can influence downstream processes.

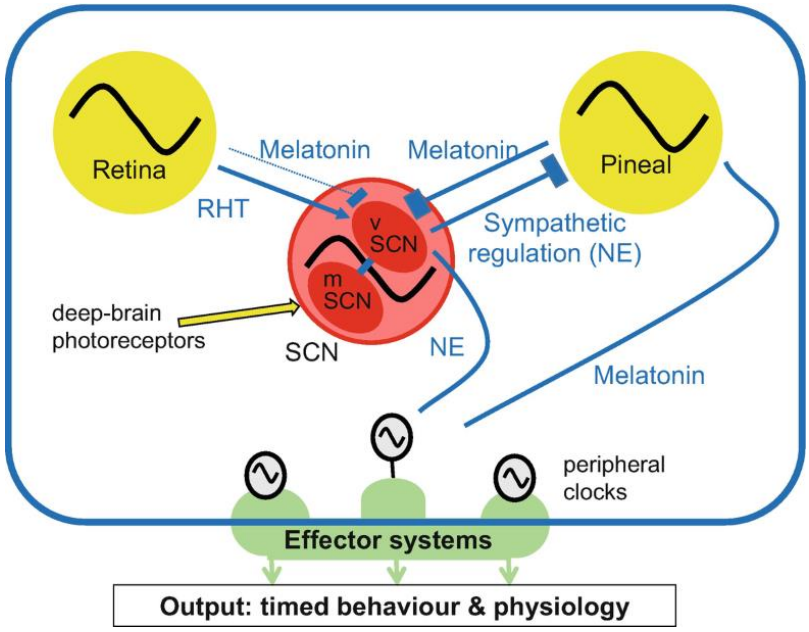

Figure 3 The neuroendocrine loop model. The three circadian pacemakers are shown as circles containing sine waves (yellow circles = photoreceptive structures). Blue lines show the interactions between structures (rectangles = inhibiting, arrows = activating, open-ended = connecting). Adapted from (Helm, 2020).

Alternatively, the model of "internal resonance" suggests that the three oscillators synchronize and amplify each other through resonance (Gwinner, 1989). The reduction of the amplitude of one of the three oscillators would thus decrease the amplitude of the other two oscillators. This implies that elimination of the endogenous melatonin rhythm should lead to a damped rhythmicity of the circadian oscillators under constant conditions. Furthermore, oscillators should be able to entrain to an increased range of zeitgeber periods and adjust more quickly to the new phase of the zeitgeber in the absence of an endogenous melatonin rhythm (Gwinner and Brandstatter, 2001). This hypothesis was tested in house sparrows (Janik et al., 1992). Pinealectomized house sparrows became arrhythmic under constant conditions, and in synchronized conditions their range of entrainment increased, supporting the model.

1.1.4 Circadian clocks in seasonal timing

Seasonal timing of physiology and behaviour plays an important role in many animals. Yearly migration, hibernation, moult and reproduction are all examples for seasonally timed events. In photoperiodic species, changing day length (photoperiod) is measured to stay synchronized with seasonal changes in the environment, and the circadian clock is thought be involved in this process (Bünning, 1960). The model of 'external coincidence' (Pittendrigh and Minis, 1964) suggests the existence of an endogenously generated circadian rhythm of photosensitivity, where a long day response occurs when the organism is exposed to light during its photosensitive phase. Inductive light periods reoccurring approximately every 24 hours have been shown in the photosensitive white-crowned sparrow (*Zonotrichia leucophrys gambelii*) (Follett et al., 1974). Light exposure during the photosensitive phase of the organism's internal ~ 24 hour rhythm is, according to the model, more important for the induction of photoperiodic responses than the duration of perceived light.

In birds, deep brain photoreceptors have been found to detect changes in photoperiod (Nakane et al., 2010). According to the current working model, light information received by deep brain photoreceptors is signalled to the pars tuberalis (PT), a region of the pituitary gland where the production of thyroid stimulating hormone (TSH) is either induced or inhibited, depending on the time of the year, and TSH initiates important seasonal responses in physiology (Nakane and Yoshimura, 2014). Appenroth et al. (2020) have shown that rhythmic clock gene expression in the mediobasal hypothalamus (MBH) and PT persisted under constant conditions in Svalbard ptarmigan (*Lagopus muta hyperborea*). Furthermore, a rhythmic sensitivity to light that requires a functional circadian system has been shown to drive the seasonal biology of Svalbard ptarmigan, providing evidence for the involvement of the circadian clock in a seasonal photoperiodic response (Appenroth et al., 2020).

1.1.5 Adaptive value of circadian clocks

Circadian clocks are found in organisms ranging from bacteria to mammals, and their ubiquity indicates adaptive significance. Endogenously generated rhythms that are entrained by environmental factors offer several advantages over exogenously driven, passive rhythms. For instance, irregular environmental conditions, such as changing weather, have far smaller effects on rhythms in physiology and behaviour when an endogenous clock is present. It is hypothesized that circadian clocks may have evolved to provide organisms with selective advantage in two ways: (i) by synchronizing physiology and behaviour to cycles of environmental conditions (extrinsic adaptive value), and (ii) by coordinating internal physiological processes (intrinsic adaptive value).

1.1.5.1 Extrinsic adaptive values

According to the hypothesis of extrinsic adaptive value, circadian clocks help organisms respond to daily challenges by programming their biological functions at favourable times of the day. Experiments where the circadian clock was disrupted support the assumption that staying synchronized with the environment gives an organism selective advantage. Cyanobacterial strains with different clock properties, some with functional circadian clocks and some with disrupted clocks grown in competition, showed that in rhythmic environments bacteria with clock periods matching the environmental rhythm out-competed bacteria with clock periods differing from the environmental rhythm (Woelfle et al., 2004). Plants are also believed to gain advantage from circadian clocks. A study on *Arabidopsis thaliana* showed that plants with a clock period matching the environment survived better than plants with clocks whose periods were out of phase with the environmental period (Dodd et al., 2005). Wild types with clocks matching the environment contained more chlorophyll, fixed carbon better and grew faster than plants with long- and short period mutations. Moreover, a study on diurnal antelope ground squirrels (*Ammospermophilus leucurus*) showed that SCN-lesioned animals were more active at night time and thus easier prey in the wild, and they showed a lower survival rate than individuals with an intact SCN (DeCoursey et al., 1997). Spoelstra et al. (2015) conducted a study on mice carrying a short-period mutation (*tau* mutation). Wild-types, homozygous and heterozygous individuals in a Mendelian ratio were allowed to breed and be naturally predated in a semi natural enclosure. Individuals carrying the *tau* mutation were more active during the day and homozygous individuals showed a lower survival rate. After 14 months the relative frequency of the *tau* allele had dropped from 50% to 20% (Spoelstra et al.,

2016). The strong selection against the short-period genotypes in this study, together with other observations of lower survival rates in organisms with clock periods differing from the environment support the hypothesis of extrinsic adaptive value.

1.1.5.2 Intrinsic adaptive values

Circadian clocks are also believed to provide organisms with advantage by maintaining temporal order within the organism. Circadian rhythms have been discovered at multiple levels of biological organization, such as locomotor activity, body temperature, blood sugar, adrenal activity, liver glycogen content, and RNA and DNA metabolism (Halberg, 1960). Several studies have focused on effects of altered circadian clocks on animal health. A study on golden hamsters (*Mesocricetus auratus*) showed that a short-period mutation of the circadian system caused cardiovascular and renal diseases in these animals, suggesting that a mismatch between the clock and the environment can be deleterious (Martino et al., 2008). *Clock* mutant mice were found to develop several metabolic syndromes and they became hyperphagic and obese (Turek et al., 2005) and BMAL1 deficient mice had reduced life spans and developed several characteristics of premature aging (Kondratov et al., 2006). Furthermore, loss of clock function caused by several mutated clock genes lead to a decrease in reproductive fitness in males of *Drosophila melanogaster* (Beaver et al., 2002). Loss of clock function in these studies affected different outputs of the clock, therefore it is difficult to determine whether these effects were caused by the loss of a functional clock, or by the loss of a particular gene.

In humans, shift work is associated with an increased risk of obesity, diabetes and cardiovascular disease (Kroenke et al., 2007, Morikawa et al., 2007, Tüchsen et al., 2006) and chronic misalignment between behavioural rhythms and the endogenous circadian timing system has been proposed to be the underlying cause (Kohsaka and Bass, 2007, Sack et al., 1992).

Overall, these studies support the hypothesis of intrinsic adaptive value, however, the role of circadian clocks in the maintenance of internal order has not been proven with certainty to confer adaptive value to organisms.

1.1.6 Circadian rhythms in aperiodic environments

In the context of adaptive value, it is interesting to have a closer look at organisms inhabiting aperiodic environments. If the endogenous circadian clock does not provide organisms with intrinsic adaptive value, a lack of selective pressure is predicted to cause regression in their circadian biology (Sharma, 2003). In the lab, *D. melanogaster* has due to its rapid live cycle

been object of several studies testing the persistence of circadian rhythms by maintenance of the flies in constant conditions for many generations. *D. melanogaster* kept under constant light (LL) for more than 700 generations still exhibited circadian rhythms in eclosion and were able to entrain to different light-dark cycles (Paranjpe et al., 2003), and they showed circadian rhythms in locomotor activity after 600 generations under DD (Sheeba et al., 2002). However, in the light of evolution 600 – 700 generations are a short time, and one may ask if the flies were given enough time to adapt to an aperiodic environment.

In this respect it interesting to look at organisms naturally living in aperiodic environments, where evolution has had plenty of time to adapt to aperiodicity. Polar environments provide a good opportunity to study circadian rhythms, as organisms in these areas experience extended periods in the absence of light-dark cycles as a zeitgeber. During summer, when the sun does not set in arctic regions, the Arctic ground squirrel (*Urocitellus parryii*) maintains daily rhythms in behaviour and physiology (Williams et al., 2012, Williams et al., 2017) and *Isospora plectrophenaxia*, a parasite of the snow bunting, keeps a 24-hour rhythm of oocyst output (Dolnik et al., 2011). However, the distribution of Arctic ground squirrels ranges into lower latitudes, and snow buntings are migratory birds that winter in temperate areas. Thus, they experience rhythmic environmental light-dark cycles for much of the year. Reindeer (*Rangifer tarandus*) and Svalbard ptarmigan, on the other hand, spend the entire year in the Arctic, where an environmental light-dark cycle is absent for large parts of the year. Both species show no overt circadian rhythms in activity during arctic summer and winter (Reierth and Stokkan, 1998a, Reierth et al., 1999, Van Oort et al., 2005). A study by Lu et al. (2010) showed that melatonin rhythms in reindeer acutely responded to the environmental light-dark cycle, but not to circadian phase. To examine the molecular clock in reindeer, Lu et al. (2010) generated *Per2* and *Bmal1* luciferase reporter constructs and introduced them into reindeer fibroblasts through transduction. Luciferase is an enzyme that together with its substrates luciferin and ATP produces bioluminescence in various organisms in nature. In the experiment, the DNA coding sequence for luciferase was fused with the regulatory regions of the genes *Per2* and *Bmal1*, resulting in expression of luciferase when transcription of the target genes was upregulated. To validate the approach mouse fibroblasts were infected with the same reporter constructs (**Figure 4***a*). In contrast to mouse fibroblasts, reindeer fibroblasts did not exhibit overt circadian oscillations (**Figure 4***b*) indicating a weak molecular clockwork (Lu et al., 2010).

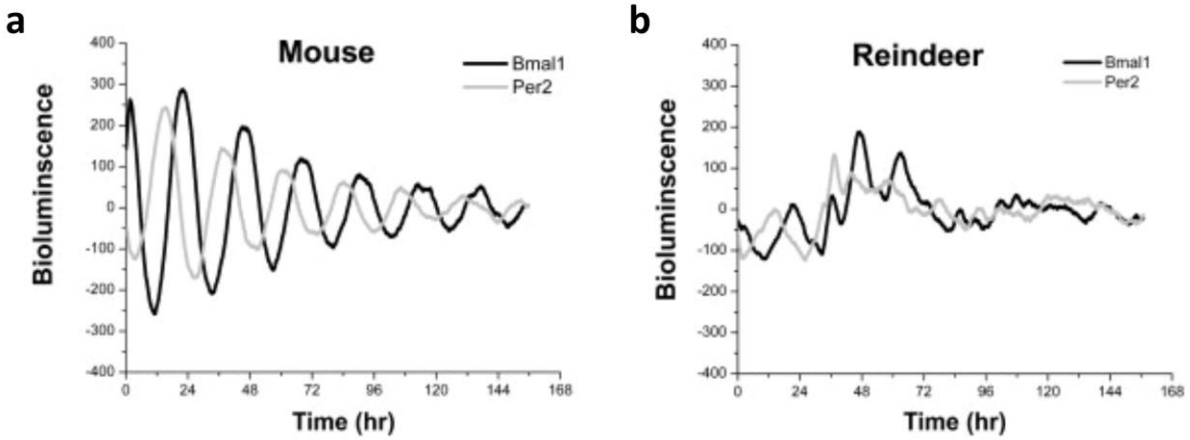

Figure 4 Molecular rhythms in mouse and reindeer fibroblasts. Cultured fibroblasts were transduced with *Per2* and *Bmal1* luciferase reporters and synchronized with forskolin before bioluminescence recording. Data is presented as spline fit. (a) mouse fibroblasts. (b) Reindeer fibroblasts. Adapted from (Lu et al., 2010).

Both reindeer and Svalbard ptarmigan lose daily behavioural rhythmicity in the absence of an external light-dark cycle, and the similarity in behaviour patterns suggests similar clock properties in both species. However, the dynamics of the molecular clock in Svalbard ptarmigan have not been examined yet, and this study will focus on endogenous circadian rhythms in this species.

1.2 Svalbard ptarmigan

1.2.1 An interesting organism to study circadian biology

Svalbard ptarmigan (*Lagopus muta hyperborea*) **(Figure 5)** are permanent inhabitants of the islands of Svalbard, an archipelago in the High Arctic (74-81°N) about 700 km north of mainland Norway. Svalbard experiences extreme changes in daylength throughout the year. From late April to late August the sun stays permanently above the horizon, whereas from November to the end of January the sun stays lower than 6° below the horizon. These special light conditions, creating polar day and polar night, make animals living on Svalbard especially interesting to study adaptations to circadian biology, as the main zeitgeber for the circadian clock is missing for large parts of the year.

Figure 5 Male Svalbard ptarmigan used in the experiment.

1.2.2 Characteristics of Svalbard ptarmigan

Svalbard ptarmigan are larger and heavier than both willow ptarmigan (*Lagopus lagopus*) and rock ptarmigan (*Lagopus muta*) on mainland Norway, and their body mass varies significantly throughout the year (**Figure 6**). To survive the long winter night, Svalbard ptarmigan deposit huge stores of fat (Mortensen and Blix, 1989). However, not only their appetite and fat stores change with season, but also their plumage. The summer plumage is brown-yellowish-black, and males usually have a white breast and abdomen. In winter both sexes are white with black tail-feathers, and the males have a black stripe running from the eyes to the beak. In winter Svalbard ptarmigan often sit in holes they dig in the snow to protect themselves from very low temperatures.

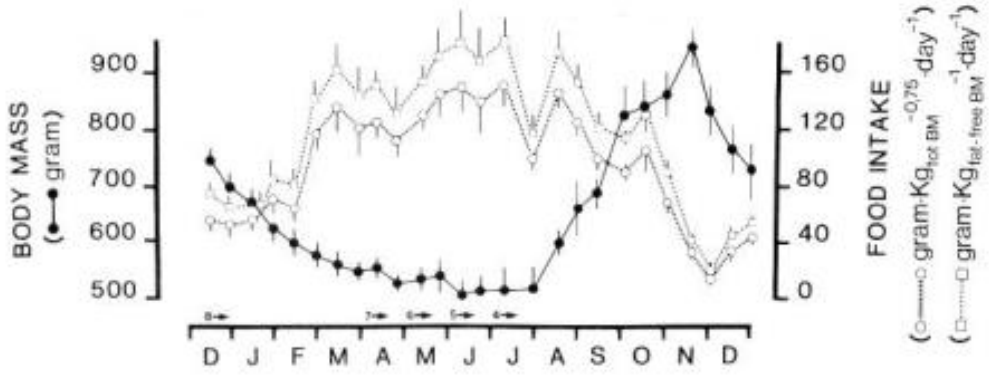

Figure 6 Changes in body mass and food intake in captive Svalbard ptarmigan exposed to natural light and temperature conditions at 79°N for 13 months. The birds were provided with standardized high-quality feed and water or snow *ad libitum* during the entire period. Vertical bars show SE. Adapted from (Stokkan et al., 1986).

1.2.3 Activity and body temperature rhythms in Svalbard ptarmigan

Reierth and Stokkan (1998) studied rhythms in feeding activity in Svalbard ptarmigan under natural photoperiodic conditions at 79°N in Svalbard and at 70°N in Tromsø (**Figure 7**). Feeding activity was intermittent during the polar day and night at 79°N. At 70°N, feeding activity was intermittent during summer, but in winter the birds seemed to be entrained. When an external light-dark cycle was present in autumn and spring, all birds were diurnal. Periodogram analysis revealed ultradian rhythmicity between May and August (Reierth and Stokkan, 1998a). In a recent study, Appenroth et al. (2020) exposed Svalbard ptarmigan to different photoperiods. Initially kept under LD 12:12 (12 hours of light, 12 hours of dark), the photoperiod was gradually reduced to LD 6:18, then one group of birds was gradually transferred into LD 16:8 and finally into LL while the second group stayed under LD 6:18. A third group of birds was transferred from LD 6:18 to DD. Locomotor activity and core body temperature (T_b) were recorded throughout the experimental design. The birds showed circadian rhythmicity in locomotor activity under external light-dark cycles that disappeared under LL and DD. Ultradian rhythms were also observed in this study, especially in birds under LL. T_b rhythms under LD were pronounced, with higher temperatures during the light phase, however, rhythms weakened under constant conditions. A rise in T_b in anticipation of light onset was observed, suggesting a circadian system to be in control of T_b rhythms under LD that weakens under constant photic conditions.

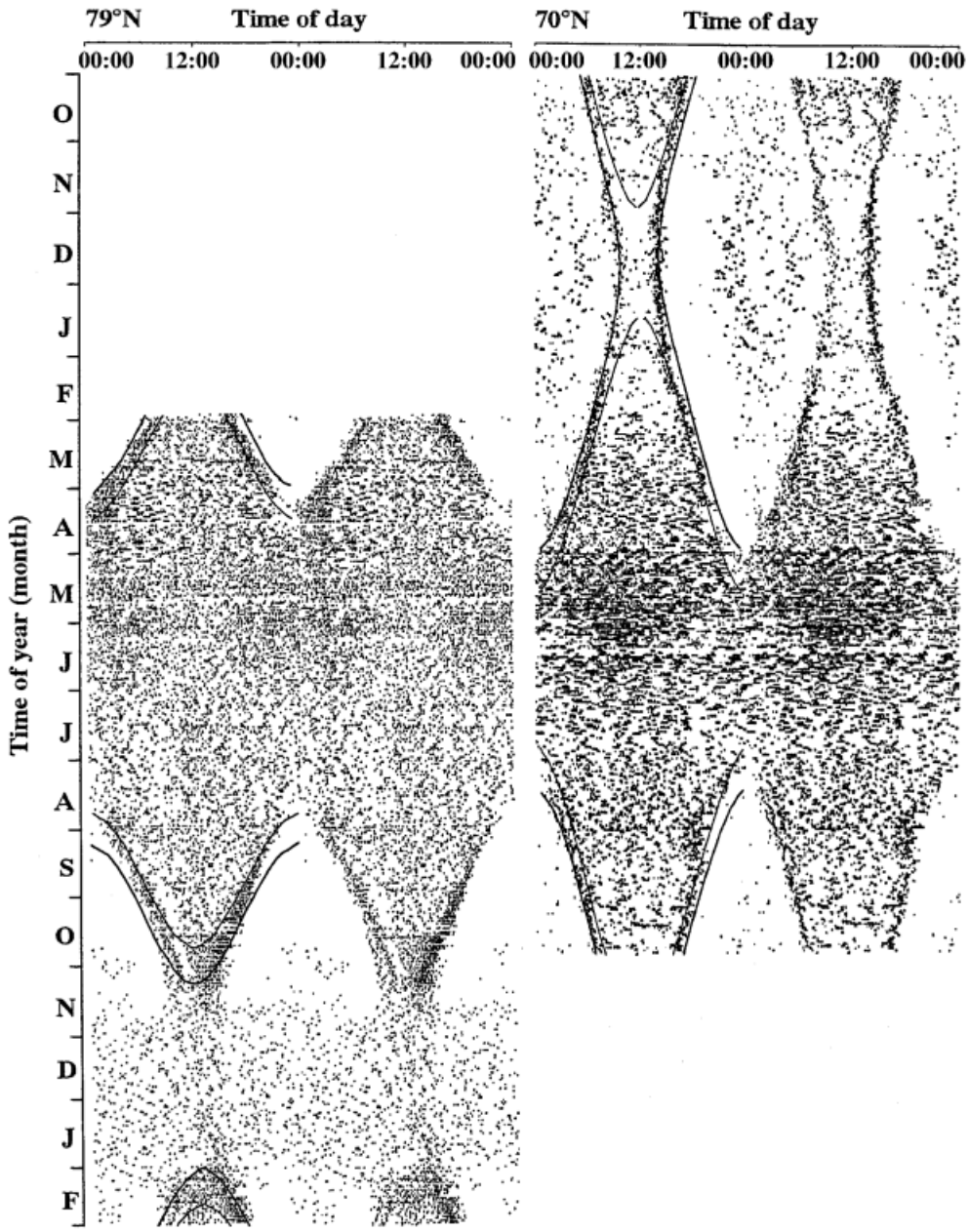

Figure 7 Double plotted actograms showing examples of Svalbard ptarmigan activity recordings at 79°N (left) and 70°N (right). Time of the day (hours) is shown on the x axis, and time of the year (months) is shown on the y axis. Thick solid lines drawn on the actograms show start and end of civil twilight, and thin solid lines show sunrise and sunset. Adapted from (Reierth and Stokkan, 1998a).

1.2.4 Variation in plasma melatonin

As mentioned earlier, the production of melatonin by the pineal gland is an important component of the avian circadian system. It influences, for instance, rhythms in body temperature, (Binkley et al., 1971) locomotor and feeding activity (Heigl and Gwinner, 1995) in house sparrows. The plasma level of melatonin is high during the night and low during the day in both diurnal and nocturnal animals, and the circadian rhythm in melatonin secretion is thought to be a physiological link between the animal and its photoperiodic environment. A study on Svalbard ptarmigan at 70°N, experiencing the natural photoperiod of this latitude, showed varying plasma levels of melatonin throughout the day with increased levels at night all year, except for May-July (**Figure 8**) (Reierth et al., 1999). From May to July no daily rhythm in plasma melatonin was observed. Both melatonin production and the amplitude of melatonin production were reduced in mid-winter. A rhythm of light intensity was present all year round, but the amplitude of melatonin production was much reduced around summer and winter solstice. These results suggest a seasonal change in flexibility of the circadian system Svalbard ptarmigan, that may be an important adaptation to life in the arctic.

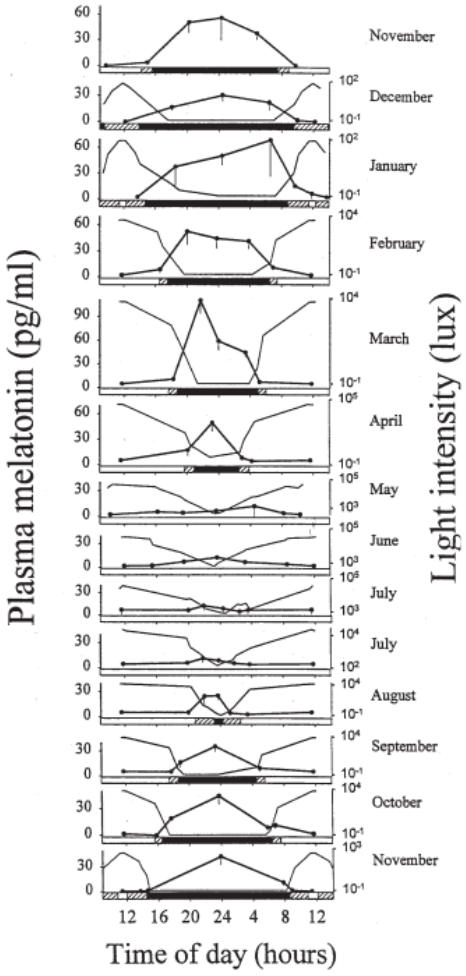

Figure 8 Daily variations in plasma melatonin in Svalbard ptarmigan throughout one year (black dots = mean ± standard error of the mean). The line without black dots represents measured light intensity in lux (missing for the first month). White bars represent sun above the horizon, shaded bars represent civil twilight and black bars represent night. Adapted from (Reierth et al., 1999).

1.2.5 Adaptive value of the circadian clock in Svalbard ptarmigan

Daily activity patterns may be less important to inhabitants of arctic environments, but the circadian system may be preserved due to its importance in seasonal synchronization. In Svalbard ptarmigan, rhythmic clock gene expression within the key tissues in the seasonal neuroendocrine cascade, the MBH and the PT, persists under constant conditions (Appenroth et al., 2020). Furthermore, a circadian rhythm in photosensitivity in Svalbard ptarmigan was

shown by Appenroth et al. (2020), supporting the model of 'external coincidence' and thereby the assumption that the circadian clock is involved in measuring photoperiod. Thus, a circadian clock seems to be an important part of seasonal synchronization in Svalbard ptarmigan, but fails to maintain daily rhythms in activity under constant environmental conditions.

1.3 Aim of the study

"For a large number of problems there will be some animal of choice or a few such animals on which it can be most conveniently studied" (Krogh, 1929). This concept, known as Krogh's principle, emphasises the importance of choice of organisms when studying biological problems. Svalbard ptarmigan are permanent inhabitants of the High Arctic, experiencing extreme photoperiodic conditions throughout the year. Living in an area where the main zeitgeber for the circadian clock is absent for large parts of the year, Svalbard ptarmigan can be seen as an ideal organism to study adaptations to circadian biology. Previous studies have focused on the output of a circadian clock in Svalbard ptarmigan under natural or simulated natural light conditions. However, a lack of circadian behaviour in the absence of a light-dark cycle does not prove that a functional molecular clock is not present in Svalbard ptarmigan. A possible reason for arrhythmicity under constant photic conditions could be a weak coupling between the clock and its output. The molecular clock in Svalbard ptarmigan has not been investigated yet, and in this study we aim to characterize the behavioural and molecular circadian biology of Svalbard ptarmigan, following two strategies:

1) An *in vivo* experiment to study activity and body temperature under controlled light conditions
2) *In vitro* experiments to examine the dynamics of the molecular clock

With these experiments we aim to answer the following five questions:

1) What happens to activity, feeding behaviour and body temperature rhythms after a sudden change from LD to DD/LL?
2) How quickly do Svalbard ptarmigan re-entrain to light-dark cycles after a change from DD/LL to LD?
3) Are there differences in ultradian rhythmicity under different light conditions?
4) Can we observe circadian oscillations in ptarmigan fibroblast clocks?
5) Can ptarmigan fibroblast clocks entrain to simulated body temperature cycles?

2 Materials and Methods

2.1 Experimental animals

Svalbard ptarmigan (*Lagopus muta hyperborea*) were hatched from eggs laid by Svalbard ptarmigan held in capture in cages outdoors at the University of Tromsø (69° 39'N, 18° 57'E). Chicks were either raised outdoors on the ground or in cages, or indoors. Seven birds (three females and four males) were transferred to cages in three isolated rooms indoors (**Figure 9**). Throughout the experiment the birds were provided *ad libitum* with standardized protein food (Ref. No.: 4120 TAU, Fiskå Mølle AS) and fresh water. The average temperature in the rooms was 8 °C (max: 12.5 °C, min: 6 °C). All birds were kept in accordance with EU directives under licence provided by the Norwegian Food Safety Authority (Mattilsynet, FOTS 14209).

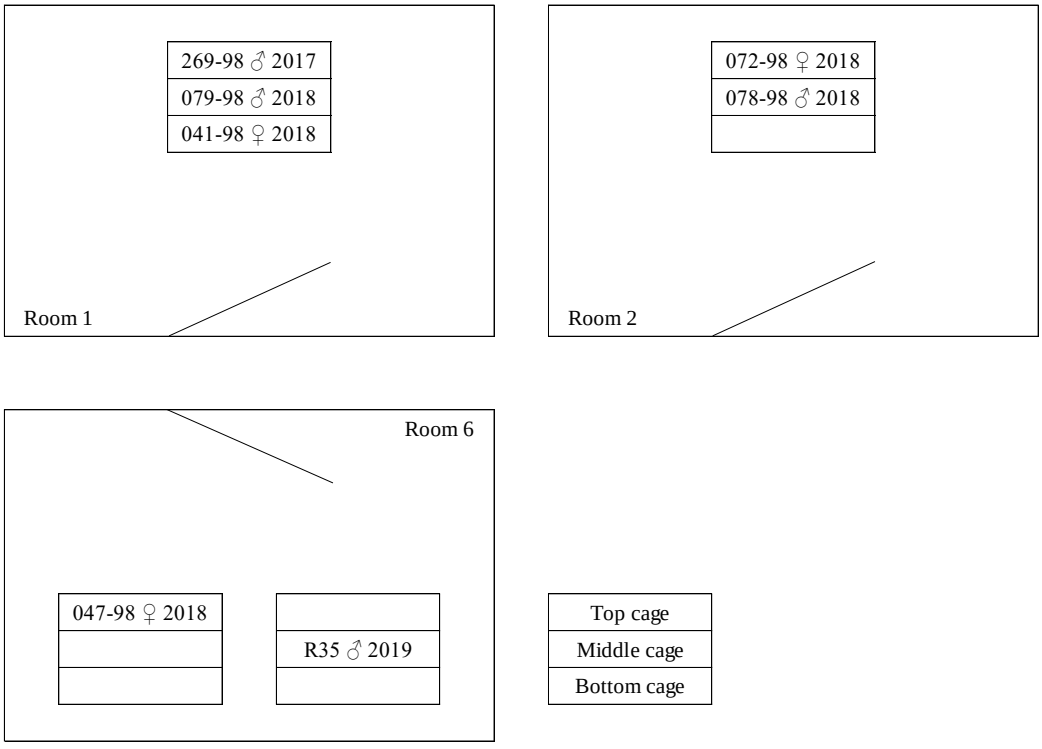

Figure 9 Plan of the three isolated rooms where the experimental birds were housed. Distribution of the birds + their identification, gender and year of birth.

2.2 Chemicals

Table 1 Chemicals used for iButton surgeries

Reagent	Code (company)
Isoflurane	ESDG9623C (Baxter)
Chlorhexidine 1 mg/ml	007227 (Fresenius Kabi)
0.9% Sterile Saline	7533 (B. Braun)
Metacam 2 mg/ml Meloxicam	386860 (Boehringer Ingelheim)
Metacam 1.5 mg/ml Meloxicam	000209 (Boehringer Ingelheim)
100% medical oxygen 10l Conexia	101530 (Linde)

Table 2 Chemicals used for cell culture work

Reagent	Code (company)
Dulbecco's Modified Eagle's Medium - high glucose	D5796-500ML (Sigma-Aldrich)
Dulbecco's Phosphate Buffered Saline	MS00F51003 (Biowest)
Fetal Bovine Serum	S009E20107 (Biowest)
Penicillin/Streptomycin	15140-122 (Gibco)
Trypsin	15090-046 (Gibco)
Gelatin solution	G1393-100ML (Sigma-Aldrich)
Dimethyl sulfoxide	B0515A (NEB)
Forskolin	F3917 (Sigma-Aldrich)
Melatonin	M5250 (Sigma-Aldrich)
Dexamethasone	D4902 (Sigma-Aldrich)
Poly-L-lysine solution	P4832-50mL (Sigma-Aldrich)
Ultra Pure Water	L 005 (Biochrom)
DMEM powder, with l-glutamine and 1000 mg glucose, without phenol red and sodium bicarbonate	D-2902 (Sigma-Aldrich)
D-glucose powder	G7021 (Sigma-Aldrich)
1 M HEPES buffer	H0887 (Sigma-Aldrich)
Sodium bicarbonate solution 7.5%	S8761 (Sigma-Aldrich)
Beetle Luciferin, Potassium Salt	E1601 (Promega)
Flouroshield™ with DAPI	F6057-20ML (Sigma-Aldrich)

Table 3 Chemicals used for ligation, transformation and cloning

Reagent	Code (company)
LB Broth (Miller)	L3522-1KG (Sigma-Aldrich)
LB Broth with agar (Miller)	L3147-1KG (Sigma-Aldrich)
Ampicillin	A9393-5G (Sigma-Aldrich)
Kanamycin	60615-5G (Sigma-Aldrich)
Zero Blunt® TOPO® PCR Cloning Kit	450245 (Thermo Fisher)
NEB® 5-alpha Competent *E. coli* (High Efficiency)	C2987I (NEB)
SOC Outgrowth Medium	B9020S (NEB)
pGL3 basic E2	48747 (Addgene)
pLV6-Bmal-luc	68833 (Addgene)
AAV-P(Cry1)-forward-intron336-Venus-NLS-D2	110054 (Addgene)

Table 4 Chemicals and kits used for plasmid extractions

Reagent	Code (company)
2-Propanol	19516-500ML (Sigma-Aldrich)
Ethanol absolute	20821.310 (VWR)
QIAprep® Spin Miniprep Kit (250)	27106 (Qiagen)
QIAGEN® Plasmid Midi Kit (100)	12145 (Qiagen)
HiSpeed® Plasmid Maxi Kit (10)	12662 (Qiagen)

Table 5 Chemicals used for Big Dye sequencing reactions

Reagent	Code (company)
M13 forward (-20) primer	N52002 (Thermo Fisher Scientific)
BigDye™ Terminator v3.1 Cycle Sequencing Kit	4337457 (Thermo Fisher Scientific)

Table 6 Chemicals used for transfections

Reagent	Code (company)
Lipofectamine™ 3000 Transfection Kit	L3000-001 (Thermo Fisher Scientific)
ViaFect™ Transfection Reagent	E4983 (Promega)
TransIT®-LT1 Transfection Reagent	MIR 2304 (Mirus)
METAFECTENE® PRO Transfection Reagent	T040-1.0 (Biontex)
CellLight™ Actin-GFP, BacMam 2.0	C10506 (Thermo Fisher Scientific)
pEYFP-Mito	Gift from Kenneth Bowitz Larsen

Table 7 Forward and reverse primers used for qPCR reactions

Gene	Forward primer 5' - 3'	Reverse primer 5' - 3'
Clock	TGGAAAGATTTGATACCAGC	GACGAATGATCTGATACTGC
Bmal1	TTCATCCTAAAGACATTGCC	GCATCTATAAGCCTTTCTCG
Cry1	CGTTTGTTTGTTATTCGTGG	TAGCCAGCTTCTTAATTGC
Cry2	GTTGCAAATTACGAAAGACC	GCTTCACCTTCTTATACAGC
Per2	AAATGGAACTTCTGGAATGG	AGATTCCTGTGGTTTAATGC
Per3	AATGGAAATTGTGCAGAGG	TCCTTGATGCAATATACAGC
Ppib	CTGACGAGAACTTCAAGC	TGGTGATGAAGAACTGGG

Table 8 Kits and chemicals used for RNA extractions, cDNA conversion and qPCR reactions

Reagent	Code (company)
RNeasy® Mini Kit (50)	74104 (Qiagen)
QIAshredder (50)	79654 (Qiagen)
RNase-Free DNase Set (50)	79254 (Qiagen)
Nuclease-Free Water	P119E (Promega)
High Capacity RNA-to-cDNA Kit	4387406 (Thermo Fisher Scientific)
GoTaq® qPCR Master Mix	A600A (Promega)

2.3 Implantation of iButton temperature loggers

Surgical implantations of iButton temperature loggers (DS1922L, Maxim Integrated) were performed on 16. – 17. September 2020 by Daniel Appenroth, assisted by Alexander West, Vebjørn Melum and Fredrik Markussen. Isoflurane in 100% medical oxygen was administered to the birds through a face mask with the help of an Ohmeda vaporizer (BOC Healthcare) and a Vapor 200 isoflurane vaporizer (Draeger Medical), and the birds lost consciousness approximately 2-4 minutes later. Oxygen flow was set to 0.5 L/min throughout surgery. Isoflurane was initially set to 4% and gradually decreased. Breathing was closely observed, and isoflurane concentration was set accordingly.

The birds were placed on the surgical bench on their backs and the feathers were sprayed with 70% ethanol. At the experimental area the feathers were removed, and the edges of the area were taped down with autoclave tape to keep the surgical area free from feathers and dust. The surgical area was disinfected with chlorhexidine. The skin was cut on the left side, caudal of the rib cage, and opened by a small cut. The blunt ends of scissors were used to open a sufficient hole. Subcutaneous fat was cut with blunt cuts, and muscle walls were cut either by blunt cuts or by cutting a small hole that was widened by blunt cuts. The opening was kept to a minimum. The cavity and the iButton were wetted with 0.9% sterile saline, and the iButton was inserted into the abdominal cavity. The abdominal cavity was closed by suturing the muscles with 2-3 stitches with wax coated braided silk 2-0 (Syneture), and the skin was sutured with 5-6 stitches. Finally, the wound was rinsed with chlorhexidine. The procedure lasted for 20-30 minutes per bird.

After surgery, the birds were injected subcutaneously with 0.2 mg/kg body mass meloxicam (diluted 1:10 with 0.9% sterile saline). They received 4-6 drops of 1.5 mg/ml meloxicam in their drinking water (250 – 300 ml) as well as *Bistorta vivipara* and *Vaccinium vitis-idaea* as supplements to their normal food. After one week the birds were checked for inflammation and infections (all birds were well).

2.4 Circadian light experiment

Birds were kept in 12 hours of light and 12 hours of dark (LD 12:12) for 16 days prior to the start of the experiment. Light was provided by 85-watt fluorescent strip lights (L 58W 830 Lumilux, Osram) delivering approximately 1000 lx at floor level, and permanent dim red light was provided by Northlight red light bulbs, 15 lm (Clas Ohlson) to allow husbandry in the dark. The experiment started on the 25th of September 2020. For the first 10 days of the experiment the birds stayed in LD 12:12, then light was changed to DD. After 20 days in DD, light was changed back to LD 12:12, and 20 days later to LL. The birds stayed in LL for 21 days, then the light in room 1 was set to LD 12:12, birds in room 2 and room 6 stayed in LL. During the experiment locomotor activity and feeding activity of the birds was constantly recorded using home-built passive infrared activity recorders. Data (passive infrared activity counts per minute) was collected using an Actimetrics CL200 USB interface coupled to a computer with the ClockLab data acquisition software version 2.61 (Actimetrics). Body temperature (T_b) was sampled by the iButtons every 30 minutes throughout the experiment. At the end of the experiment the iButtons were recovered and read with the software program OneWireViewer (Maxim Integrated, Version 0.3.19.47). One iButton was installed in each room to measure the ambient temperature (T_a).

2.5 Cell cultures

Work with cell cultures was performed under a laminar flow hood (Thermo Scientific) to keep cells free from contamination. The following cells were cultured and used in experiments: Svalbard ptarmigan skin fibroblast cultures established by Dr Alexander West following the protocol of skin biopsy processing (Du and Brown, 2021), rat-1 cells stably transfected with a *Per1* luciferase reporter (a kind gift from Prof Qing Jun Meng) and human U2OS cells (ATCC® HTB-96™). Vials with cells stored in a liquid nitrogen tank (Thermolyne) were thawed in a 37 °C water bath (Julabo), cells were suspended in cell culture media (Dulbecco's Modified Eagle's Medium (DMEM) supplied with 20% Fetal Bovine Serum (FBS) and penicillin/streptomycin) and centrifuged for five minutes at 3000 rpm in a SL 40 Centrifuge (Thermo Scientific). Cell pellets were resuspended in cell culture media and transferred to T75 cell culture flasks (Thermo Scientific). Cell culture flasks used for ptarmigan fibroblasts were coated with a 1:10 gelatin solution in Dulbecco's Phosphate Buffered Saline (PBS). Cultures were maintained at 37 °C (5% CO_2) in a Culture Safe Touch 190 CO_2 Incubator (Leec), provided with new cell culture media when required and split when confluent.

2.6 Transfections and bioluminescence recording

2.6.1 Cloning plasmids for transfections

To prepare the agar plates 25 g LB agar and 1 l ultra-pure water were added to a glass bottle (VWR) and autoclaved (CertoClav Sterilizer). The agar was heated in a microwave (Panasonic) until boiling and cooled down for ~ 60 minutes. 2 ml ampicillin were added to the agar (final concentration: 100 µg/ml), and the agar containing ampicillin was then pipetted to 9-cm petri dishes (VWR) and cooled down to room temperature.

Bacteria containing the plasmids AAV-P(Cry1)-forward-intron336-Venus-NLS-D2, pGL3 basic E2 and pLV6-Bmal-luc were spread on separate agar plates containing ampicillin, using sterile 10 µl pipette tips (VWR). Plates were sealed with parafilm and maintained at 37 °C overnight. The next morning 2 ml LB broth containing ampicillin (100 µg/ml) were added to each of three 50 ml falcon tubes. A single bacterial colony was picked from each agar plate using sterile 10 µl pipette tips and transferred to the individual falcon tubes. The lids were left one quarter open to allow aeration. Falcon tubes were placed with a 45° angle in a shanking incubator (Stuart) for approximately six hours. Next to a lit Bunsen burner (Usbeck), 50 ml LB broth and 100 µl LB broth containing bacteria from the falcon tubes were added to each of three Erlenmeyer flasks and left in the shaking incubator overnight. The next day 50 ml from each Erlenmeyer flask were transferred to an individual 50 ml falcon tube. The falcon tubes were centrifuged at 1000 rpm for 30 minutes. Plasmids were extracted using a QIAGEN® Plasmid Midi Kit following the manufacturer's instructions, and DNA concentrations were measured using Nanodrop 2000c (Thermo Scientific).

2.6.2 Optimizing transfection reactions

2.6.2.1 Preparing cell culture plates with microscope coverslips

1 ml 70% ethanol was added to each well on two 12-well cell culture plates (Falcon) and one microscope coverslip was placed in the ethanol in each well and left at room temperature for 15 minutes. The ethanol was discarded and the wells with the coverslips were washed with ultra-pure water. 500 µl Poly-L-lysine solution were added to each well and left at room temperature for five minutes. Then the Poly-L-lysine solution was discarded, the wells were washed with ultra-pure water and plates were left to dry at 37 °C.

2.6.2.2 Testing different transfection reagents and concentrations

A few hours later ~ 10^5 cells were seeded to each well (rat-1 cells to one plate and ptarmigan fibroblasts to the second plate) and left at 37 °C (5% CO_2) until the next day. For transfections, a Lipofectamine™ 3000 Transfection Kit and a ViaFect™ Transfection Reagent were used following the manufacturer's transfection optimizing protocols. pYEFP-Mito was used as DNA. After ~ 24 hours the media with the reagents was discarded and replaced with normal cell culture media.

Before mounting the microscope slides, coverslips in the wells were washed with PBS three times and left to dry at room temperature for five minutes. The coverslips were taken out of the wells with tweezers and mounted on microscope slides (Thermo Scientific) with Fluoroshield™ with DAPI. Slides were wrapped in aluminium foil and stored at 4 °C. The brightfield microscope Axio Observer 7 (Zeiss) was used to visualize the cells and determine the transfection efficiency.

Due to unsatisfactory transfection results two more transfection reagents were tested. Approximately 30 000 ptarmigan fibroblasts were seeded to each well on four µ-slides 8 Well (ibidi) and maintained at 37 °C (5% CO_2). Transfections were carried out two days later using a TransIT®-LT1 Transfection Reagent and a METAFECTENE® PRO transfection reagent at different concentrations as shown in **Figure 10**. The transfection reagent and DNA (Actin-GFP), together with DMEM (without supplies), made up 50 µl that were added to each well containing 150 µl cell culture media (50 µl + 150 µl). Cells were visualized and images were taken with the live cell imaging system Celldiscoverer 7 (Zeiss).

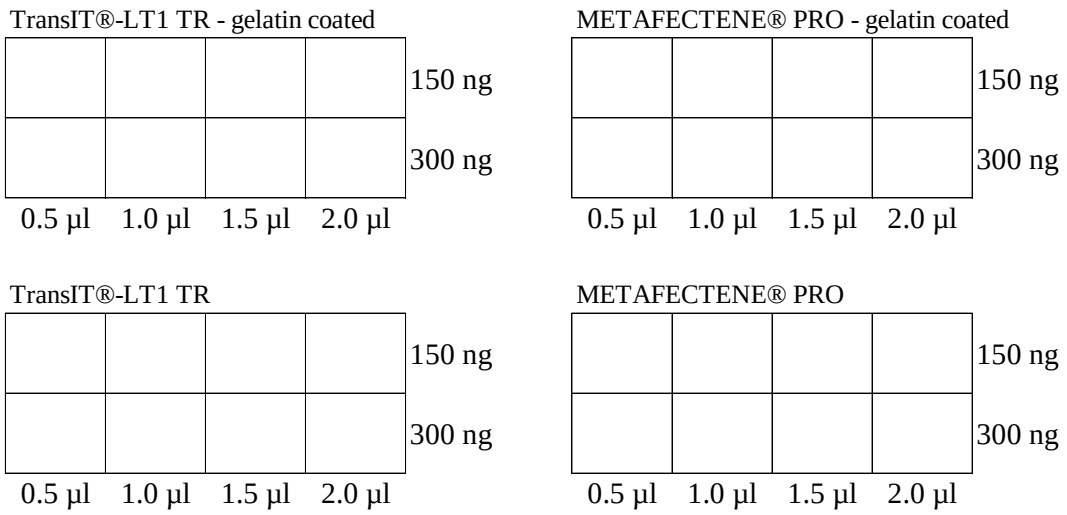

Figure 10 Scheme of the four µ-slides 8 Well used to test the transfections. TransIT®-LT1 Transfection Reagent and METAFECTENE® PRO were used as transfection reagents (TR). Four different TR concentrations (0.5 µl, 1.0 µl, 1.5 µl and 2.0 µl), and two different DNA concentrations (150 ng and 300 ng) were tested (DNA: Actin-GFP). Cells were grown on slides coated with gelatin solution as well as slides without a gelatin coat.

Cells were growing well in wells with and without a gelatin coat, and a combination of 2 µl TransIT®-LT1 Transfection Reagent and 200 ng DNA (in a 200 µl volume) was decided to be the best way to carry out transfections in future experiments.

2.6.3 Bioluminescence recording

The recording medium was made following the recording medium protocol (Yamazaki and Takahashi, 2005). Approximately 10^5 U2OS cells were seeded in each of 10 35-mm cell culture dishes (Falcon) and maintained at 37 °C (5% CO_2) until the next day. Cells in five dishes were transfected with the *Per2* luciferase promoter reporter pGL3 basic E2, and cells in the other five dishes were transfected with the *Bmal1* luciferase promotor reporter pLV6-Bmal-luc, following the protocol that worked best when testing the transfections. Transfected cells were maintained at 37 °C (5% CO_2) for ~ 24 hours, then they were treated with DMEM supplied with 50% FBS for one hour. Subsequently, cells were washed with PBS and 3 ml recording medium were added to each dish. Dishes were air-sealed with parafilm and put into a photon detection unit (LM-2400, Hamamatsu) kept at 37 °C. Photons were counted for one minute every 15 minutes. After five days the temperatures in the incubator where the photon detection unit was kept were set to cycle between 36 °C and 39 °C for five days, each cycle lasting 24 hours. Temperatures were recorded by an iButton. The same procedures were repeated for ptarmigan fibroblasts, with temperatures cycling between 39 °C and 42 °C (around the average temperature obtained from recovered iButtons from the *in vivo* experiment = ~ 40.5 °C).

2.7 Cloning

Primer pairs for the clock genes *Bmal1*, *Clock*, *Per2*, *Per3*, *Cry1*, *Cry2*, and the reference gene *Ppib* were cloned and sequence validated to test their target specificity.

2.7.1 qPCR

To amplify the primers, 10 µl GoTaq® qPCR Master Mix, 1 µl forward primer, 1 µl reverse primer 7 µl Nuclease-Free Water, and 1 µl cDNA (sample from ptarmigan fibroblasts) were added to each PCR tube (Hard-Shell PCR Plates 96-well, Bio-Rad) and qPCR reactions were carried out with a CFX Connect Real-Time PCR System (Bio-Rad) as shown in **Table 9** for all of the seven genes (primer efficiency > 90%).

Table 9 Program used for qPCR reactions

Temperature (°C)	Duration	Cycles
95	2 min	1
95	15 sec	39
57	15 sec	
60	1 min	

2.7.2 Ligation

For ligation, a Zero Blunt® TOPO® PCR Cloning Kit was used. 4 µl PCR product, 1 µl salt solution and 1 µl of the vector pCR Blunt ll TOPO were added to each of seven tubes on a PCR 8-tube strip (one tube for each primer pair). The tubes were left at room temperature for five minutes and then placed on ice.

2.7.3 Transformation

Transformations were carried out using an antiseptic technique next to a lit Bunsen burner. 25 µl 5-alpha competent *E. coli* and 1 µl of plasmid DNA from ligations were added to each of seven 1.5 ml Eppendorf tubes. The tubes were placed on ice for 30 minutes, exposed to a heat shock at 42 °C for 30 seconds to facilitate entry of the plasmid DNA to the bacteria, and placed back on ice for five minutes. 950 µl SOC Outgrowth Medium were added to each tube, then the tubes were placed in the shaking incubator at 37 °C and 250 rpm for 60 minutes.

100 µl bacterial solution from each tube were dispersed on separate agar plates using a sterile glass spreader. Plates were incubated at 37 °C overnight, and the next morning they were sealed with parafilm and stored at -4 °C.

2.7.4 Plasmid growth and extractions

2 ml LB broth containing ampicillin (100 µg/ml) were added to each of seven 15 ml falcon tubes next to a lit Bunsen burner. Then, using a sterile 10 µl pipette tip, two colonies were picked from each plate and transferred to the individual falcon tubes. The falcon tubes were left in the shaking incubator overnight with the lids a quarter open to allow air into the tubes. Plasmid DNA was extracted using a QIAprep® Spin Miniprep Kit following the manufacturer's instructions. DNA concentration was measured using Nanodrop 2000c.

2.7.5 Big Dye sequencing reaction

For Big Dye PCR reactions, a BigDye™ Terminator v3.1 Cycle Sequencing Kit was used. 0.5 µl 10 µmol/ml M13 forward primer, 0.5 µl Big Dye, 3 µl 5x sequence buffer, 15 µl Nuclease-Free Water and 100 ng DNA from plasmid extractions were added to each tube on a PCR 8-tube strip. Tubes were placed in the Mastercycler Gradient and the program was set as shown in **Table 10.** Sequencing products were sent to the in-house sequencing facility, where capillary electrophoresis was performed by a 3130xl Genetic Analyzer (Applied Biosystems), and the data was sent back. ApE (Version 2.0.61, 2020) was used to find the cloning site, and target sequence and cloning site were aligned using Clustral Omega (EMBL-EBI).

Table 10 Parameters used in Big Dye sequencing reactions

Temperature (°C)	Duration	Cycles
96	5 min	1
96	10 sec	40
50	5 sec	
60	4 min	

2.8 Fibroblast stimulation experiments

Approximately 10^5 cells (ptarmigan fibroblasts) were seeded in each of four wells on six 6-well cell culture plates (Thermo Scientific) and maintained at 37 °C (5% CO_2) for three days. On the 3rd day, the cells on each plate received a different treatment. Plate 1 was left untreated as a negative control. 2 µl 100 nM dexamethasone were added to each of the four wells on plate 2, 2 µl 10 µM forskolin were added to each of the four wells on plate 3, 2 µl of a 1:1000 dimethyl sulfoxide (DMSO) dilution were added to each of the four wells on plate 4 as a control for dexamethasone and forskolin and 2 µl 100 pg/ml melatonin (a physiological concentration in Svalbard ptarmigan (Reierth et al., 1999)) were added to each of the four wells on plate 5. On plate 6 the cell culture media was replaced with cell culture media supplied with 50% FBS. All plates were maintained at 37 °C (5% CO_2) for one hour, then the reagents were discarded, plates were washed with PBS, sealed with parafilm, snap-frozen on dry ice and stored at -80 °C.

2.8.1 RNA extractions, cDNA conversion and qPCR

RNA was extracted from the stimulated ptarmigan fibroblasts using QIAshredders and a RNeasy® Mini Kit following the manufacturer's instructions. RNA concentrations were measured using Nanodrop 2000c.

For cDNA conversion, 10 µl buffer and 1 µl enzyme from a High Capacity RNA-to-cDNA Kit and 9 µl RNA sample (with a 100 ng/µl concentration) were added to each tube (PCR 8-tube strips, VWR). Tubes were placed in a Mastercycler Gradient (Eppendorf) and the temperature was set to 37 °C for one hour, 95 °C for five minutes and then cooled down to 4 °C.

Prior to qPCR reactions cDNA was normalized to a concentration of 10 ng/µl. Primers for the clock genes *Clock*, *Bmal1*, *Cry1*, *Cry2*, *Per2*, *Per3*, and for the reference gene *Ppib* were used in qPCR reactions. 10 µl GoTaq® qPCR Master Mix, 1 µl forward primer, 1 µl reverse primer, 7 µl Nuclease-Free Water and 1 µl cDNA were added to each PCR tube. qPCR reactions were carried out as shown in **Table 11**, **Table 12** and **Table 13**.

Table 11 qPCR program for the genes *Clock* and *Ppib*

Temperature (°C)	Duration	Cycles
95	2 min	1
95	15 sec	39
54	15 sec	
60	1 min	

Table 12 qPCR program for the genes *Bmal1* and *Cry1*

Temperature (°C)	Duration	Cycles
95	2 min	1
95	15 sec	39
60	1 min	

Table 13 qPCR program for the genes *Cry2*, *Per2* and *Per3*

Temperature (°C)	Duration	Cycles
95	2 min	1
95	15 sec	39
57	15 sec	
60	1 min	

2.9 Circadian stimulation experiment

Approximately 10^5 cells (ptarmigan skin fibroblasts) were seeded in each of four wells on 19 6-well cell culture plates and maintained at 37 °C (5% CO_2) for three days. From day three, cells on the plates were treated with cell culture media supplied with 50% FBS to stimulate their clocks. After one hour the media supplied with 50% FBS was replaced with normal cell culture media. Stimulations started on a Tuesday at 9 a.m. with plate 19, and subsequently cells on plates were stimulated down to plate 1 as shown in **Table 14**. Plates were collected as shown in **Table 15**. In this way, cells were stimulated in advance and collected over an eight-hour period rather than every four hours for 72 hours. For collections, cell culture media was discarded, cells were washed with PBS, plates were sealed with parafilm, snap-frozen on dry ice and stored at -80 °C. RNA was extracted, converted to cDNA, and qPCR reactions were performed as described above.

Table 14 Day and time of stimulations for each plate

Day and time of synchronizatons	Plates (hours before collection)		
Tuesdy, 9 a.m.	19 (72 h)		
Tuesday, 6 p.m.	16 (60 h)	17 (64 h)	18 (68 h)
Wednesday, 9 a.m.	13 (48 h)	14 (52 h)	15 (56 h)
Wednesdy, 6 p.m.	10 (36 h)	11 (40 h)	12 (44 h)
Thursday, 9 a.m.	7 (24 h)	8 (28 h)	9 (32 h)
Thursday, 6 p.m.	4 (12 h)	5 (16 h)	6 (20 h)
Friday 9, a.m.	1 (0 h)	2 (4 h)	3 (8 h)

Table 15 Day and time of collection for each plate

Day and time of collections	Plates			
Friday, 7 a.m.	4	10	16	
Friday, 10 a.m.	1	7	13	19
Friday, 11 a.m.	5	11	17	
Friday, 2 p.m.	2	8	14	
Friday, 3 p.m.	6	12	18	
Friday, 6 p.m.	3	9	15	

2.10 Circadian temperature cycling experiment

Approximately 10^5 cells (ptarmigan fibroblasts) were seeded to 12 6-well cell culture plates and maintained at 37 °C (5% CO_2) until they were confluent. Before the start of the experiment the cell culture media in each well was replaced with 4 ml fresh cell culture media. Cells were maintained at temperatures cycling between 36.5 °C and 39.5 °C for four cycles (each cycle lasting 24 hours) and subsequently maintained at 39.5 °C. One cell culture plate with cells was collected every four hours starting at 36.5 °C of the last temperature cycle as shown in **Figure 11**. For collections, cell culture media was discarded, cells were washed with PBS, plates were sealed with parafilm, snap-frozen on dry ice and stored at -80 °C. RNA was extracted, converted to cDNA, and qPCR reactions were performed as described above.

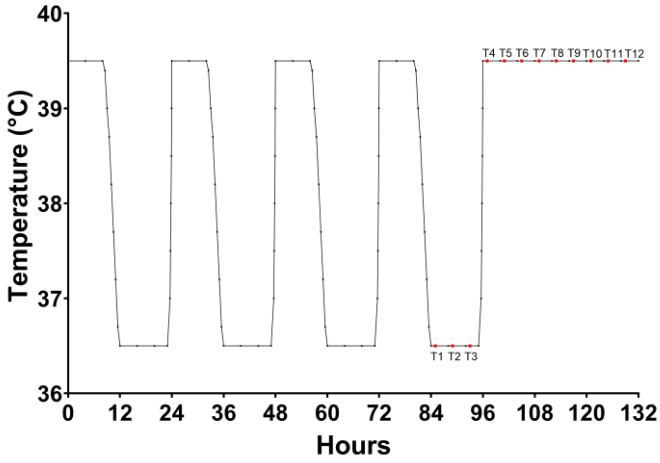

Figure 11 Cycling temperatures in the incubator. Ptarmigan fibroblasts were kept at temperatures cycling between 36.5 °C and 39.5 °C and subsequently maintained at 39.5 °C. Collections were performed every four hours starting at T1.

2.11 Data analysis

Raw data was handled using Microsoft Excel (2016). All graphs and statistical analyses were made with the software GraphPad Prism 9.0.0 except for actograms which were made using the Fiji (Rueden et al., 2017, Schindelin et al., 2012) plugin ActogramJ (Schmid et al., 2011), and JTK_Cycle (Hughes et al., 2010) and RStudio 1.4.1106 were used to identify rhythms in gene expression.

2.11.1 Periods for activity and body temperature oscillations

Activity data was normalized against its 99 percentiles for each bird. Locomotor activity, feeding activity and T_b were illustrated as actograms using ActogramJ. For activity data the minimum value was set to 0 and the maximum value to 1 (0 = no activity; 1 = 99 percentile value). For T_b data the minimum value was set to 39 and the maximum value to 42. The chosen values are defined by T_b taken from recovered iButtons from the *in vivo* experiment. Periods of locomotor activity, feeding activity and T_b were calculated with ActogramJ and the Lomb-Scargle periodogram (Scargle, 1982, Lomb, 1976) and data was exported to GraphPad Prism 9.0.0 for illustration.

2.11.2 Persistence of Tb under constant conditions and anticipation of light change

T_b data from each bird was normalized against its mean and illustrated by diagrams, and a nonlinear regression was drawn as a damped sine wave. A paired t test was performed to test for differences between half-lives of damped sine waves under DD and LL. T_b mean of five hours before lights changed from lights-on to lights-off was divided by the T_b mean of the entire period of 24 hours to subtract the baseline and data was defined as pre-dawn T_b index. This was done for the day before the lights changed from DD to LD as well as for the entire period under LD for each bird. The same calculations were done for the three birds that were transferred from LL to LD (for the last day under LL and the entire period under LD). Repeated measures one-way ANOVA and a subsequent Dunnett's multiple comparisons test, where the values from the last day under LD were used as a control group, were performed to test for differences in anticipation of light onset between the days.

2.11.3 Ultradian rhythms

Periods of the highest ultradian peaks were calculated in Microsoft Excel (2016) and illustrated using GraphPad Prism 9.0.0. One-way ANOVA and a subsequent Turkey's multiple comparisons test were performed to test for differences between light treatments.

2.11.4 Bioluminescence recording data

A 24-hour moving average was subtracted from the data, and data was visualized in GraphPad Prism 9.0.0. For temperature cycling data the centre of gravity of circadian oscillations for the last 24 hours of recordings was calculated using CircWave 1.4 and compared between the genes to calculate the phase relationship.

2.11.5 qPCR data

Analysis of qPCR data was performed in Microsoft Excel (2016). The delta cycle threshold values (ΔCt) were calculated for each gene using **Equation 1**.

Equation 1

$$\Delta Ct = Ct\ gene\ of\ interest - Ct\ reference\ gene$$

ΔΔCt was calculated using **Equation 2.**

Equation 2

$$\Delta\Delta Ct = \Delta Ct - control\ mean$$

Since the calculations were in logarithm base 2, the value of $2^{-\Delta\Delta Ct}$ was calculated to get the expression fold change. Graphs were made using GraphPad Prism 9.0.0.

3 Results

3.1 Circadian light experiment

This experiment was designed to characterize activity and body temperature in Svalbard ptarmigan after a transfer from a rhythmic light-dark environment to constant light conditions, and after a transfer from constant light conditions back to a rhythmic light-dark environment. Birds were kept under LD for 10 days, DD for 20 days, LD again for 20 days, LL for 21 days, then three birds were transferred back to LD for 13 days (**Figure 12**) while the other birds stayed under LL (**Figure 13**). Throughout the experiment locomotor and feeding activity were constantly recorded (passive infrared activity counts per minute) and T_b was measured every 30 minutes by temperature loggers implanted into the abdominal cavity. For the analysis, the experiment was divided into segments of 10 days (20 days for the second time under LD and 13 days for the last segment) and Lomb-Scargle periodograms were calculated for each segment.

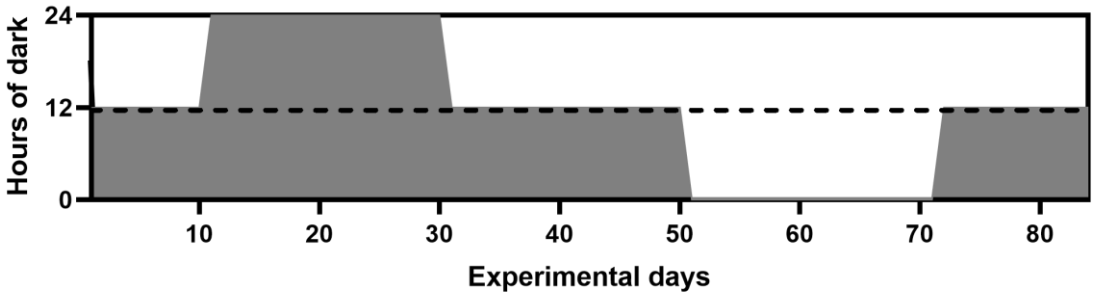

Figure 12 Schematic of light conditions for birds in room 1 throughout the experiment. Grey shading indicates lights off, white background indicates lights on.

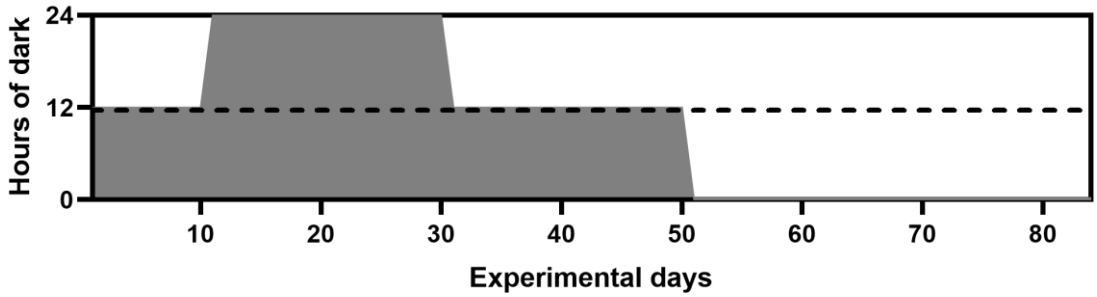

Figure 13 Schematic of light conditions for birds in room 2 and room 6 throughout the experiment. Grey shading indicates lights off, white background indicates lights on.

3.1.1 Rhythmicity under light-dark cycles

Results for a representative male bird (ID: 269-98) for locomotor activity, feeding activity and T_b are shown in **Figure 14**, **Figure 15** and **Figure 16**. In the presence of an external light-dark cycle all birds showed a clear daily rhythm in activity and T_b, with concentrated feeding bouts in the morning and evening (**Figure 14**, **Figure 15** and **Figure 16***a*,*d*,*g*). The periodograms revealed a main period of 24 hours ($P < 0.05$). All other experimental birds also showed significant periods of 24 hours (**Appendix A**, **B** and **C**). These observations were consistent between all LD periods throughout the experimental design.

3.1.2 Rhythmicity after transfer to constant darkness

After a transfer from LD to DD, a circadian component crossed the threshold for significance ($P < 0.05$) in all birds for locomotor activity and four birds for feeding activity. The circadian component for locomotor and feeding activity was much weaker under constant conditions than under LD. A prevalent and statistically significant ($P < 0.05$) circadian component in T_b was present during the first 10 days under DD (**Figure 16***b*), however, during the second part under DD (**Figure 16***c*) the circadian rhythm disappeared in five birds. T_b rhythms were much more consistent than activity rhythms (**Figure 14**, **Figure 15** and **Figure 16**).

3.1.3 Rhythmicity after transfer to constant light

The observations made for birds under LL were similar to those under DD. A circadian component crossed the threshold for significance in all birds for locomotor activity and five birds for feeding activity, but it was much weaker under LL than in a rhythmic light-dark environment. Periodograms also revealed a statistically significant ($P < 0.05$) circadian component in T_b in all birds during the first 10 days under LL (**Figure 16***e*) that disappeared in five birds during the second part under LL (**Figure 16***f*). Birds were more active under LL than under DD, especially during the last part, which is also reflected in higher T_b (**Figure 14**, **Figure 15** and **Figure 16**).

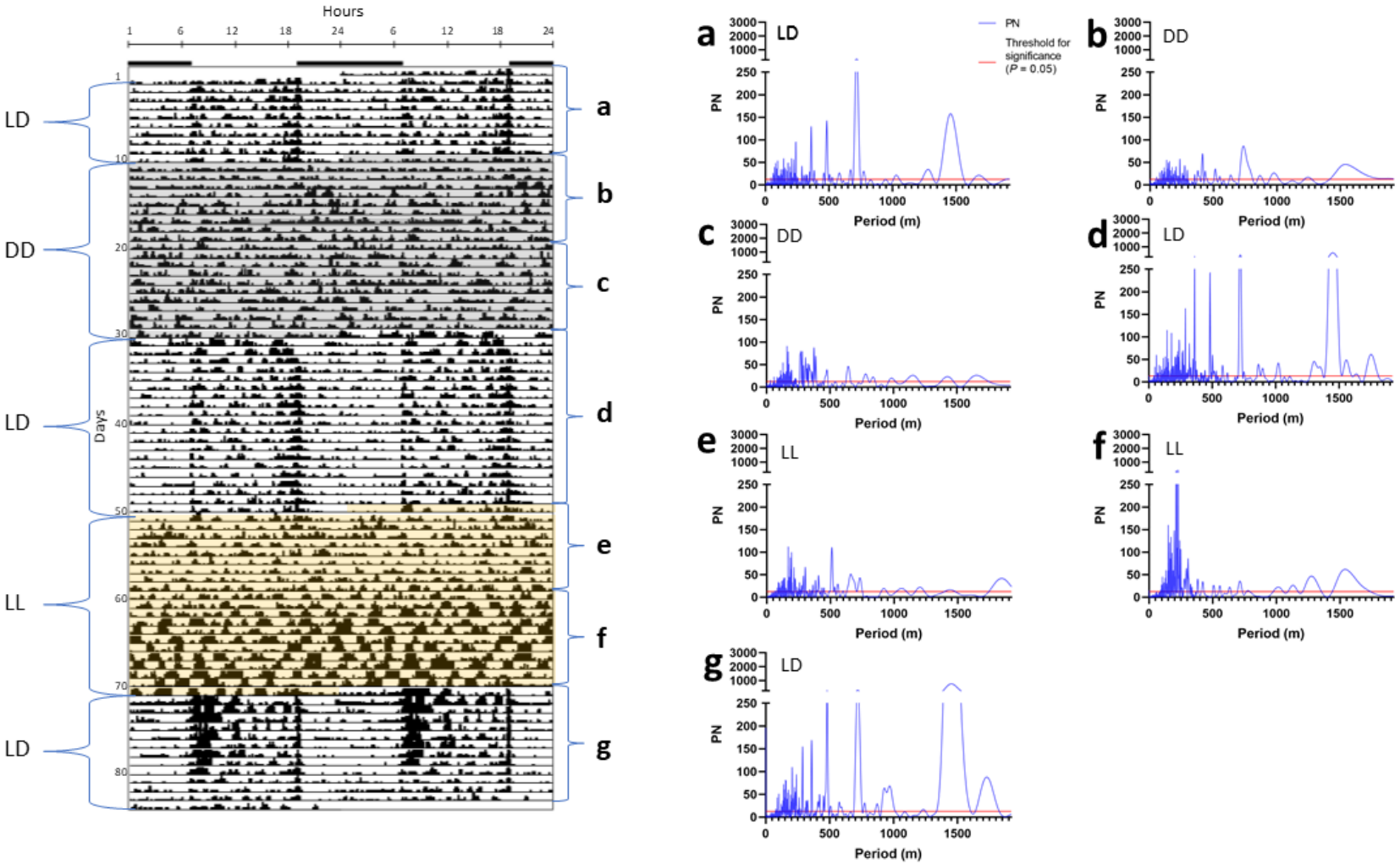

Figure 14 Locomotor activity of a representative male bird (ID: 269-98). Double plotted actogram (left) and corresponding periodograms (right). Each line on the actogram represents two days, and the second day is repeated in the next line. Black bars indicate activity. Data was normalized against its 99 percentiles, and the minimum value set to 0 (no activity) and the maximum value to 1 (99 percentiles). Grey shading indicates DD, yellow shading LL. Black bars above the actogram = lights off, white bars = lights on (refers to LD). The experiment was divided into segments (a-g on the right side of the actogram) and Lomb-Scargle periodograms were calculated for each segment. PN = Lomb-Scargle power

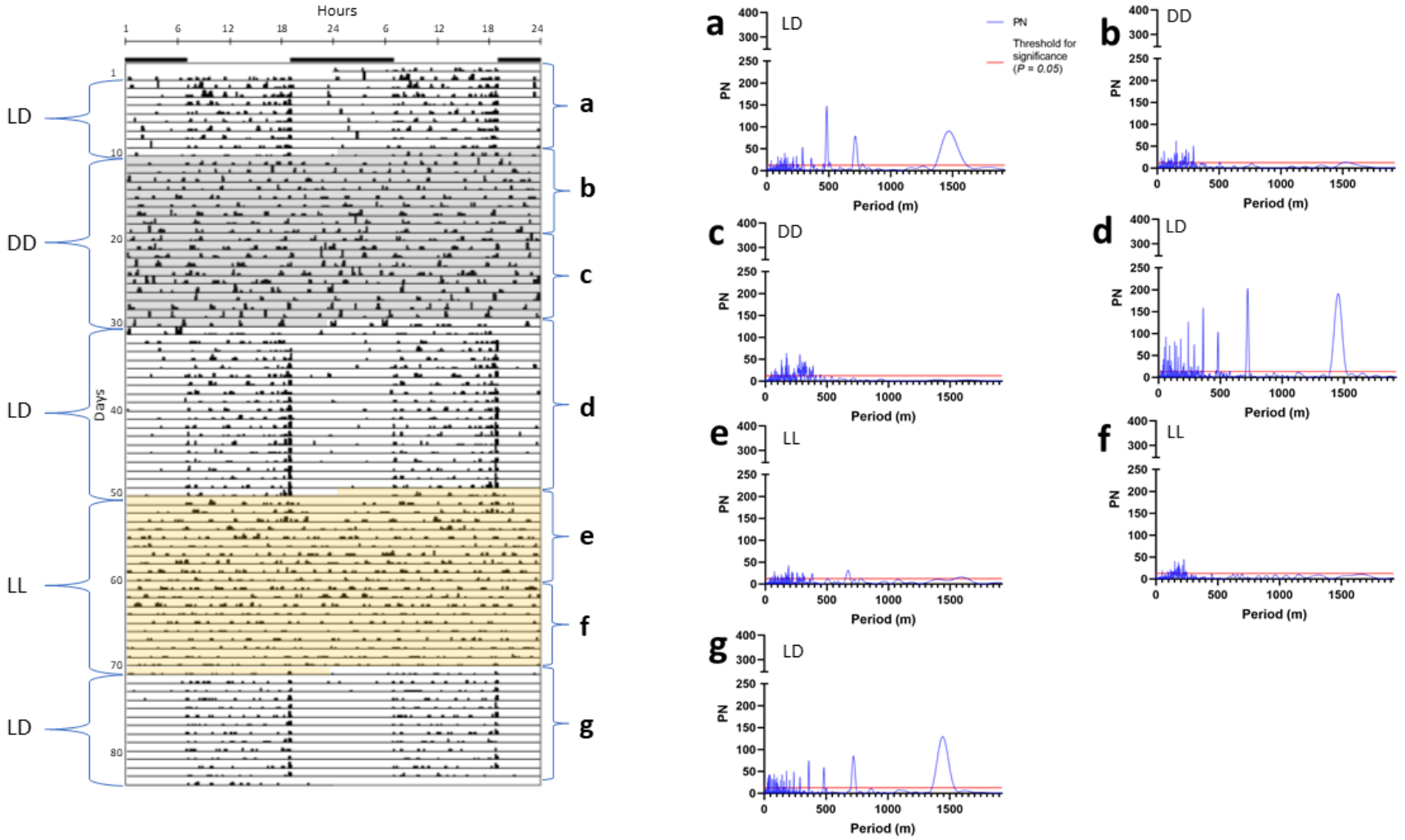

Figure 15 Feeding activity of a representative male bird (ID: 269-98). Double plotted actogram (left) and corresponding periodograms (right). Each line on the actogram represents two days, and the second day is repeated in the next line. Black bars indicate activity. Data was normalized against its 99 percentiles, and the minimum value set to 0 (no activity) and the maximum value to 1 (99 percentiles). Grey shading indicates DD, yellow shading LL. Black bars above actogram = lights off, white bars = lights on (refers to LD). The experiment was divided into segments (a-g on the right side of the actogram) and Lomb-Scargle periodograms were calculated for each segment. PN = Lomb-Scargle power

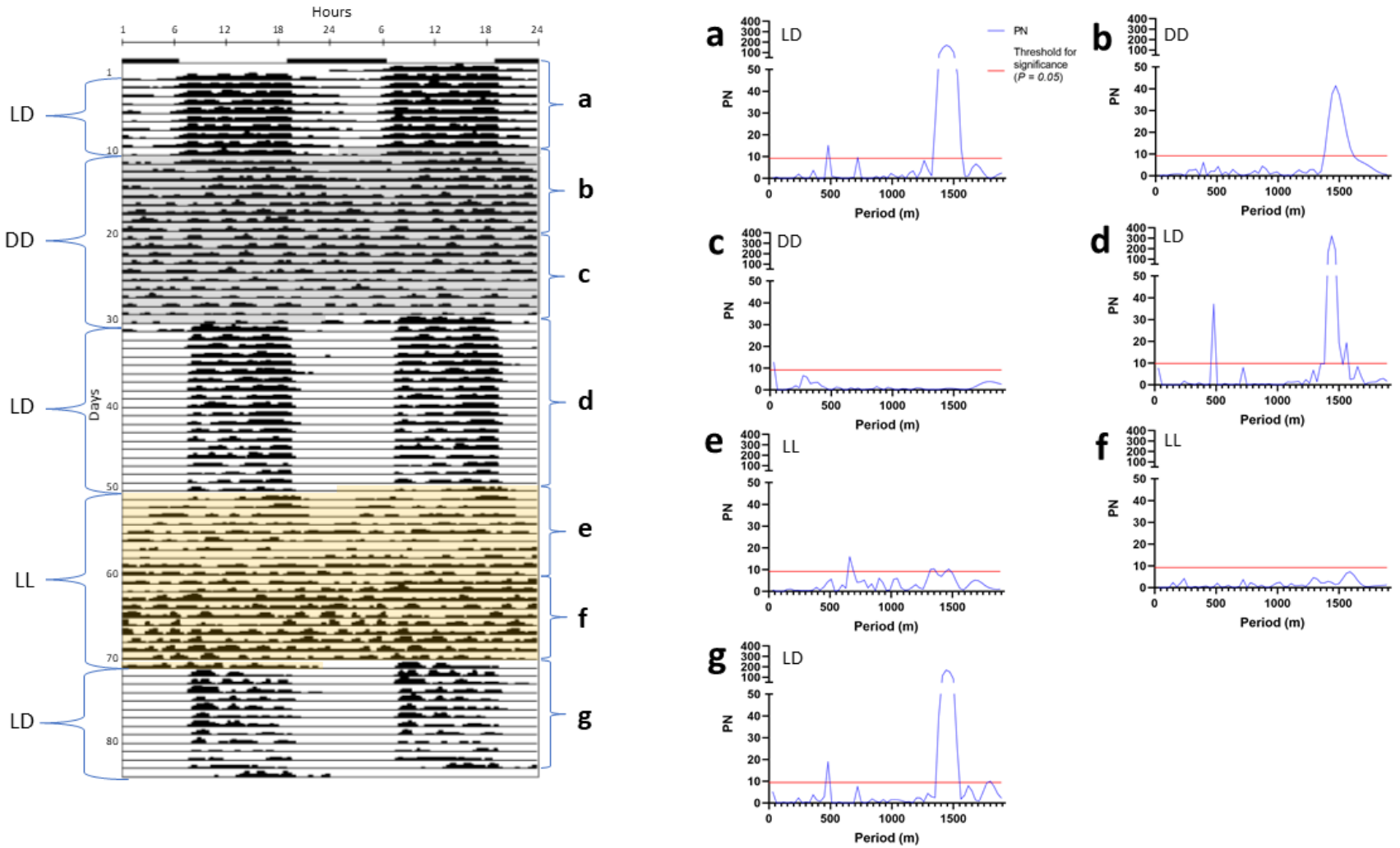

Figure 16 T_b of a representative male bird (ID: 269-98). Double plotted actogram (left) and corresponding periodograms (right). Each line on the actogram represents two days, and the second day is repeated in the next line. Black bars indicate increased T_b. The minimum value was set to 39 and the maximum value to 42. Grey shading indicates DD, yellow shading LL. Black bars above actogram = lights off, white bars = lights on (refers to LD). The experiment was divided into segments (a-g on the right side of the actogram) and Lomb-Scargle periodograms were calculated for each segment. PN = Lomb-Scargle power

3.1.4 Persistence of Tb under constant conditions

As discussed in sections 1.1.2 and 1.1.3, T_b rhythms dampened after several days under constant conditions. To quantify how long a rhythm in T_b amplitude persists after a transfer from a rhythmic light-dark environment to constant light conditions, T_b amplitude under DD and LL was plotted, and a nonlinear regression was drawn as a dampened sine wave. Results for the representative bird, as well as the half-lives of the dampened sine waves of all seven experimental birds are shown in **Figure 17** (see **Appendix D** for all birds). A paired t test showed that half-lives were significantly shorter under LL compared to DD ($P < 0.005$).

3.1.5 Anticipation of light change

Rising body temperature anticipates dawn in LD entrained ptarmigan indicating the involvement of an entrained circadian oscillator (Appenroth et al., 2021a). To examine the rate of re-entrainment of the T_b cycle to LD following exposure to constant conditions, T_b amplitude after the light was changed from DD to LD and from LL to LD was plotted (**Figure 18**, **Appendix E**). One-way repeated measures ANOVA and a subsequent Dunnett's multiple comparisons test showed that the first four days under LD were significantly different ($P < 0.05$) to the last day under LD after the light changed from DD to LD. The transition period from LL to LD did not pass a one-way ANOVA ($P > 0.05$).

3.1.6 Ultradian rhythmicity

A significant ultradian component in locomotor and feeding activity was present throughout the entire experiment. To test if the frequency of the ultradian components changed under different lighting conditions we further analyzed feeding activity by comparison of ultradian periods between all seven experimental birds (**Figure 19**). One-way ANOVA and a subsequent Turkey's multiple comparisons test revealed a significant difference ($P < 0.05$) between ultradian periods under the second LD treatment to ultradian periods under constant conditions.

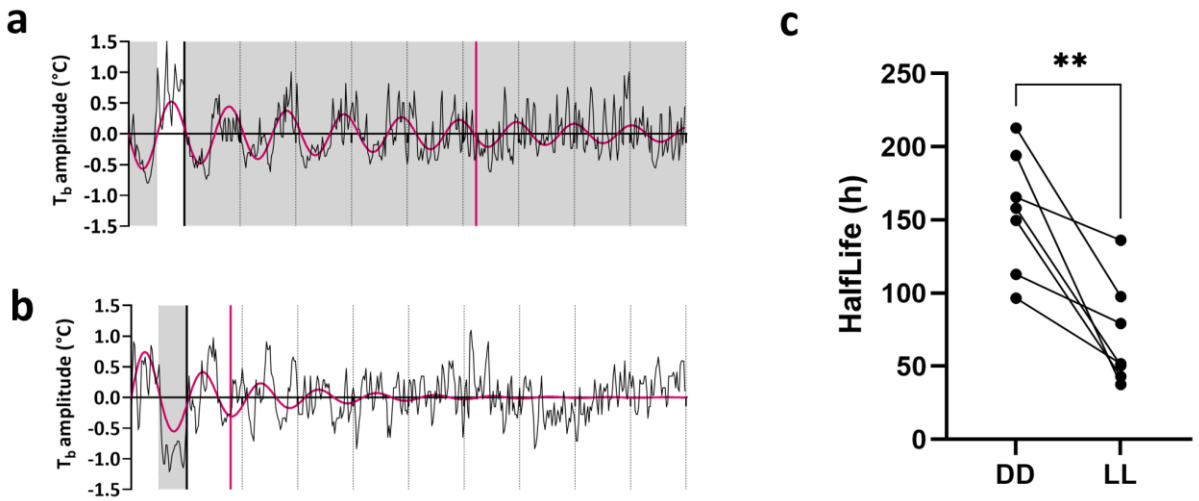

Figure 17 (a-b) T_b amplitude of a representative male bird (ID: 269-98) for 10 days. (a) Last day under LD and following nine days under DD, and (b) last day under LD and following nine days under LL. Vertical dotted lines separate days, white background = lights on, grey background = lights off. A nonlinear regression was drawn as a dampened sine wave (red), vertical red line = half-life of dampened sine wave. (c) Half-lives of dampened sine waves of all seven birds under DD and LL. A paired t test revealed a significant difference between DD and LL ($P < 0.005$, indicated by asterisks).

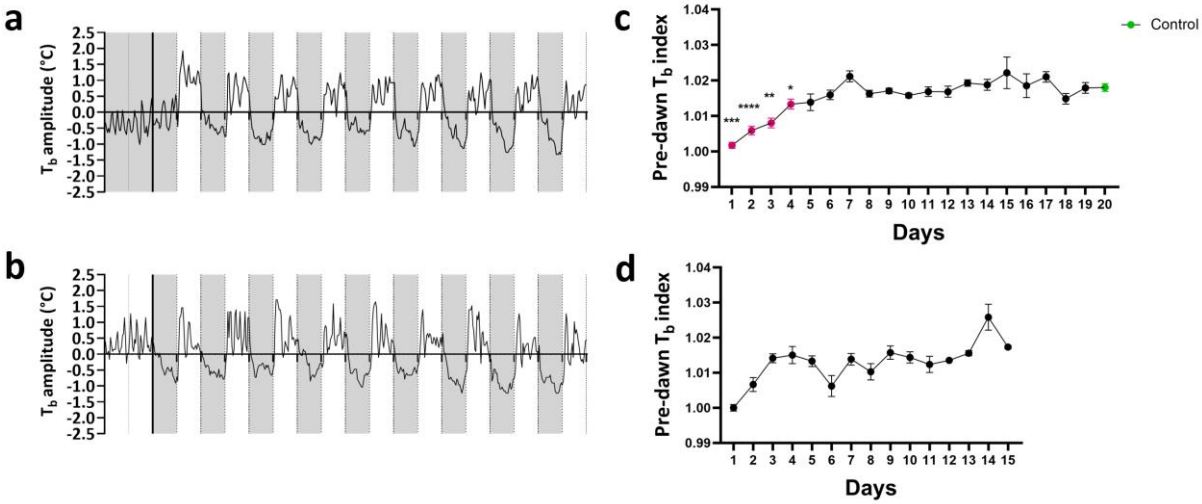

Figure 18 (a-b) T_b amplitude of a representative male bird (ID: 269-98) for 10 days. (a) Transition from DD to LD and (b) transition from LL to LD. Vertical dotted lines separate 12 hours. White background = lights on, grey background = lights off. (c) Pre-dawn T_b index indicating anticipation of light change, calculated for the last day under DD and all following days under LD for all seven birds (mean ± SEM). One-way ANOVA and a subsequent Dunnett's multiple comparisons test revealed a significant difference ($P < 0.05$) in anticipation of light change between the first four days and the last day. (d) Pre-dawn T_b index for the last day under LL and all following days under LD for the three birds that were transferred back to LD (mean ± SEM). Data did not pass a one-way ANOVA ($P > 0.05$). **Pre-dawn T_b index** = T_b mean for five hours before the lights changed divided by the T_b mean of the entire period (=24 h).

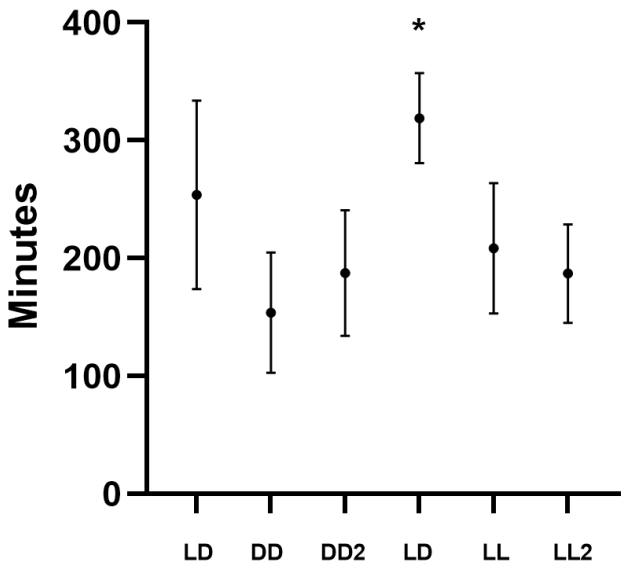

Figure 19 Comparison between ultradian periods for feeding activity for all seven experimental birds. Data is presented as the mean ± SD of seven periods (seven birds) for each light treatment. One-way ANOVA and a subsequent Turkey's multiple comparisons test revealed a significant difference ($P < 0.05$) between ultradian periods under the second LD treatment to ultradian periods under constant conditions, indicated by the asterisk.

3.2 Cell culture work

The *in vitro* experiments were designed to get insight into the dynamics of a molecular clock in Svalbard ptarmigan. Fibroblast cells show robust circadian rhythms in clock gene transcription in laboratory rodents (Balsalobre et al., 2000a, Welsh et al., 2004) and were therefore chosen as a model to study the molecular clock in ptarmigan.

3.2.1 Transfections and bioluminescence recording

U2OS cells exhibit robust circadian rhythms in clock gene transcription (Baggs et al., 2009, Zhang et al., 2009) and were therefore chosen as a positive control for the protocol. Svalbard ptarmigan skin fibroblasts and U2OS cells were transfected with *Per2* and *Bmal1* luciferase promoter reporters and real-time bioluminescence was recorded to examine the characteristics of a molecular clock in Svalbard ptarmigan. We first tested transfection efficiency using pYEFP-Mito and Actin-GFP reporter plasmids. A combination of 2 µl TransIT®-LT1 Transfection Reagent and 200 ng DNA (in a 200 µl volume) lead to sufficient transfection results to carry on with subsequent experiments (**Figure 20**). We first tested our protocol by transfecting rhythmic U2OS cells with *Per2* and *Bmal1* luciferase promoter reporters (**Figure 21***a*, **Appendix F**). Cells were synchronized with 50% FBS for one hour, and real-time light

emission (bioluminescence) was measured for several days. Quantification of the reporter luminescence revealed oscillations with an average period of 21.25 ± 1.02 hours in *Per2* and *Bmal1* transcription in U2OS cells and data was smooth (**Figure 21***a,c*). As expected, oscillations of these two genes were in antiphase to each other (11.08 hours difference between phases) (**Figure 21***e*).

The same procedure was performed for ptarmigan fibroblasts to test for a rhythm in clock gene transcription in these cells (**Figure 21***b,d,* **Appendix G**). Transfection efficiency was high, as judged by strong luciferase signals. Circadian oscillations were observed in *Per2* and *Bmal1* transcription with an average period of 22.28 ± 1.47 hours in ptarmigan fibroblasts, but data was rather jagged and oscillations did not dampen (**Figure 21***b,d*). The oscillations of the two genes were almost in phase (0.04 hours difference between phases) (**Figure 21***e*).

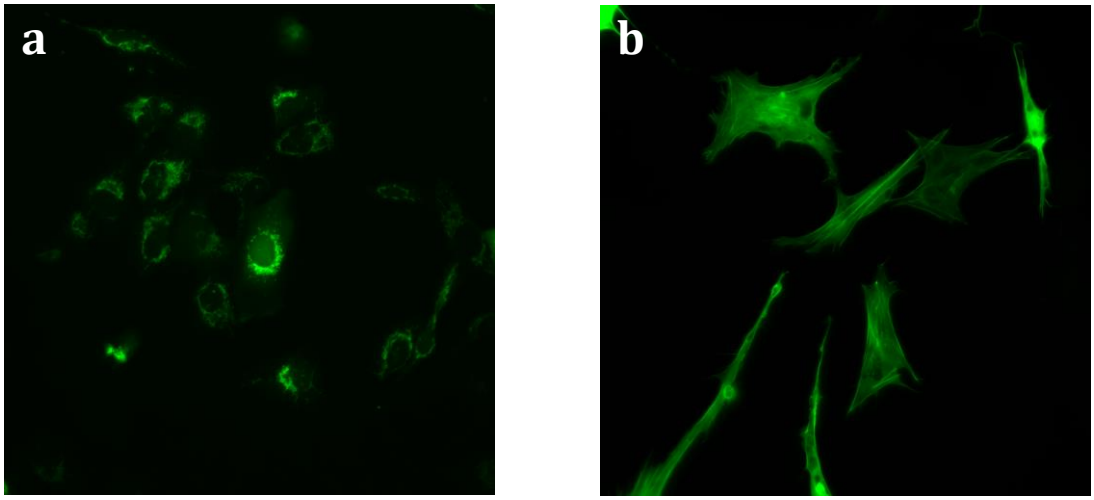

Figure 20 Transfected cells as a result from transfection optimizations (a) U2OS cells transiently transfected with pYEFP-Mito and (b) Ptarmigan fibroblasts transiently transfected with Actin-GFP.

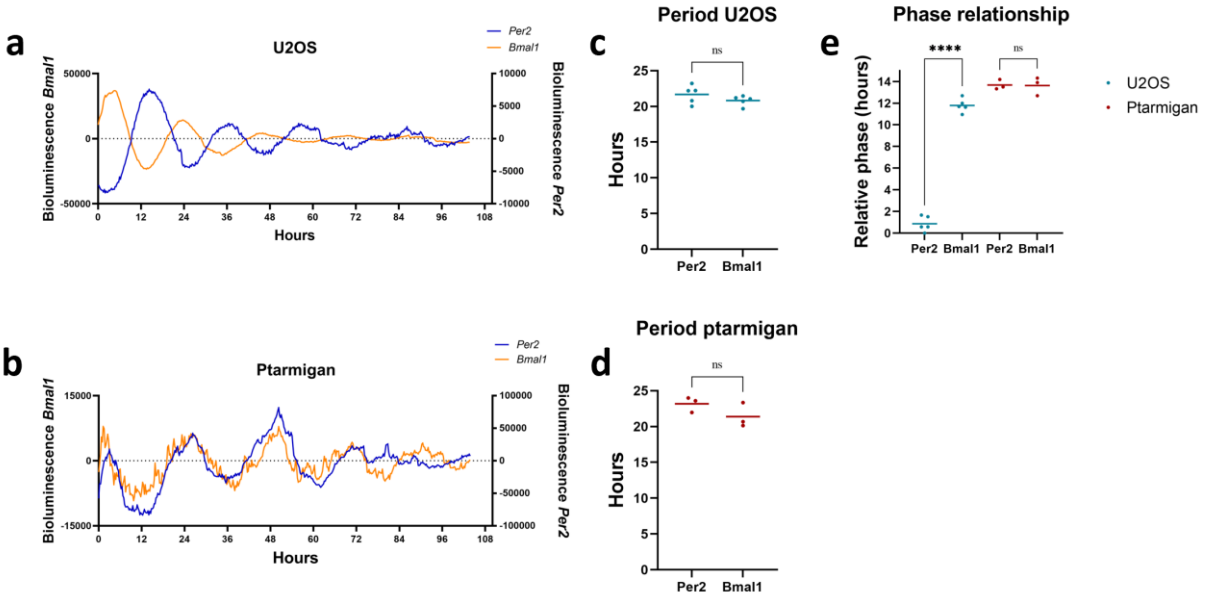

Figure 21 Molecular rhythms in U2OS cells and ptarmigan fibroblasts. U2OS cells and ptarmigan fibroblasts were transiently transfected with *Per2* and *Bmal1* luciferase reporters. Cells were synchronized with 50% FBS for one hour, then bioluminescence was recorded (photon counts per minute, one minute was measured every 15 minutes). (a) U2OS cells (baseline subtracted data), x = 0 = 12 hours after start of recording. (b) Ptarmigan fibroblasts (baseline subtracted data), x = 0 = 12 hours after start of recording. (c) *Per2* and *Bmal1* periods in U2OS cells. (d) *Per2* and *Bmal1* periods in ptarmigan fibroblasts. (e) Phase relationship between *Per2* and *Bmal1* in U2OS cells and ptarmigan fibroblasts. y = relative phase in hours starting from 12 hours after start of recording. The mean difference between *Per2* and *Bmal1* phases in U2OS cells was 11.08 hours compared to 0.04 hours in ptarmigan fibroblasts. Data is presented as the mean of replicates. Unpaired t tests were performed to test for differences between periods and differences between phases. Ns = not significant, **** = $P < 0.0001$.

3.2.2 Sequence validation of primers

Per2 and *Bmal1* luciferase reporters are mouse promotor reporters and may not reflect the activity of ptarmigan clock gene promoters. Therefore, an experiment using qPCRs was designed, as qPCRs are sensitive and highly specific to the genes of interest. To test the target specificity of the qPCR primers, primer pairs for the clock genes *Bmal1*, *Clock*, *Per2*, *Per3*, *Cry1*, *Cry2*, and the reference gene *Ppib* were cloned and sequence validated (**Figure 22 - 28**). The identity percentage between the PCR product and the ptarmigan genome was 100% for all genes, except for *Per3* with an identity percentage of 99.08%.

Bmal1

```
L.muta hyperborea_cloned        TTCATCCTAAAGACATTGCCAAAGTGAAGGAGCAGCTATCTTCTTCTGACACTGCACCAC  60
L.muta hyperborea_genome        TTCATCCTAAAGACATTGCCAAAGTGAAGGAGCAGCTATCTTCTTCTGACACTGCACCAC  60
                                ************************************************************

L.muta hyperborea_cloned        GAGAAAGGCTTATAGATGC  79
L.muta hyperborea_genome        GAGAAAGGCTTATAGATGC  79
                                ******************
```

Identity percentage: 100%

Figure 22 Identity percentage between the PCR product and the Svalbard ptarmigan genome in the clock gene *Bmal1*.

Clock

```
L.muta hyperborea_cloned        TGGAAAGATTTGATACCAGCCCCACACCTTCCGCTTCCTCCAGGAGTTCAAGAAAATCTT  60
L.muta hyperborea_genome        TGGAAAGATTTGATACCAGCCCCACACCTTCCGCTTCCTCCAGGAGTTCAAGAAAATCTT  60
                                ************************************************************

L.muta hyperborea_cloned        CACATACTGCAGTATCAGATCATTCGTC  88
L.muta hyperborea_genome        CACATACTGCAGTATCAGATCATTCGTC  88
                                ****************************
```

Identity percentage: 100%

Figure 23 Identity percentage between the PCR product and the Svalbard ptarmigan genome in the clock gene *Clock.*

Per2

```
L.muta hyperborea_cloned        AAATGGAACTTCTGGAATGGATCAGCCTTGGAAGAAAAGTGGGAAAAATAGGAAATCAAA  60
L.muta hyperborea_genome        AAATGGAACTTCTGGAATGGATCAGCCTTGGAAGAAAAGTGGGAAAAATAGGAAATCAAA  60
                                ************************************************************

L.muta hyperborea_cloned        ACGCATTAAACCACAGGAATCT  82
L.muta hyperborea_genome        ACGCATTAAACCACAGGAATCT  82
                                **********************
```

Identity percentage: 100%

Figure 24 Identity percentage between the PCR product and the Svalbard ptarmigan genome in the clock gene *Per2.*

Per3

```
L.muta hyperborea_cloned        AATGGAAATTGTGCAGAGGAAACACCAGAACCAGTGACTTTGCAGCAGATGTGTGCAGAT  60
L.muta hyperborea_genome        AATGGAAATTGTGCAGAGGAAACACCAGAACCAGTGACTTTGCAGCAGGTGTGTGCAGAT  60
                                ********************************************** ***********

L.muta hyperborea_cloned        GTCAACCGGATAAAGAATCTGGGACAGCAGCTGTATATTGCATCAAGGA  109
L.muta hyperborea_genome        GTCAACCGGATAAAGAATCTGGGACAGCAGCTGTATATTGCATCAAGGA  109
                                ************************************************
```

Identity percentage: 99.08%

Figure 25 Identity percentage between the PCR product and the Svalbard ptarmigan genome in the clock gene *Per3.*

Cry1

```
L.muta hyperborea_cloned        CGTTTGTTTGTTATTCGTGGACAGCCAGCAGATGTTTTCCCCAGGCTTTTTAAGGAATGG  60
L.muta hyperborea_genome        CGTTTGTTTGTTATTCGTGGACAGCCAGCAGATGTTTTCCCCAGGCTTTTTAAGGAATGG  60
                                ************************************************************

L.muta hyperborea_cloned        AGCATTGCAAAACTCTCTATTGAATATGATTCTGAGCCATTTGGGAAGGAGAGAGATGCA  120
L.muta hyperborea_genome        AGCATTGCAAAACTCTCTATTGAATATGATTCTGAGCCATTTGGGAAGGAGAGAGATGCA  120
                                ************************************************************

L.muta hyperborea_cloned        GCAATTAAGAAGCTGGCTA  139
L.muta hyperborea_genome        GCAATTAAGAAGCTGGCTA  139
                                ******************
```

Identity percentage: 100%

Figure 26 Identity percentage between the PCR product and the Svalbard ptarmigan genome in the clock gene *Cry1*.

Cry2

```
L.muta hyperborea_cloned        GTTGCAAATTACGAAAGACCAAGGATGAACGCCAATTCGTTGCTGGCCAGCCCTACTGGA  60
L.muta hyperborea_genome        GTTGCAAATTACGAAAGACCAAGGATGAACGCCAATTCGTTGCTGGCCAGCCCTACTGGA  60
                                ************************************************************

L.muta hyperborea_cloned        CTCAGTCCCTACCTGCGTTTTGGCTGTTTGTCCTGCCGCTTATTTTACTACCGTCTCTGG  120
L.muta hyperborea_genome        CTCAGTCCCTACCTGCGTTTTGGCTGTTTGTCCTGCCGCTTATTTTACTACCGTCTCTGG  120
                                ************************************************************

L.muta hyperborea_cloned        GAGCTGTATAAGAAGGTGAAGC  142
L.muta hyperborea_genome        GAGCTGTATAAGAAGGTGAAGC  142
                                **********************
```

Identity percentage: 100%

Figure 27 Identity percentage between the PCR product and the Svalbard ptarmigan genome in the clock gene *Cry2*.

Ppib

```
L.muta hyperborea_cloned        CTGACGAGAACTTCAAGCTGAAGCATTACGGCCCCGGCTGGGTGAGCATGGCCAACGCCG  60
L.muta hyperborea_genome        CTGACGAGAACTTCAAGCTGAAGCATTACGGCCCCGGCTGGGTGAGCATGGCCAACGCCG  60
                                ************************************************************

L.muta hyperborea_cloned        GCAAGGACACCAACGGCTCCCAGTTCTTCATCACCA  96
L.muta hyperborea_genome        GCAAGGACACCAACGGCTCCCAGTTCTTCATCACCA  96
                                ********************************
```

Identity percentage: 100%

Figure 28 Identity percentage between the PCR product and the Svalbard ptarmigan genome in the reference gene *Ppib*.

3.2.3 Fibroblast stimulation experiment

Mammalian circadian clock gene expression can be synchronized in cultured cells by various signaling molecules (Balsalobre et al., 2000a, Balsalobre et al., 2000b). To test whether ptarmigan fibroblast clocks can be stimulated *in vitro*, ptarmigan fibroblasts were treated for one hour with different reagents: 50% FBS, dexamethasone, forskolin and melatonin. RNA was extracted from cells, converted to cDNA and qPCRs were performed (**Figure 29** and **Figure 30**). Significant differences were found between serum and its untreated control for the clock gene *Per2* ($P < 0.001$). Dexamethasone and forskolin revealed significant differences to their control (treated with DMSO) for the genes *Clock* ($P < 0.05$), *Per2* ($P < 0.01$ for dexamethasone and $P < 0.05$ for forskolin), *Per3* ($P < 0.05$) and for dexamethasone *Bmal1*($P < 0.05$).

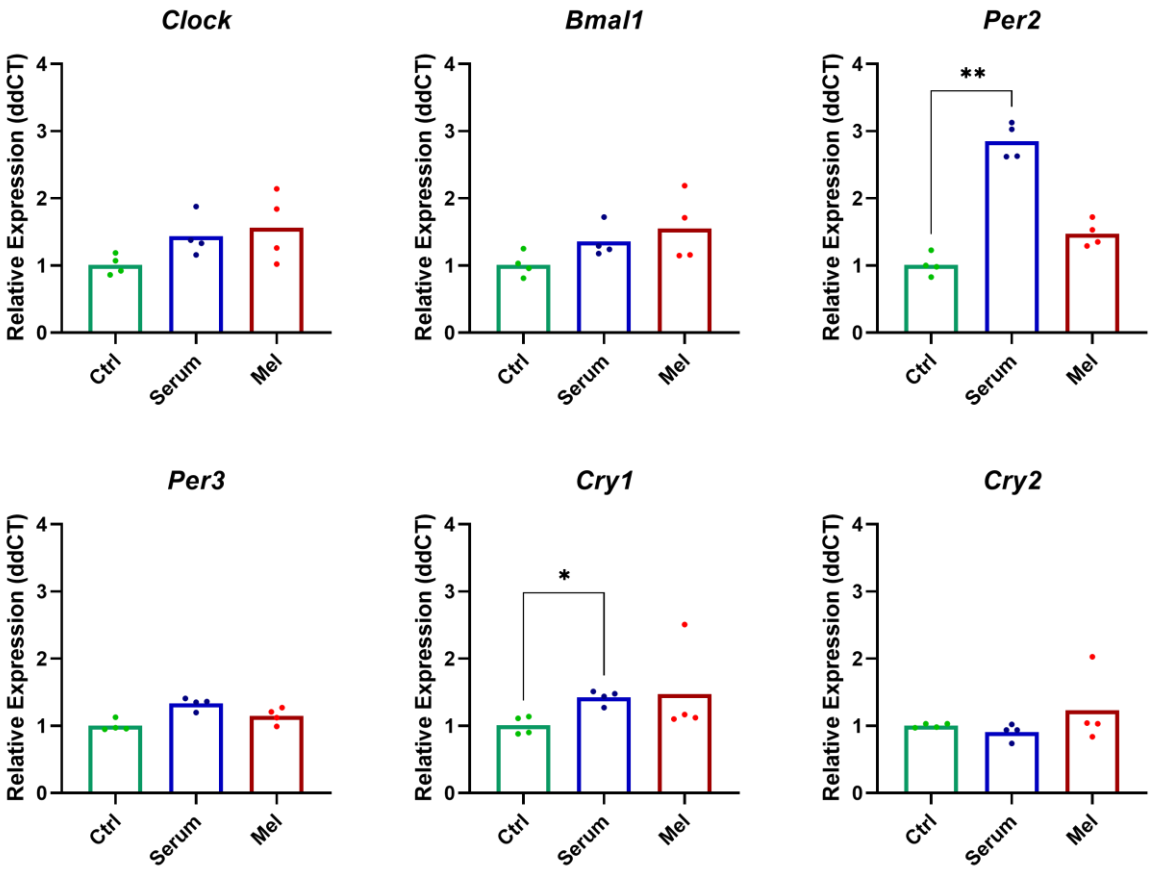

Figure 29 Relative expression of clock genes. Ptarmigan fibroblasts were stimulated for one hour with different reagents: 50% FBS and melatonin. RNA was extracted from cells, converted to cDNA and qPCRs were performed for each clock gene. Data was processed as described in the "Materials and methods" section and is presented as the mean of four replicates for each treatment. One way ANOVA and a subsequent Dunnett's multiple comparisons test were performed to test for differences between the treatments and an untreated control. * = $P < 0.05$, ** = $P < 0.01$

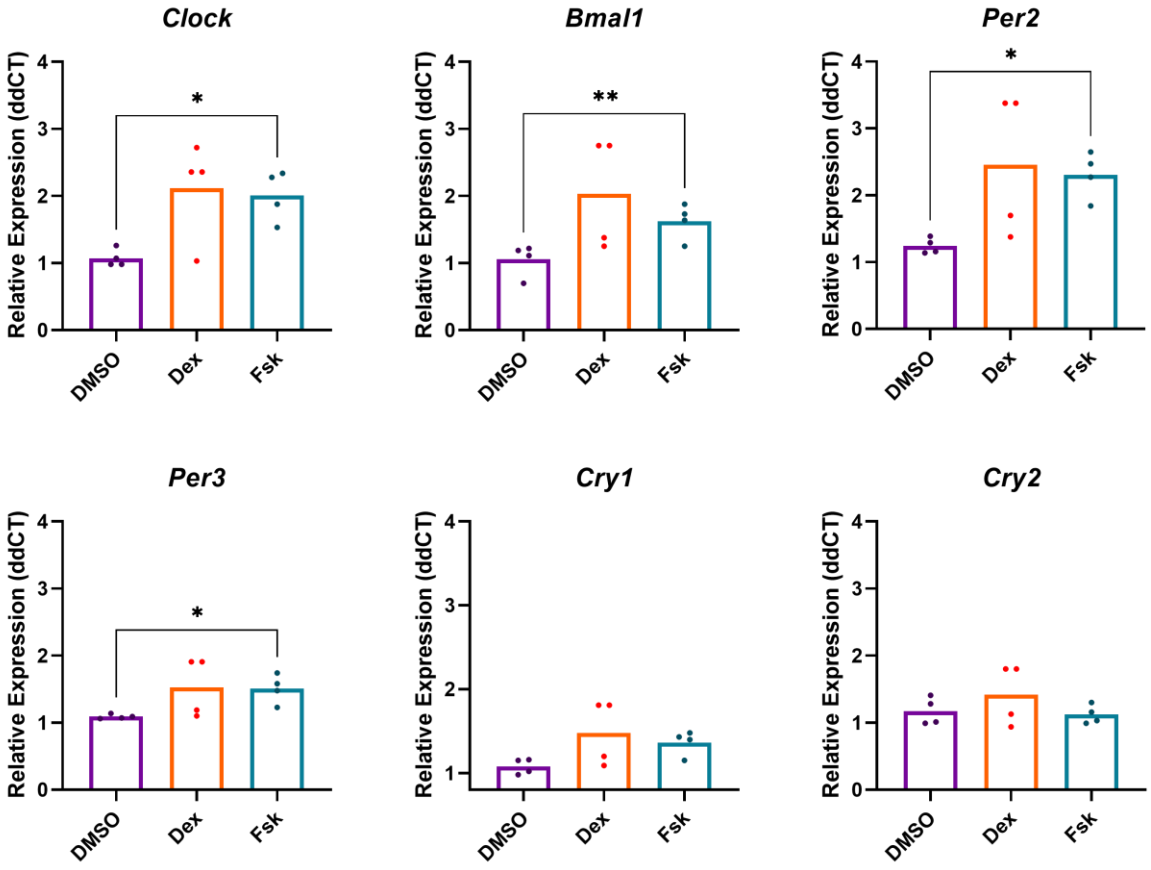

Figure 30 Relative expression of clock genes. Ptarmigan fibroblasts were stimulated for one hour with different reagents: dexamethasone and forskolin. RNA was extracted from cells, converted to cDNA and qPCRs were performed for each clock gene. Data was processed as described in the "Materials and methods" section and is presented as the mean of four replicates for each treatment. One way ANOVA and a subsequent Dunnett's multiple comparisons test were performed to test for differences between the treatments and a control treated with dimethyl sulfoxide (DMSO). * = $P < 0.05$, ** = $P < 0.01$

3.2.4 Circadian stimulation experiment

Having established that a serum shock stimulated ptarmigan *Per2* expression we tested for a rhythmic clock gene expression in ptarmigan skin fibroblasts. Ptarmigan fibroblasts were stimulated with 50% FBS for one hour, and cells were subsequently collected every four hours for 72 hours. RNA was extracted from cells, converted to cDNA and qPCRs were performed for the clock genes *Bmal1*, *Clock*, *Per2*, *Per3*, *Cry1*, *Cry2* and the reference gene *Ppib*. Relative expression of clock genes is shown in **Figure 31**. Strikingly, none of the genes showed a clear rhythm in expression and none of the genes passed a one-way ANOVA ($P > 0.05$).

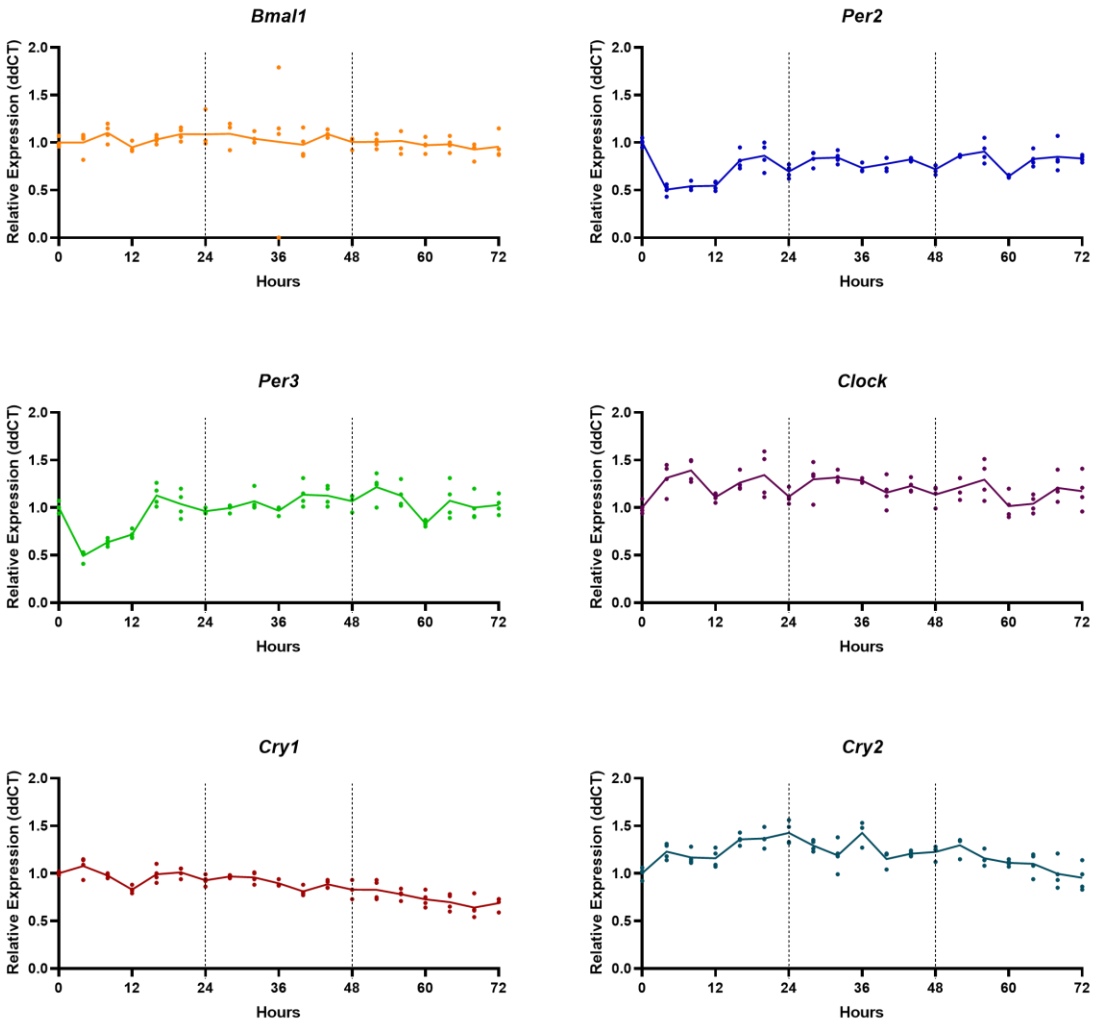

Figure 31 Relative expression of the clock genes *Bmal1*, *Clock*, *Per2*, *Per3*, *Cry1* and *Cry2* over 72 hours. Ptarmigan fibroblasts were treated with 50% FBS for one hour and subsequently collected every four hours. RNA was extracted, converted to cDNA and qPCRs were performed for each clock gene. Data was processed as described in the "Materials and methods" section and is presented as the mean of four replicates for each time point. None of the genes passed a one-way ANOVA.

3.2.5 Circadian temperature cycling experiments

It has been shown that circadian gene expression can be synchronized by simulated body temperature cycles with daily differences of 3 °C and 1 °C in mice and human fibroblast cultures (Saini et al., 2012). We first transfected rhythmic U2OS cells with *Per2* and *Bmal1* luciferase reporters and kept them at temperatures cycling between 36 °C and 39 °C, while real-time bioluminescence was recorded for several cycles. To test whether cultured ptarmigan fibroblasts can be stimulated by simulated body temperature cycles, the same procedure was performed for ptarmigan fibroblasts at temperatures cycling between 39 °C and 42 °C (average

body temperature taken from experimental birds = 40.5 °C). Each temperature cycle lasted for 24 hours.

U2OS data was messy and luciferase signals were rather weak (**Figure 32***a*, **Appendix H**). *Per2* transcription showed damped oscillations and transcription was high when temperatures were high, and *Bmal1* transcription did not show clear oscillations for most dishes with cells. However, ptarmigan data was smooth and showed high luciferase signals (**Figure 32***b*, **Appendix I**). Transcription of *Per2* and *Bmal1* was nearly in phase (1.83 hours difference between phases), and *Per2* transcription was strikingly negatively correlated to temperatures.

To go into further detail a second experiment was performed. Ptarmigan fibroblast cultures were kept at temperatures cycling between 36 °C and 39 °C for four cycles, then the temperature was continuously kept at 39 °C. Cells were collected every four hours starting at the second half of the fourth temperature cycle. RNA was extracted from cells, converted to cDNA and qPCRs were performed for all clock genes and the reference gene *Ppib*. *Per2*, *Per3*, *Bmal1*, *Cry1* and *Clock* showed damped oscillations which were in phase, but no response to cycling temperatures was observed in and *Cry2* (**Figure 33**).

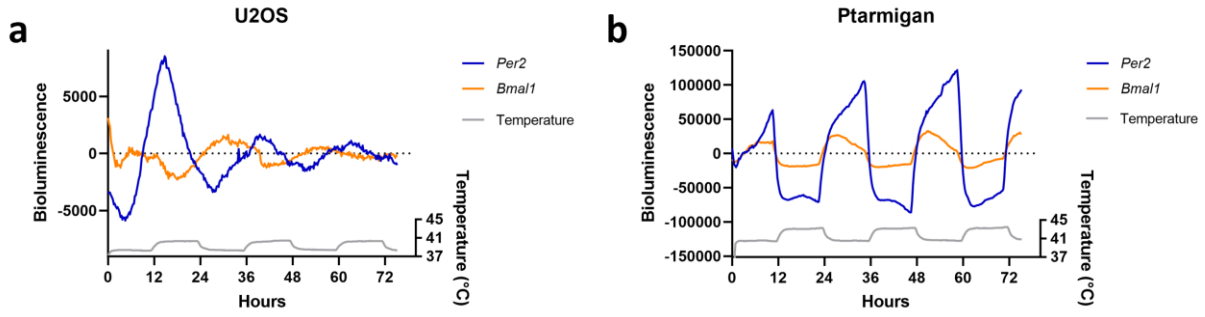

Figure 32 Clock gene transcription under simulated body temperature cycles. U2OS cells and ptarmigan fibroblasts were transiently transfected with *Per2* and *Bmal1* luciferase reporters and kept at cycling temperatures while real-time bioluminescence was measured (photon counts per minute, one minute was measured every 15 minutes). (a) U2OS cells (baseline subtracted data), x = 0 = 12 hours after start of recording. (b) Ptarmigan fibroblasts (baseline subtracted data), x = 0 = 12 hours after start of recording.

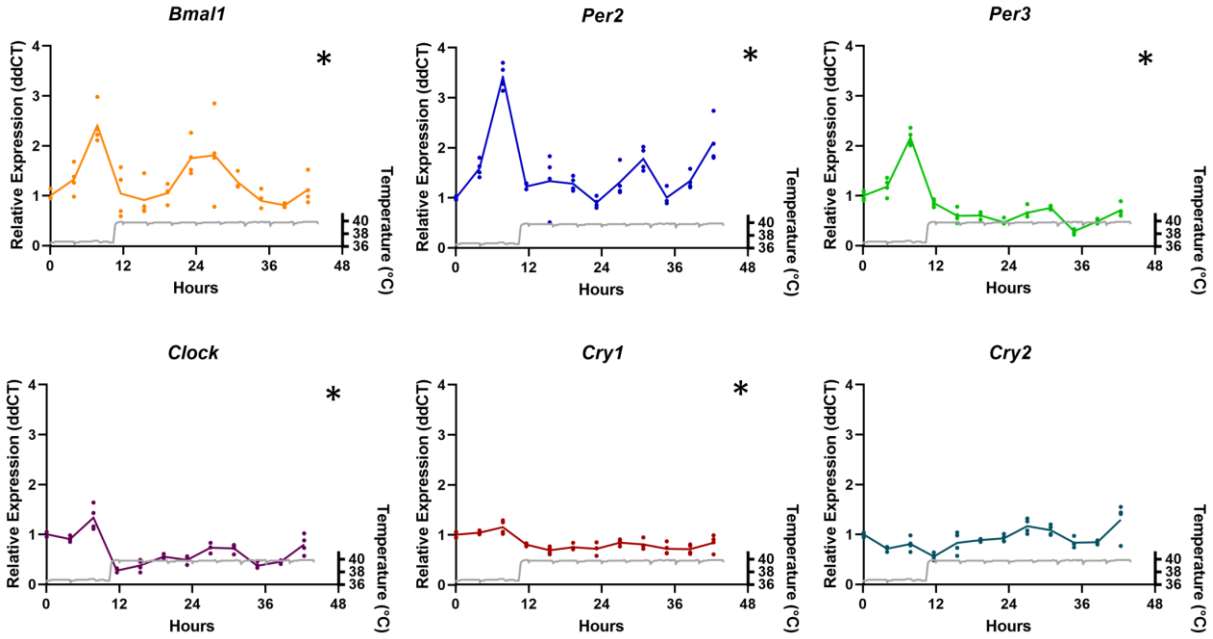

Figure 33 Clock gene expression after exposure to temperature cycles. Ptarmigan fibroblast cultures were kept at temperatures cycling between 36 °C and 39 °C for four cycles (each cycle lasting 24 hours), then the temperature was continuously kept at 39 °C. Cells were collected every four hours starting at the second half of the fourth temperature cycle. RNA was extracted from cells, converted to cDNA and qPCRs were performed. Data was processed as described in the "Materials and methods" section and is presented as the mean of four replicates (for each gene) for each time point. JTK_Cycle was used to identify rhythms in gene expression. * = $P < 0.01$.

4 Discussion

4.1.1 Changes in activity and body temperature after the transition from a rhythmic light-dark environment to constant conditions

Under natural light conditions Svalbard ptarmigan show daily behavioral rhythmicity under rhythmic light-dark cycles, but no daily rhythmicity during the polar day, and no or little daily rhythmicity during the polar night (Reierth and Stokkan, 1998a). Similarly, in a simulated natural light-dark environment, daily rhythms in T_b were observed under rhythmic light-dark conditions where T_b rose in anticipation of lights on, but rhythms disappeared under DD and LL (Appenroth et al., 2021a). These findings suggest that Svalbard ptarmigan use a circadian system to control T_b under LD, but this system appears to weaken under DD and LL (Appenroth et al., 2021a). In this study, Svalbard ptarmigan were exposed to controlled light conditions and sudden transitions from environmental light-dark cycles to constant conditions to study activity and T_b after controlled transitions from LD to constant conditions.

Consistent with previous observations, all birds in this study showed clear circadian rhythmicity in both activity and T_b with diurnal activity patterns under LD. T_b was high during the light-phase and low during the dark-phase, as would be expected since T_b is usually high during the active phase and low during the rest phase (Heldmaier et al., 1989, Refinetti and Menaker, 1992).The observed morning and evening bouts in feeding activity have also been described in the past (Reierth and Stokkan, 1998a, Reierth and Stokkan, 1998b). Morning and evening bouts of activity have been reported in other bird species as well, such as greenfinches (*Chloris chloris*) chaffinches (*Fringilla coelebs*) and bramblings (*Fringilla montifringilla*) (Aschoff and Meyer‐Lohmann, 1955, Aschoff, 1966). They are suggested to be controlled by two separate oscillators with different responses to light (Daan and Aschoff, 1975, Daan and Pittendrigh, 1976).

After the birds were transferred from LD to DD/LL Lomb-Scargle actograms revealed different phenotypes with weak but statistically significant circadian peaks in several cases, both for locomotor and feeding activity. These could possibly be a result of husbandry, where birds might have used visits as clues to keep track of time, although visits were done at different times of the day to avoid possible entrainment by disturbances. However, circadian peaks might have been caused by an endogenous timekeeping system that weakens rapidly but is still present after an abrupt change in illumination. After prolonged exposure to constant light birds became

more active. Increasing daylength in spring time stimulates gonadal growth in Svalbard ptarmigan, and higher activity under LL most probably reflects an increased desire to breed as a response to prolonged light exposure (Sharp, 1996).

Rhythms in T_b persisted for several days in all birds after an abrupt transfer to from LD to DD. Appenroth et al. (2021) suggested a circadian system to be in control of T_b under LD that weakens under constant conditions. In this case it may be assumed that the circadian system might need several cycles to weaken after a sudden change in light conditions. During the second part (last 10 days) under DD, periodograms showed weak but significant circadian rhythms in T_b in two birds, the other birds lost their rhythm completely. This corresponds with the disappearing rhythms in T_b under prolonged DD/LL observed by Appenroth et al. (2021). In this study, rhythms in T_b persisted for a significantly shorter time under LL than under DD. This might be due to negative masking, meaning that the birds responded directly to the change in light conditions rather than to a circadian system.

4.1.2 Changes in body temperature in anticipation of light onset

Under simulated natural light conditions T_b in Svalbard ptarmigan has been observed to rise in anticipation of lights-on under LD (Appenroth et al., 2021a). In this study, anticipation of light onset by the means of a rise in T_b was calculated for all seven birds after they were abruptly transferred from DD back to LD. Calculated anticipation for the first four days under LD was significantly different to the last day under LD. This suggests that birds needed approximately four days to entrain to an environmental light-dark cycle. No significant difference in anticipation of light change between days were found after a sudden transition from LL to LD. However, the sample size of this group was smaller (three birds only), and similar results of a larger group of birds would certainly be more convincing. The fact that the birds were able to anticipate the onset of light not long after a sudden change from DD to LD supports the hypothesis that T_b in Svalbard ptarmigan is controlled by an endogenous time-measuring system in a rhythmic light-dark environment.

4.1.3 Ultradian rhythmicity

In this study a sustained ultradian rhythmicity in locomotor and feeding activity was observed during the entire period of recording. Ultradian rhythms in Svalbard ptarmigan have been observed in the past in feeding activity under constant light (Reierth and Stokkan, 1998a), and in locomotor activity especially under LL (Appenroth et al., 2021a). Ultradian rhythms in activity have also been shown in other bird species such as Japanese quail (Guzmán et al.,

2017). The presence of ultradian rhythms in both locomotor and feeding activity in this study suggests ultradian patterns in the interplay of foraging and rest. In their natural habitat, Svalbard ptarmigan experience short summers and the time for growth and reproduction is limited. Ultradian rhythms in activity give Svalbard ptarmigan the opportunity to take advantage of the polar day by several alternating periods of foraging and rest around the clock.

Significant ultradian rhythmicity in locomotor activity has also been shown in both Svalbard reindeer and Norwegian reindeer (van Oort et al., 2007). The frequency of ultradian cycles increased from winter to summer and is thought to be due to a seasonal increase in appetite and quality of forage. In this study, the birds showed no significant increase in frequency of ultradian cycles under LL compared to DD, however, ultradian periods of feeding activity were significantly longer under LD than under DD/LL. The ultradian component hence seems to gain importance when the circadian component is weak. However, we do not know if ultradian rhythms in Svalbard ptarmigan are driven by hunger and satiety or underly an endogenous timing mechanism.

The common vole (*Microtus arvalis*) exhibits a highly robust ultradian behavior that is suggested to be a result of evolutionary pressure, as synchronous foraging reduces the likelihood of being preyed on by kestrels (Daan and Slopsema, 1978). The circadian system is not required for the expression of rhythmic ultradian behavior in voles, as ultradian rhythms persisted after lesioning the SCN (Gerkema et al., 1990). Furthermore, energy depletion or sleep debt do not seem to be the driving force behind the ultradian rhythms in voles, as ultradian behavior in locomotor activity was not substantially affected by deprivation of food, water or sleep (Daan and Slopsema, 1978, Gerkema and van der Leest, 1991). These findings suggest an endogenous self-sustained oscillator to drive ultradian rhythms in voles (Bourguignon and Storch, 2017). Recent findings suggest that ultradian rhythms in locomotor activity may rely on an oscillator based on dopamine, called dopaminergic ultradian oscillator (DUO). Dopamine is a neurotransmitter considered to be one of the key elements in promotion of wakefulness (Brown et al., 2012). Extracellular dopamine levels have been shown to fluctuate in synchrony with ultradian rhythms in locomotor activity in the striatum of *Bmal1* deficient mice under DD (Blum et al., 2014). Moreover, disruption of the dopamine transporter gene lengthened the period of locomotor activity rhythms in mice. Dopamine neurons are suggested to play a central role in the generation of ultradian rhythmicity (Bourguignon and Storch, 2017), however, it remains unclear if the rhythmicity is cell autonomous.

In this study ultradian feeding bouts were more concentrated under DD than under LD/LL. Tyler et al. (2016) suggested a mechanism independent of the circadian system that times activity, regarding food and safety in ruminants. Ruminants are more prone to attack by nocturnal predators and less able to detect predators during dark (Kie, 1999). Therefore, they time their active phase as much as possible during light. Activity in reindeer was observed to increasingly shift into twilight with decreasing daylight in winter, and to withdraw from twilight with increasing daylength towards summer (Tyler et al., 2016). Animals hence increased their tolerance of risk when their energy demands were not satisfied by feeding during daylight under short days and avoided risk in summer when plenty of daylight did not limit feeding opportunities. The same behavior has been observed in Svalbard ptarmigan (Reierth and Stokkan, 1998a) and several species of non-boreal songbirds and small mammals when exposed to photoperiods of high latitudes in captivity (Daan and Aschoff, 1975). The concentrated feeding bouts under DD in this study may be because ptarmigan perceive darkness as risk, and they may rather feed a bit longer when already having risked exposure to possible danger instead of constantly feeding a bit.

4.1.4 Are ptarmigan skin fibroblasts rhythmic?

4.1.4.1 Stimulation and bioluminescence recordings

U2OS cells would be expected to show clear daily oscillations in clock gene transcription (Baggs et al., 2009, Zhang et al., 2009), and this was also observed in this study. As expected, *Per2* and *Bmal1* expression cycled in antiphase to each other, and the data provides a reasonable positive control for the ptarmigan data.

Real-time bioluminescence recordings revealed daily oscillations in ptarmigan fibroblast clock gene transcription after stimulation. However, transcription of *Per2* and *Bmal1* would be expected to cycle in antiphase (Saini et al., 2012) but instead cycled in phase. Furthermore, oscillations did not dampen as would be expected in clock genes. Temperatures in the incubator where cell cultures were maintained and in the photon detection unit were measured (**Figure 34**) and data revealed small temperature fluctuations occurring with daily regularity in the photon detection unit (**Figure 34***b*). It may be that the promotor reporters we used are very

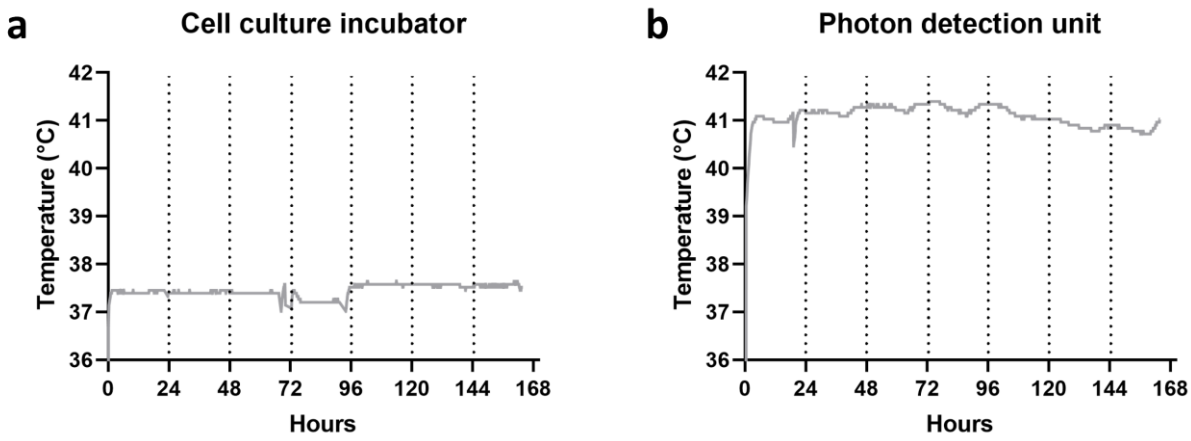

Figure 34 Temperature measurements by an iButton. (a) Temperatures in the cell culture incubator where cell cultures were maintained. (b) Temperatures in the photon detection unit.

sensitive to temperatures and oscillations may have been caused by the observed temperature fluctuations rather than by an endogenous timing mechanism.

Similar experiments have been done in the past with reindeer fibroblasts (Lu et al., 2010). Real-time bioluminescence recordings of *Per2* and *Bmal1* transcription in reindeer showed no significant oscillations. Reindeer and Svalbard ptarmigan show similar activity patterns under natural light conditions of high latitudes, however, under controlled light conditions Svalbard ptarmigan do show indications of a circadian system that weakens in the absence of an external light-dark cycle. It needs to be clarified in the future whether the observed oscillations in ptarmigan *Per2* and *Bmal1* transcription were caused by the measured temperature fluctuations to make more detailed statements about the circadian system in Svalbard ptarmigan.

4.1.4.2 Stimulation and qPCR

Gene expression was rather flat for all genes (*Bmal1, Clock, Per2, Per3, Cry1* and *Cry2*), and none of the genes passed a one-way ANOVA, which strongly indicates the absence of a molecular rhythm. This is consistent with the luciferase assays, if the assumption that oscillations were caused by temperature fluctuations is true. A weak transient response to stimulation was present, which was already seen when stimulating clock genes with different reagents earlier in this study. Strangely, *Per2* and *Per3* expression decreased immediately after stimulation. The luciferase assays suggest that the cells are very temperature sensitive, and the decrease in gene expression might reflect a perceived increase in temperature after cells were out of the incubator for a few minutes while the cell culture media was changed. Future careful testing would be needed to resolve this question.

4.1.4.3 Clock gene expression under simulated body temperature cycles

U2OS *Per2* and *Bmal1* data acquired under simulated body temperature cycles was messy. *Per2* transcription showed damped oscillations, and *Bmal1* transcription did not show clear oscillations for most dishes with cells. Additionally, luciferase signals were tenfold weaker than signals measured for ptarmigan fibroblasts. This can probably be attributed to transfection difficulties. In contrast to previous observations, where *Per2* expression was high when temperatures were low (Kaneko et al., 2020), *Per2* transcription was high when temperatures were high. Kaneko et al. (2020) started sampling after U2OS cells had been exposed to cycling temperatures for five days, while in this study we started the bioluminescence recording right after U2OS cells were exposed to temperature cycles. Thus, U2OS cells in this study might not have been given enough time to entrain to the temperature cycles. Moreover, as data was messy it is difficult to make concrete conclusions.

The pattern of *Per2* transcription in ptarmigan fibroblasts nearly mirrored the pattern of temperature cycles at which cells were kept, and the amplitude of the oscillations increased with passing days, indicating a strong response to cycling temperatures. As already observed for ptarmigan fibroblasts in the stimulation experiment transcription of *Per2* and *Bmal1* cycled in phase, indicating a response to temperatures rather than a response to a molecular clock.

Ptarmigan fibroblasts kept at cycling temperatures for four days and collected during the transfer to constant temperatures showed different responses for different clock genes. *Per2*, *Per3*, *Bmal1* and *Clock* showed a damped oscillation in gene expression, which is likely a response to temperature cycles that immediately damped after a transfer to constant temperatures. The qPCR showed that gene expression was in phase, which agrees with the luciferase assays. However, a dampening rhythm may be evidence of a dampening oscillator, which suggests that the clock is interacting in some respect. Interestingly, once in constant conditions the peaks of *Bmal1* and *Per2*/*Per3* were separated, which hints at a return to more expected dynamics where *Bmal1* and *Per2*/*Per3* cycle in antiphase.

By performing qPCRs, we measured expression of clock genes while by recording bioluminescence we measured transcription of clock genes, hence there may be small differences between the experiments. Furthermore, the luciferase reporters we used are mouse promotor reporters, which may not reflect the activity of ptarmigan clock gene promoters, while qPCRs are highly specific to the genes of interest. *Cry2* did not respond to cycling temperatures, indicating a lower level of temperature sensitivity. The data also suggests that *Cry2* expression is not driven by BMAL1:CLOCK, which is unexpected. However, the data was not

convincingly clear, and the experiment will have to be repeated to make a stronger statement. Moreover, due to compromises with a study on a different species carried out simultaneously, the experiment was performed at temperatures lower than the physiological temperatures of ptarmigan (temperatures in the incubator cycled between 36.5 °C and 39.5 °C, while average T_b in birds in this study was approximately 40.5 °C). However, ptarmigan fibroblasts were growing well when maintained at 37 °C, and qPCR data overall agrees with the luciferase assays, suggesting that temperatures were not a major problem. Nevertheless, we recommend repeating the experiment in the future with physiological temperatures of ptarmigan.

Appenroth et al. (2021) assessed the transcriptional regulation of *Cry1* and *Per2* within the MBH and PT in Svalbard ptarmigan *in vivo* and showed that both genes were rhythmic under LD and within the first 24 hours after a transfer to LL (Appenroth et al., 2021b). The mammalian SCN is protected against sensitivity to body temperature entrainment, which may possibly be the case in other regions of the brain as well, such as the MBH and PT. We need to bear in mind that here we examined one specific tissue, and that the fibroblast clockwork we investigated in is not necessarily an indicator for the entire animal.

4.1.4.4 Looking at individual cells

Clock genes in cultured cells are thought to either be stimulated to cycle in expression by a serum shock, or they may already cycle but are out of phase with one another. In this case a serum shock would synchronize gene expression (**Figure 35**).

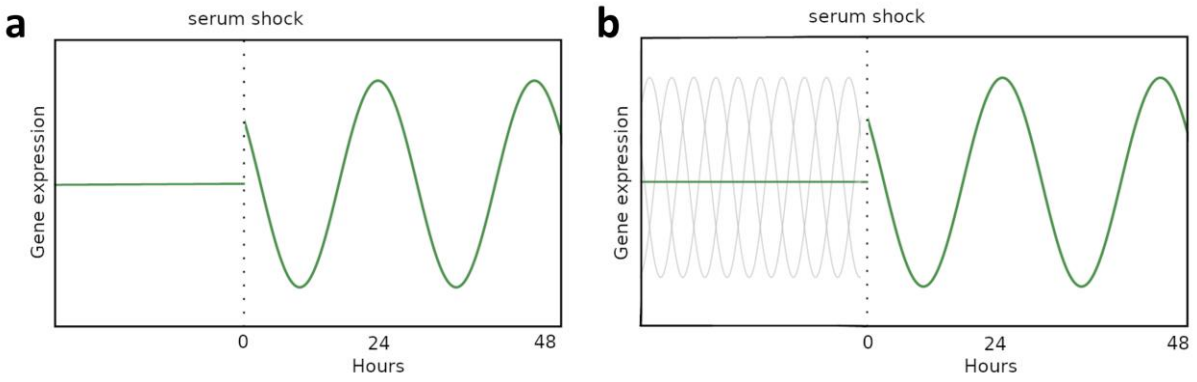

Figure 35 Two possible effects of a serum shock on clock gene expression in cultured cells. (a) Individual cells are not rhythmic, and a serum shock stimulates clock genes to cycle in expression. (b) Individual cells are rhythmic but out of phase with one another, hence gene expression seems flat. A serum shock synchronizes the cells to cycle in phase.

In this study, results were obtained from many thousand cells, and we do not know whether cells were stimulated or synchronized. It would therefore be a useful approach for the future to look at gene expression in individual cells. An attempt was made in this study to use a fluorescence-based method to monitor gene expression in single cells. As a positive control, U2OS cells were transfected with a fluorescent reporter of *Cry1* transcription, AAV-P(Cry1)-forward-intron336-Venus-NLS-D2, and a series of images was taken of individual cells over 72 hours. Due to limited time towards the end of this project as well as technical difficulties, such as low transfection efficiency and cells moving out of focus while a series of images over extended time periods were taken (**Figure 36**), the experiment was discontinued. The experimental design of this experiment needs to be improved in the future to obtain data from individual cells. In this regard, we intended to transfect cells with biosensors for H_2O_2, ATP:ADP ratio and NADH:NAD^+ ratio. Cycles in metabolism as an output of the circadian clock cause cycles in H_2O_2 abundance and cycling changes in ATP:ADP and NADH:NAD^+ ratios. Using these biosensors allows to study the output of a molecular clock and compare it to findings about the clock itself.

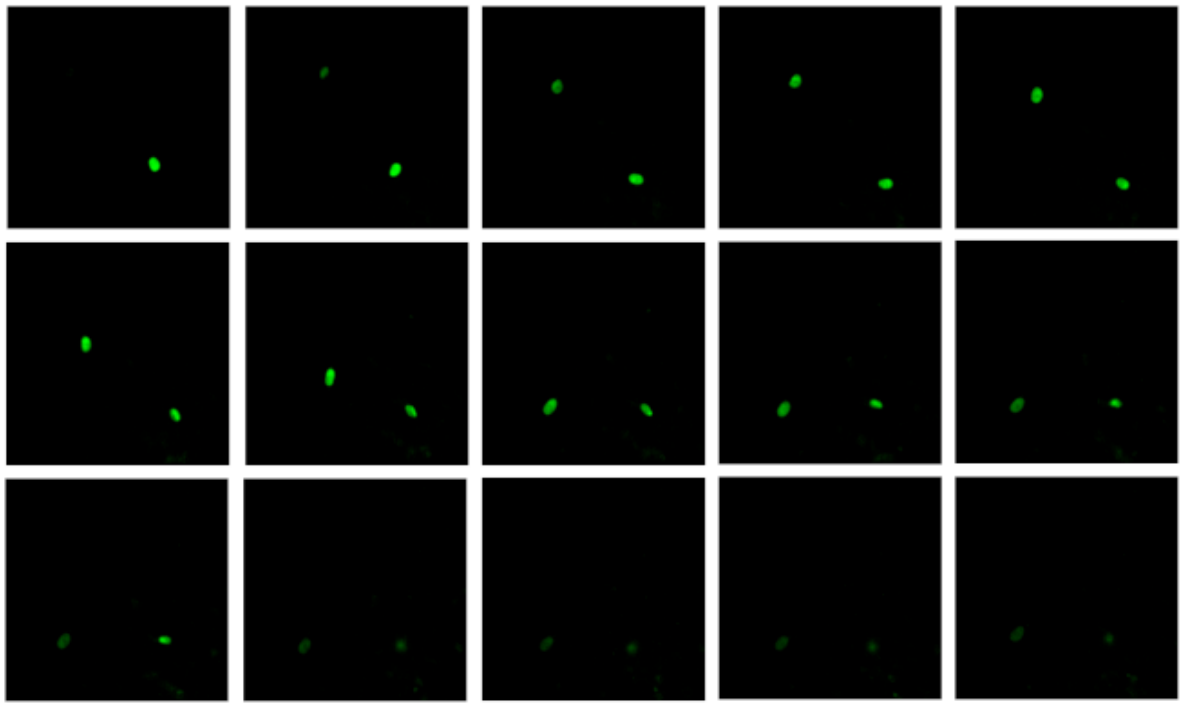

Figure 36 U2OS cells transiently transfected with a fluorescent reporter of *Cry1* transcription (AAV-P(Cry1)-forward-intron336-Venus-NLS-D2). One image was taken every hour over a period of 72 hours with the live cell imaging system Celldiscoverer 7 (Zeiss). This figure shows a series of images with four hours differences between each image, from the start of the experiment (top left corner and sequentially from left to right) until cells went out of focus (bottom row).

4.1.5 Adaptive value of circadian clocks in the Arctic

Van Oort et al. (2005) states that maintaining a strong endogenous clock in a non-rhythmic environment is of little selective advantage for herbivores. Svalbard reindeer and Svalbard ptarmigan are both herbivores experiencing a non-rhythmic environment for most of the year, and both show very weak circadian behavior in the absence of a rhythmic light-dark environment. This unusual phenotype reflects a rather unusual selective pressure and may therefore be seen as an adaptation to life in the Arctic. However, sustained circadian behavior and physiology has been reported in several species inhabiting the Arctic, such as polar bears (*Ursus maritimus*) (Ware et al., 2020), Arctic ground squirrels (*Urocitellus parryii*) (Williams et al., 2012, Williams et al., 2017) and bumblebees (*Bombus terrestris* and *B. Pascuorum*) (Stelzer and Chittka, 2010). These differences in circadian output between species may be seen as a flexible solution to different evolutionary histories.

In Svalbard ptarmigan a circadian clock is maintained in tissues essential for seasonal timing and is thus suggested to be maintained for measuring photoperiod (Appenroth et al., 2021b), but behavioral output is suggested to be decoupled from a possibly functional molecular clockwork in other tissues. Looking at the molecular dynamics of the clock, our results suggest that a molecular clockwork is not functional in Svalbard ptarmigan in tissues not essential for seasonal timing.

4.1.6 Conclusion

We have shown that daily rhythms in locomotor and feeding activity in Svalbard ptarmigan immediately weakened after a sudden change of light conditions from LD to DD/LL, while rhythms in T_b persisted for at least 10 days in all experimental birds. From approximately four days after a change from DD to LD birds showed a rise in T_b in anticipation of light onset. These findings support the hypotheses that Svalbard ptarmigan are in little endogenous control of daily activity rhythms, and that T_b rhythms in Svalbard ptarmigan are under control of a circadian system that weakens under constant conditions. We have also shown that a sustained ultradian rhythmicity was present during the entire experimental design, with higher frequencies under constant lighting conditions than under light-dark cycles. Weak circadian rhythmicity in the absence of a rhythmic light-dark environment together with a higher frequency of ultradian rhythms suggest a greater importance of daily rhythms under LD and an increased importance of ultradian rhythms under DD and LL, which indicates a flexible system as an adaptation to an unusual environment. We have shown daily oscillations in *Per2* and

Bmal1 transcription in ptarmigan fibroblasts, and attribute these to a high sensitivity of clock components to small temperature fluctuations in birds. No self-sustained spontaneous rhythms in clock gene expression were found in ptarmigan fibroblasts, which indicates the absence of an endogenously driven molecular rhythm. The suggested sensitivity of avian clock components to temperature was reflected in a strong response of *Per2* and *Bmal1* transcription to simulated body temperature cycles. Taken together, our results support the hypothesis of a weak circadian system in Svalbard ptarmigan.

References

APPENROTH, D. 2016. *Core body temperature cycles in captive Svalbard rock ptarmigan (Lagopus muta hyperborea).* UiT Norges arktiske universitet.

APPENROTH, D., NORD, A., HAZLERIGG, D. G. & WAGNER, G. C. 2021a. Body Temperature and Activity Rhythms Under Different Photoperiods in High Arctic Svalbard ptarmigan (Lagopus muta hyperborea). *Frontiers in Physiology,* 12.

APPENROTH, D., WAGNER, G. C., HAZLERIGG, D. G. & WEST, A. C. 2020. Adaptive value of circadian rhythms in High Arctic Svalbard ptarmigan. *bioRxiv*.

APPENROTH, D., WAGNER, G. C., HAZLERIGG, D. G. & WEST, A. C. 2021b. Evidence for circadian-based photoperiodic timekeeping in Svalbard ptarmigan, the northernmost resident bird. *Current Biology*.

ASCHOFF, J. 1966. Circadian activity pattern with two peaks. *Ecology,* 47**,** 657-662.

ASCHOFF, J. & MEYER‐LOHMANN, J. 1955. Die Aktivität gekäfigter Grünfinken im 24‐Stunden‐Tag bei unterschiedlich langer Lichtzeit mit und ohne Dämmerung. *Zeitschrift für Tierpsychologie,* 12**,** 254-265.

BAGGS, J. E., PRICE, T. S., DITACCHIO, L., PANDA, S., FITZGERALD, G. A. & HOGENESCH, J. B. 2009. Network features of the mammalian circadian clock. *PLoS Biol,* 7**,** e1000052.

BALSALOBRE, A., BROWN, S. A., MARCACCI, L., TRONCHE, F., KELLENDONK, C., REICHARDT, H. M., SCHÜTZ, G. & SCHIBLER, U. 2000a. Resetting of circadian time in peripheral tissues by glucocorticoid signaling. *Science,* 289**,** 2344-2347.

BALSALOBRE, A., DAMIOLA, F. & SCHIBLER, U. 1998. A serum shock induces circadian gene expression in mammalian tissue culture cells. *Cell,* 93**,** 929-937.

BALSALOBRE, A., MARCACCI, L. & SCHIBLER, U. 2000b. Multiple signaling pathways elicit circadian gene expression in cultured Rat-1 fibroblasts. *Current Biology,* 10**,** 1291-1294.

BEAVER, L., GVAKHARIA, B., VOLLINTINE, T., HEGE, D., STANEWSKY, R. & GIEBULTOWICZ, J. 2002. Loss of circadian clock function decreases reproductive fitness in males of Drosophila melanogaster. *Proceedings of the National Academy of Sciences,* 99**,** 2134-2139.

BINKLEY, S., KLUTH, E. & MENAKER, M. 1971. Pineal function in sparrows: circadian rhythms and body temperature. *Science,* 174**,** 311-314.

BINKLEY, S., REILLY, K. B. & HRYSHCHYSHYN, M. 1980. N-acetyltransferase in the chick retina. *Journal of comparative physiology,* 139**,** 103-108.

BLUM, I. D., ZHU, L., MOQUIN, L., KOKOEVA, M. V., GRATTON, A., GIROS, B. & STORCH, K.-F. 2014. A highly tunable dopaminergic oscillator generates ultradian rhythms of behavioral arousal. *Elife,* 3**,** e05105.

BOURGUIGNON, C. & STORCH, K.-F. 2017. Control of rest: activity by a dopaminergic ultradian oscillator and the circadian clock. *Frontiers in neurology,* 8**,** 614.

BROWN, R. E., BASHEER, R., MCKENNA, J. T., STRECKER, R. E. & MCCARLEY, R. W. 2012. Control of sleep and wakefulness. *Physiological reviews*.

BROWN, S. A., ZUMBRUNN, G., FLEURY-OLELA, F., PREITNER, N. & SCHIBLER, U. 2002. Rhythms of mammalian body temperature can sustain peripheral circadian clocks. *Curr Biol,* 12**,** 1574-83.

BUHR, E. D., YOO, S. H. & TAKAHASHI, J. S. 2010. Temperature as a universal resetting cue for mammalian circadian oscillators. *Science,* 330**,** 379-85.

BÜNNING, E. Circadian rhythms and the time measurement in photoperiodism. Cold Spring Harbor Symposia on Quantitative Biology, 1960. Cold Spring Harbor Laboratory Press, 249-256.
CANTWELL, E. L. & CASSONE, V. M. 2002. Daily and circadian fluctuation in 2-deoxy [14C]-glucose uptake in circadian and visual system structures of the chick brain: effects of exogenous melatonin. *Brain research bulletin,* 57**,** 603-611.
CANTWELL, E. L. & CASSONE, V. M. 2006. Chicken suprachiasmatic nuclei: I. Efferent and afferent connections. *J Comp Neurol,* 496**,** 97-120.
CASSONE, V. M., BROOKS, D. S. & KELM, T. A. 1995. Comparative distribution of 2[125I]iodomelatonin binding in the brains of diurnal birds: outgroup analysis with turtles. *Brain Behav Evol,* 45**,** 241-56.
CASSONE, V. M. & MENAKER, M. 1984. Is the avian circadian system a neuroendocrine loop? *Journal of Experimental Zoology,* 232**,** 539-549.
CASSONE, V. M. & MOORE, R. Y. 1987. Retinohypothalamic projection and suprachiasmatic nucleus of the house sparrow, Passer domesticus. *J Comp Neurol,* 266**,** 171-82.
CUNINKOVA, L. & BROWN, S. 2008. Peripheral circadian oscillators: interesting mechanisms and powerful tools. *Annals of the New York Academy of Sciences,* 1129**,** 358-370.
DAAN, S. & ASCHOFF, J. 1975. Circadian rhythms of locomotor activity in captive birds and mammals: their variations with season and latitude. *Oecologia,* 18**,** 269-316.
DAAN, S. & PITTENDRIGH, C. S. 1976. A functional analysis of circadian pacemakers in nocturnal rodents. *Journal of comparative physiology,* 106**,** 267-290.
DAAN, S. & SLOPSEMA, S. 1978. Short-term rhythms in foraging behaviour of the common vole, Microtus arvalis. *Journal of comparative Physiology,* 127**,** 215-227.
DECOURSEY, P. J., KRULAS, J. R., MELE, G. & HOLLEY, D. C. 1997. Circadian performance of suprachiasmatic nuclei (SCN)-lesioned antelope ground squirrels in a desert enclosure. *Physiology & Behavior,* 62**,** 1099-1108.
DODD, A. N., SALATHIA, N., HALL, A., KÉVEI, E., TÓTH, R., NAGY, F., HIBBERD, J. M., MILLAR, A. J. & WEBB, A. A. 2005. Plant circadian clocks increase photosynthesis, growth, survival, and competitive advantage. *Science,* 309**,** 630-633.
DOLNIK, O. V., METZGER, B. J. & LOONEN, M. J. 2011. Keeping the clock set under the midnight sun: diurnal periodicity and synchrony of avian Isospora parasites cycle in the High Arctic. *Parasitology,* 138**,** 1077.
DU, N.-H. & BROWN, S. A. 2021. Measuring Circadian Rhythms in Human Cells. *In:* BROWN, S. A. (ed.) *Circadian Clocks: Methods and Protocols.* New York, NY: Springer US.
EBIHARA, S., ADACHI, A., HASEGAWA, M., NOGI, T., YOSHIMURA, T. & HIRUNAGI, K. 1997. In vivo microdialysis studies of pineal and ocular melatonin rhythms in birds. *Neurosignals,* 6**,** 233-240.
EBIHARA, S., UCHIYAMA, K. & OSHIMA, I. 1984. Circadian organization in the pigeon, Columba livia: the role of the pineal organ and the eye. *Journal of Comparative Physiology A,* 154**,** 59-69.
FOLLETT, B. K., MATTOCKS, P. & FARNER, D. S. 1974. Circadian function in the photoperiodic induction of gonadotropin secretion in the white-crowned sparrow, Zonotrichia leucophrys gambelii. *Proceedings of the National Academy of Sciences,* 71**,** 1666-1669.
GASTON, S. & MENAKER, M. 1968. Pineal function: the biological clock in the sparrow? *Science,* 160**,** 1125-1127.

GERKEMA, M. P., GROOS, G. A. & DAAN, S. 1990. Differential elimination of circadian and ultradian rhythmicity by hypothalamic lesions in the common vole, Microtus arvalis. *Journal of Biological Rhythms,* 5**,** 81-95.
GERKEMA, M. P. & VAN DER LEEST, F. 1991. Ongoing ultradian activity rhythms in the common vole, Microtus arvalis, during deprivations of food, water and rest. *Journal of Comparative Physiology A,* 168**,** 591-597.
GUZMÁN, D. A., FLESIA, A. G., AON, M. A., PELLEGRINI, S., MARIN, R. H. & KEMBRO, J. M. 2017. The fractal organization of ultradian rhythms in avian behavior. *Scientific reports,* 7**,** 1-13.
GWINNER, E. 1989. Melatonin in the circadian system of birds: model of internal resonance. *Circadian clocks and ecology*. Hokkaido Univ. Press.
GWINNER, E. & BRANDSTATTER, R. 2001. Complex bird clocks. *Philosophical Transactions of the Royal Society of London. Series B: Biological Sciences,* 356**,** 1801-1810.
HALBERG, F. 1960. Temporal coordination of physiologic function. *Cold Spring Harb Symp Quant Biol,* 25**,** 289-310.
HEIGL, S. & GWINNER, E. 1995. Synchronization of circadian rhythms of house sparrows by oral melatonin: effects of changing period. *Journal of biological rhythms,* 10**,** 225-233.
HELDMAIER, G., STEINLECHNER, S., RUF, T., WIESINGER, H. & KLINGENSPOR, M. 1989. Photoperiod and thermoregulation in vertebrates: body temperature rhythms and thermogenic acclimation. *Journal of biological rhythms,* 4**,** 139-153.
HELM, B. 2020. Clocks and Calendars in Birds. *Neuroendocrine Clocks and Calendars.* Springer.
HUGHES, M. E., HOGENESCH, J. B. & KORNACKER, K. 2010. JTK_CYCLE: an efficient nonparametric algorithm for detecting rhythmic components in genome-scale data sets. *Journal of biological rhythms,* 25**,** 372-380.
JANIK, D., DITTAMI, J. & GWINNER, E. 1992. The effect of pinealectomy on circadian plasma melatonin levels in house sparrows and European starlings. *Journal of biological rhythms,* 7**,** 277-286.
JUSS, R., DAVIES, I., FOLLET, B. & MASON, R. 1994. Circadian rhythm in neuronal discharge activity in the quail lateral hypothalamic retinorecipient nucleus (LHRN) recorded in vitro. *J. Physiol,* 475**,** 132.
KANEKO, H., KAITSUKA, T. & TOMIZAWA, K. 2020. Response to Stimulations Inducing Circadian Rhythm in Human Induced Pluripotent Stem Cells. *Cells,* 9**,** 620.
KIE, J. G. 1999. Optimal foraging and risk of predation: effects on behavior and social structure in ungulates. *Journal of Mammalogy,* 80**,** 1114-1129.
KOHSAKA, A. & BASS, J. 2007. A sense of time: how molecular clocks organize metabolism. *Trends in Endocrinology & Metabolism,* 18**,** 4-11.
KONDRATOV, R. V., KONDRATOVA, A. A., GORBACHEVA, V. Y., VYKHOVANETS, O. V. & ANTOCH, M. P. 2006. Early aging and age-related pathologies in mice deficient in BMAL1, the core componentof the circadian clock. *Genes & development,* 20**,** 1868-1873.
KROENKE, C. H., SPIEGELMAN, D., MANSON, J., SCHERNHAMMER, E. S., COLDITZ, G. A. & KAWACHI, I. 2007. Work characteristics and incidence of type 2 diabetes in women. *American journal of epidemiology,* 165**,** 175-183.
KROGH, A. 1929. The progress of physiology. *American Journal of Physiology-Legacy Content,* 90**,** 243-251.
LOMB, N. R. 1976. Least-squares frequency analysis of unequally spaced data. *Astrophysics and space science,* 39**,** 447-462.

LU, J. & CASSONE, V. 1993. Pineal regulation of circadian rhythms of 2-deoxy [14 C] glucose uptake and 2 [125 I] iodomelatonin binding in the visual system of the house sparrow, Passer domesticus. *Journal of Comparative Physiology A,* 173**,** 765-774.

LU, W., MENG, Q.-J., TYLER, N. J., STOKKAN, K.-A. & LOUDON, A. S. 2010. A circadian clock is not required in an arctic mammal. *Current Biology,* 20**,** 533-537.

MARTINO, T. A., OUDIT, G. Y., HERZENBERG, A. M., TATA, N., KOLETAR, M. M., KABIR, G. M., BELSHAM, D. D., BACKX, P. H., RALPH, M. R. & SOLE, M. J. 2008. Circadian rhythm disorganization produces profound cardiovascular and renal disease in hamsters. *American Journal of Physiology-Regulatory, Integrative and Comparative Physiology,* 294**,** R1675-R1683.

MORIKAWA, Y., NAKAGAWA, H., MIURA, K., SOYAMA, Y., ISHIZAKI, M., KIDO, T., NARUSE, Y., SUWAZONO, Y. & NOGAWA, K. 2007. Effect of shift work on body mass index and metabolic parameters. *Scandinavian journal of work, environment & health***,** 45-50.

MORIN, L. P. 1994. The circadian visual system. *Brain Res Brain Res Rev,* 19**,** 102-27.

MORTENSEN, A. & BLIX, A. S. 1989. Seasonal changes in energy intake, energy expenditure, and digestibility in captive Svalbard rock ptarmigan and Norwegian willow ptarmigan. *Ornis Scandinavica***,** 22-28.

NAKANE, Y., IKEGAMI, K., ONO, H., YAMAMOTO, N., YOSHIDA, S., HIRUNAGI, K., EBIHARA, S., KUBO, Y. & YOSHIMURA, T. 2010. A mammalian neural tissue opsin (Opsin 5) is a deep brain photoreceptor in birds. *Proceedings of the National Academy of Sciences,* 107**,** 15264-15268.

NAKANE, Y. & YOSHIMURA, T. 2014. Universality and diversity in the signal transduction pathway that regulates seasonal reproduction in vertebrates. *Frontiers in neuroscience,* 8**,** 115.

NATESAN, A., GEETHA, L. & ZATZ, M. 2002. Rhythm and soul in the avian pineal. *Cell Tissue Res,* 309**,** 35-45.

PARANJPE, D. A., ANITHA, D., KUMAR, S., KUMAR, D., VERKHEDKAR, K., CHANDRASHEKARAN, M., JOSHI, A. & KUMAR SHARMA, V. 2003. Entrainment of eclosion rhythm in Drosophila melanogaster populations reared for more than 700 generations in constant light environment. *Chronobiology international,* 20**,** 977-987.

PARTCH, C. L., GREEN, C. B. & TAKAHASHI, J. S. 2014. Molecular architecture of the mammalian circadian clock. *Trends in cell biology,* 24**,** 90-99.

PITTENDRIGH, C. S. & MINIS, D. H. 1964. The entrainment of circadian oscillations by light and their role as photoperiodic clocks. *The American Naturalist,* 98**,** 261-294.

PLAUTZ, J. D., KANEKO, M., HALL, J. C. & KAY, S. A. 1997. Independent photoreceptive circadian clocks throughout Drosophila. *Science,* 278**,** 1632-1635.

PREITNER, N., DAMIOLA, F., ZAKANY, J., DUBOULE, D., ALBRECHT, U. & SCHIBLER, U. 2002. The orphan nuclear receptor REV-ERBα controls circadian transcription within the positive limb of the mammalian circadian oscillator. *Cell,* 110**,** 251-260.

REFINETTI, R. & MENAKER, M. 1992. The circadian rhythm of body temperature. *Physiology & behavior,* 51**,** 613-637.

REIERTH, E. & STOKKAN, K.-A. 1998a. Activity rhythm in High Arctic Svalbard ptarmigan (Lagopus mutus hyperboreus). *Canadian journal of zoology,* 76**,** 2031-2039.

REIERTH, E. & STOKKAN, K.-A. 1998b. Dual entrainment by light and food in the Svalbard ptarmigan (Lagopus mutus hyperboreus). *Journal of biological rhythms,* 13**,** 393-402.

REIERTH, E., VAN'T HOF, T. J. & STOKKAN, K.-A. 1999. Seasonal and daily variations in plasma melatonin in the high-arctic Svalbard ptarmigan (Lagopus mutus hyperboreus). *Journal of biological rhythms,* 14**,** 314-319.

REPPERT, S. M. & WEAVER, D. R. 2001. Molecular analysis of mammalian circadian rhythms. *Annual review of physiology,* 63**,** 647-676.

RIVKEES, S. A., CASSONE, V. M., WEAVER, D. R. & REPPERT, S. M. 1989. Melatonin receptors in chick brain: characterization and localization. *Endocrinology,* 125**,** 363-368.

RUEDEN, C. T., SCHINDELIN, J., HINER, M. C., DEZONIA, B. E., WALTER, A. E., ARENA, E. T. & ELICEIRI, K. W. 2017. ImageJ2: ImageJ for the next generation of scientific image data. *BMC bioinformatics,* 18**,** 1-26.

SACK, R. L., BLOOD, M. L. & LEWY, A. J. 1992. Melatonin rhythms in night shift workers. *Sleep,* 15**,** 434-441.

SAINI, C., MORF, J., STRATMANN, M., GOS, P. & SCHIBLER, U. 2012. Simulated body temperature rhythms reveal the phase-shifting behavior and plasticity of mammalian circadian oscillators. *Genes Dev,* 26**,** 567-80.

SCARGLE, J. D. 1982. Studies in astronomical time series analysis. II-Statistical aspects of spectral analysis of unevenly spaced data. *The Astrophysical Journal,* 263**,** 835-853.

SCHINDELIN, J., ARGANDA-CARRERAS, I., FRISE, E., KAYNIG, V., LONGAIR, M., PIETZSCH, T., PREIBISCH, S., RUEDEN, C., SAALFELD, S. & SCHMID, B. 2012. Fiji: an open-source platform for biological-image analysis. *Nature methods,* 9**,** 676-682.

SCHMID, B., HELFRICH-FÖRSTER, C. & YOSHII, T. 2011. A new ImageJ plug-in "ActogramJ" for chronobiological analyses. *Journal of biological rhythms,* 26**,** 464-467.

SHARMA, V. K. 2003. Adaptive significance of circadian clocks. *Chronobiology international,* 20**,** 901-919.

SHARP, P. J. 1996. Strategies in avian breeding cycles. *Animal Reproduction Science,* 42**,** 505-513.

SHEEBA, V., CHANDRASHEKARAN, M., JOSHI, A. & SHARMA, V. 2002. Locomotor activity rhythm in Drosophila melanogaster after 600 generations in an aperiodic environment. *Naturwissenschaften,* 89**,** 512-514.

SIMPSON, S. & FOLLETT, B. 1981. Pineal and hypothalamic pacemakers: their role in regulating circadian rhythmicity in Japanese quail. *Journal of comparative physiology,* 144**,** 381-389.

SPOELSTRA, K., WIKELSKI, M., DAAN, S., LOUDON, A. S. & HAU, M. 2016. Natural selection against a circadian clock gene mutation in mice. *Proceedings of the National Academy of Sciences,* 113**,** 686-691.

STELZER, R. J. & CHITTKA, L. 2010. Bumblebee foraging rhythms under the midnight sun measured with radiofrequency identification. *BMC biology,* 8**,** 1-7.

STOKKAN, K.-A., MORTENSEN, A. & BLIX, A. S. 1986. Food intake, feeding rhythm, and body mass regulation in Svalbard rock ptarmigan. *American Journal of Physiology-Regulatory, Integrative and Comparative Physiology,* 251**,** R264-R267.

TAKAHASHI, J. & MENAKER, M. 1982. Role of the suprachiasmatic nuclei in the circadian system of the house sparrow, Passer domesticus. *Journal of Neuroscience,* 2**,** 815-828.

TÜCHSEN, F., HANNERZ, H. & BURR, H. 2006. A 12 year prospective study of circulatory disease among Danish shift workers. *Occupational and Environmental Medicine,* 63**,** 451-455.

TUREK, F. W., JOSHU, C., KOHSAKA, A., LIN, E., IVANOVA, G., MCDEARMON, E., LAPOSKY, A., LOSEE-OLSON, S., EASTON, A. & JENSEN, D. R. 2005. Obesity and metabolic syndrome in circadian Clock mutant mice. *Science,* 308**,** 1043-1045.

TYLER, N. J., GREGORINI, P., FORCHHAMMER, M. C., STOKKAN, K.-A., VAN OORT, B. E. & HAZLERIGG, D. G. 2016. Behavioral timing without clockwork: photoperiod-dependent trade-off between predation hazard and energy balance in an arctic ungulate. *Journal of biological rhythms,* 31**,** 522-533.

UNDERWOOD, H., BARRETT, R. K. & SIOPES, T. 1990. The quail's eye: a biological clock. *Journal of Biological Rhythms,* 5**,** 257-265.

VAN OORT, B. E., TYLER, N. J., GERKEMA, M. P., FOLKOW, L., BLIX, A. S. & STOKKAN, K.-A. 2005. Circadian organization in reindeer. *Nature,* 438**,** 1095-1096.

VAN OORT, B. E., TYLER, N. J., GERKEMA, M. P., FOLKOW, L. & STOKKAN, K.-A. 2007. Where clocks are redundant: weak circadian mechanisms in reindeer living under polar photic conditions. *Naturwissenschaften,* 94**,** 183-194.

WARE, J. V., RODE, K. D., ROBBINS, C. T., LEISE, T., WEIL, C. R. & JANSEN, H. T. 2020. The clock keeps ticking: circadian rhythms of free-ranging polar bears. *Journal of biological rhythms,* 35**,** 180-194.

WELSH, D. K., YOO, S.-H., LIU, A. C., TAKAHASHI, J. S. & KAY, S. A. 2004. Bioluminescence imaging of individual fibroblasts reveals persistent, independently phased circadian rhythms of clock gene expression. *Current Biology,* 14**,** 2289-2295.

WHITMORE, D., FOULKES, N. S., STRÄHLE, U. & SASSONE-CORSI, P. 1998. Zebrafish Clock rhythmic expression reveals independent peripheral circadian oscillators. *Nature neuroscience,* 1**,** 701-707.

WILLIAMS, C. T., BARNES, B. M. & BUCK, C. L. 2012. Daily body temperature rhythms persist under the midnight sun but are absent during hibernation in free-living arctic ground squirrels. *Biology letters,* 8**,** 31-34.

WILLIAMS, C. T., BARNES, B. M., YAN, L. & BUCK, C. L. 2017. Entraining to the polar day: circadian rhythms in arctic ground squirrels. *Journal of Experimental Biology,* 220**,** 3095-3102.

WOELFLE, M. A., OUYANG, Y., PHANVIJHITSIRI, K. & JOHNSON, C. H. 2004. The adaptive value of circadian clocks: an experimental assessment in cyanobacteria. *Current Biology,* 14**,** 1481-1486.

YAMAZAKI, S., GOTO, M. & MENAKER, M. 1999. No evidence for extraocular photoreceptors in the circadian system of the Syrian hamster. *J Biol Rhythms,* 14**,** 197-201.

YAMAZAKI, S., NUMANO, R., ABE, M., HIDA, A., TAKAHASHI, R.-I., UEDA, M., BLOCK, G. D., SAKAKI, Y., MENAKER, M. & TEI, H. 2000. Resetting central and peripheral circadian oscillators in transgenic rats. *Science,* 288**,** 682-685.

YAMAZAKI, S. & TAKAHASHI, J. S. 2005. Real-time luminescence reporting of circadian gene expression in mammals. *Methods in enzymology,* 393**,** 288-301.

YASUO, S., YOSHIMURA, T., BARTELL, P. A., IIGO, M., MAKINO, E., OKABAYASHI, N. & EBIHARA, S. 2002. Effect of melatonin administration on qPer2, qPer3, and qClock gene expression in the suprachiasmatic nucleus of Japanese quail. *European Journal of Neuroscience,* 16**,** 1541-1546.

YOO, S.-H., YAMAZAKI, S., LOWREY, P. L., SHIMOMURA, K., KO, C. H., BUHR, E. D., SIEPKA, S. M., HONG, H.-K., OH, W. J. & YOO, O. J. 2004. PERIOD2:: LUCIFERASE real-time reporting of circadian dynamics reveals persistent circadian oscillations in mouse peripheral tissues. *Proceedings of the National Academy of Sciences,* 101**,** 5339-5346.

YOSHIMURA, T., SUZUKI, Y., MAKINO, E., SUZUKI, T., KUROIWA, A., MATSUDA, Y., NAMIKAWA, T. & EBIHARA, S. 2000. Molecular analysis of avian circadian clock genes. *Molecular brain research,* 78**,** 207-215.

ZHANG, E. E., LIU, A. C., HIROTA, T., MIRAGLIA, L. J., WELCH, G., PONGSAWAKUL, P. Y., LIU, X., ATWOOD, A., HUSS III, J. W. & JANES, J. 2009. A genome-wide RNAi screen for modifiers of the circadian clock in human cells. *Cell,* 139**,** 199-210.

ZIMMERMAN, N. H. & MENAKER, M. 1979. The pineal gland: a pacemaker within the circadian system of the house sparrow. *Proceedings of the National Academy of Sciences,* 76**,** 999-1003.

Appendix

Appendix A: Locomotor activity actograms and corresponding periodograms for all experimental birds

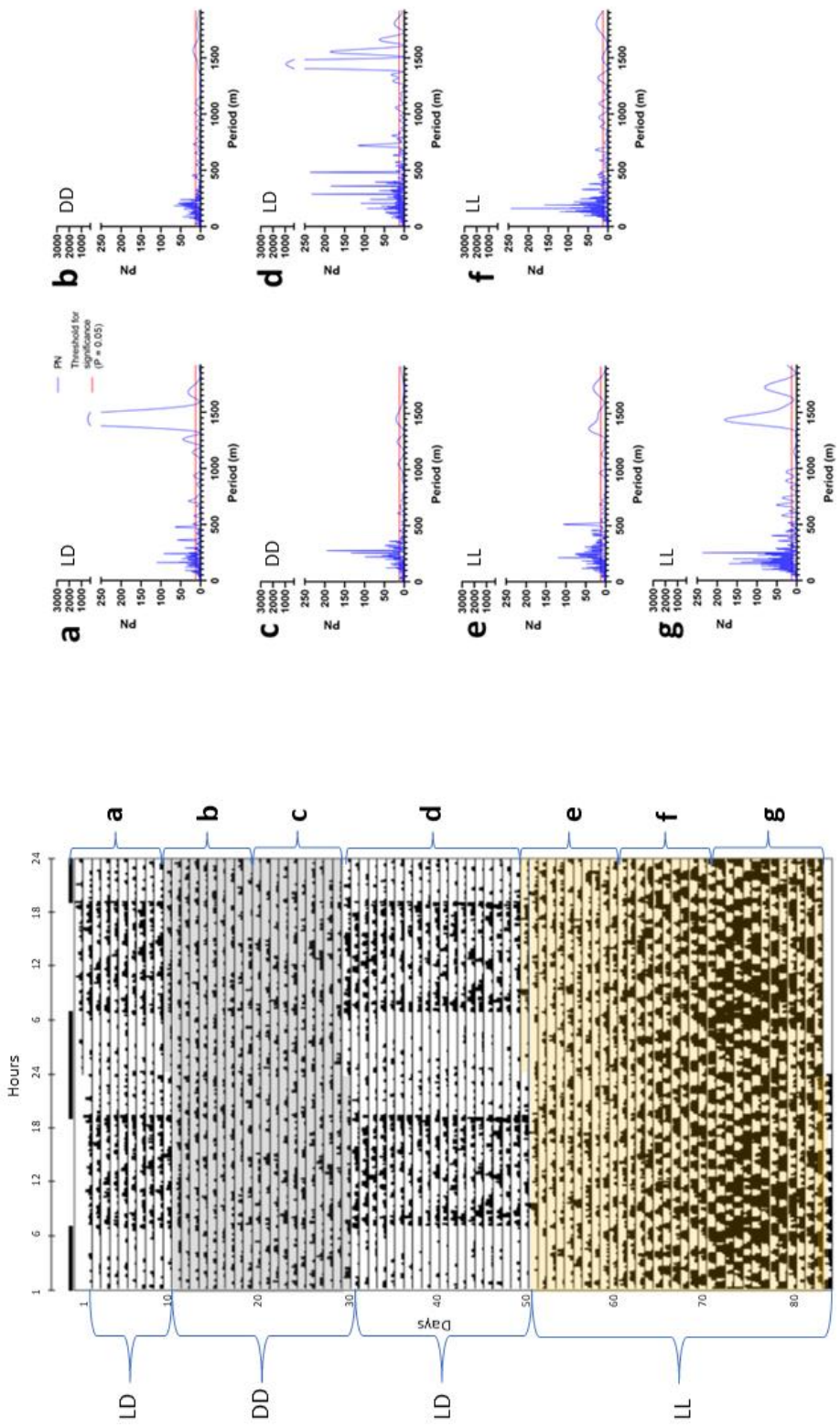

Figure A 1 Locomotor activity (ID: 072-98). Double plotted actogram (left) and corresponding periodograms (right). Each line on the actogram represents two days, and the second day is repeated in the next line. Black bars indicate activity. Data was normalized against its 99 percentiles, and the minimum value set to 0 (no activity) and the maximum value to 1 (99 percentiles). Grey shading indicates DD, yellow shading LL. Black bars above the actogram = lights off, white bars = lights on (refers to LD). The experiment was divided into segments (a-g on the right side of the actogram) and Lomb-Scargle periodograms were calculated for each segment. PN = Lomb-Scargle power

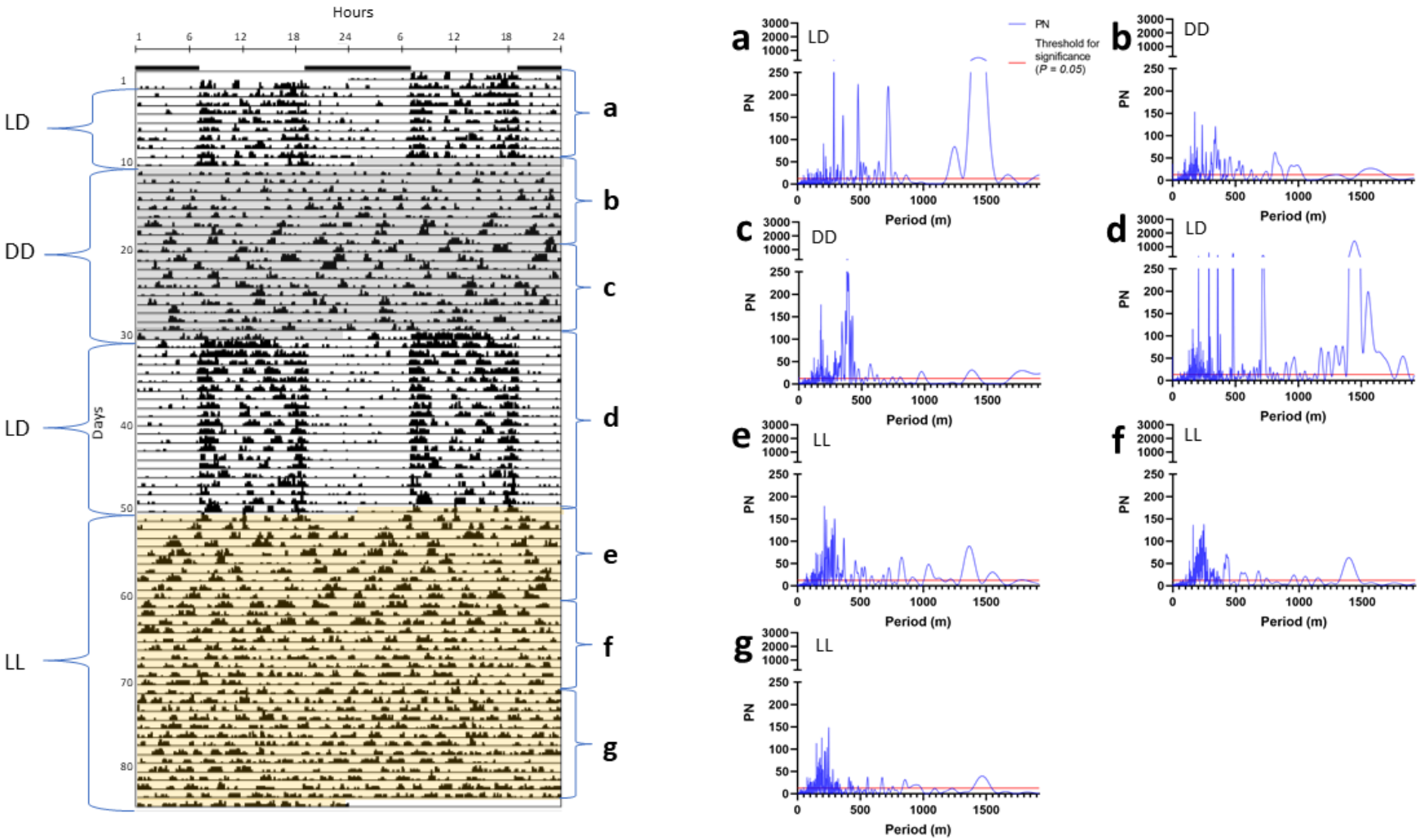

Figure A 2 Locomotor activity (ID: 078-98). Double plotted actogram (left) and corresponding periodograms (right). Each line on the actogram represents two days, and the second day is repeated in the next line. Black bars indicate activity. Data was normalized against its 99 percentiles, and the minimum value set to 0 (no activity) and the maximum value to 1 (99 percentiles). Grey shading indicates DD, yellow shading LL. Black bars above the actogram = lights off, white bars = lights on (refers to LD). The experiment was divided into segments (a-g on the right side of the actogram) and Lomb-Scargle periodograms were calculated for each segment. PN = Lomb-Scargle power

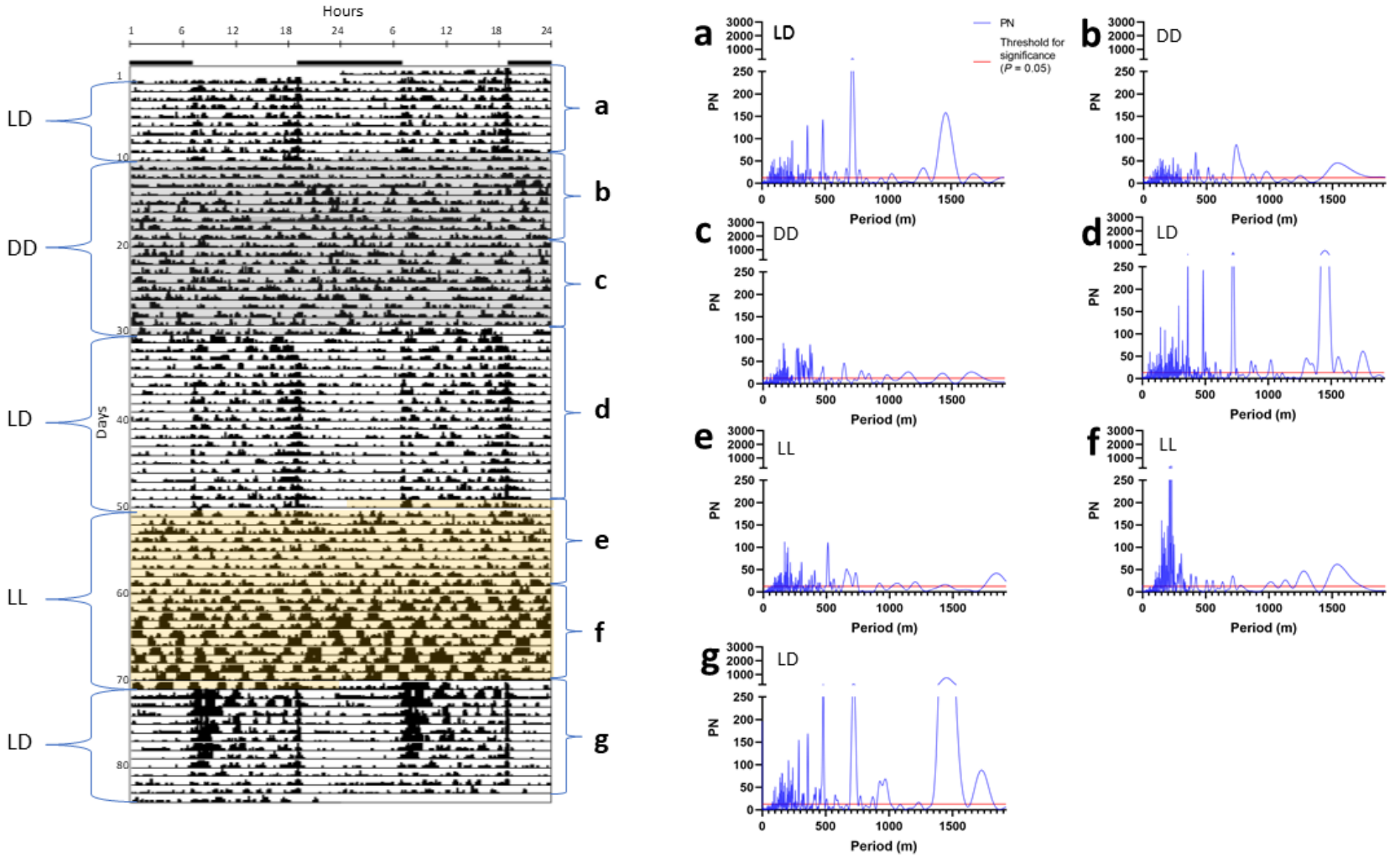

Figure A 3 Locomotor activity (ID: 269-98). Double plotted actogram (left) and corresponding periodograms (right). Each line on the actogram represents two days, and the second day is repeated in the next line. Black bars indicate activity. Data was normalized against its 99 percentiles, and the minimum value set to 0 (no activity) and the maximum value to 1 (99 percentiles). Grey shading indicates DD, yellow shading LL. Black bars above the actogram = lights off, white bars = lights on (refers to LD). The experiment was divided into segments (a-g on the right side of the actogram) and Lomb-Scargle periodograms were calculated for each segment. PN = Lomb-Scargle power

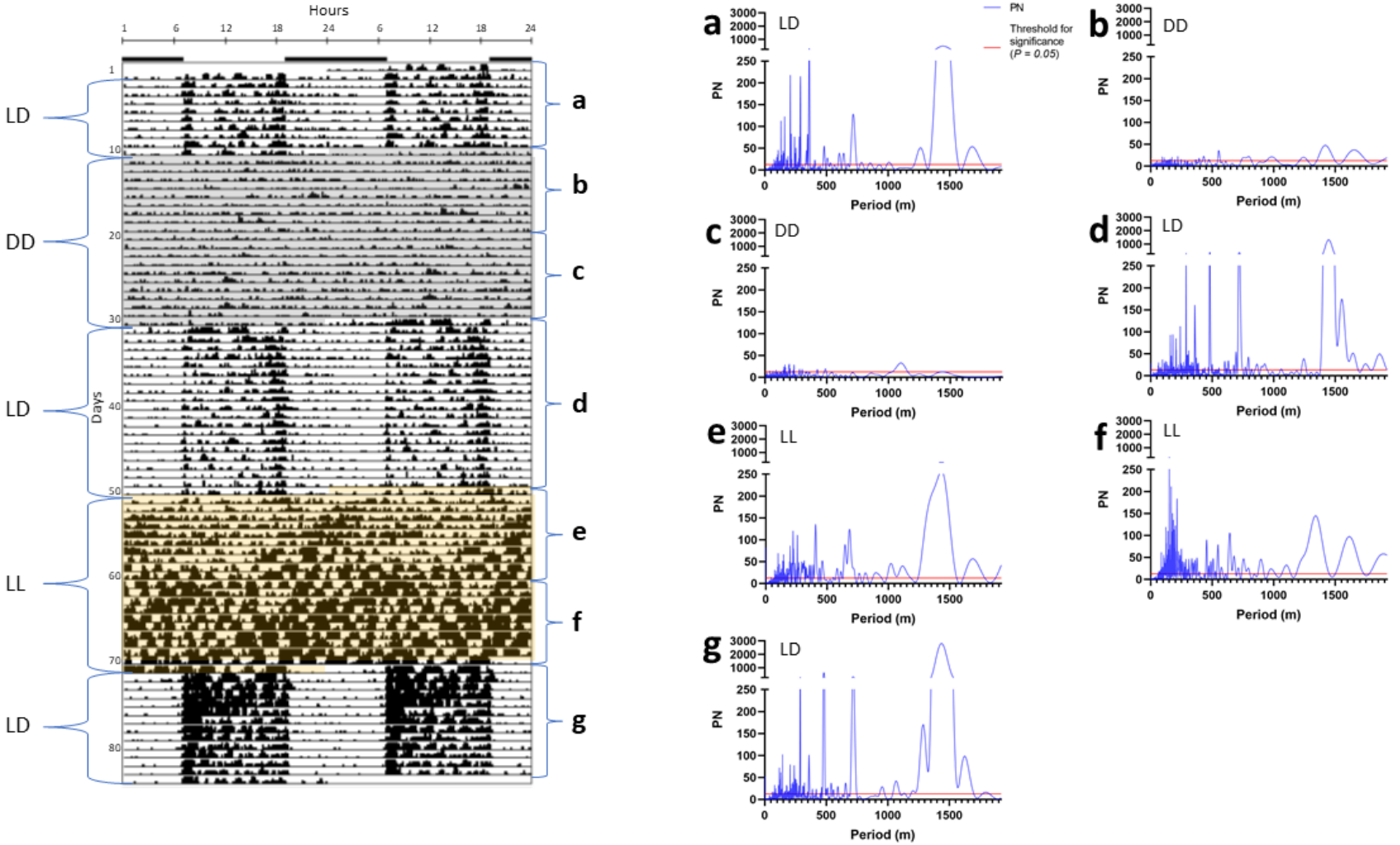

Figure A 4 Locomotor activity (ID: 079-98). Double plotted actogram (left) and corresponding periodograms (right). Each line on the actogram represents two days, and the second day is repeated in the next line. Black bars indicate activity. Data was normalized against its 99 percentiles, and the minimum value set to 0 (no activity) and the maximum value to 1 (99 percentiles). Grey shading indicates DD, yellow shading LL. Black bars above the actogram = lights off, white bars = lights on (refers to LD). The experiment was divided into segments (a-g on the right side of the actogram) and Lomb-Scargle periodograms were calculated for each segment. PN = Lomb-Scargle power

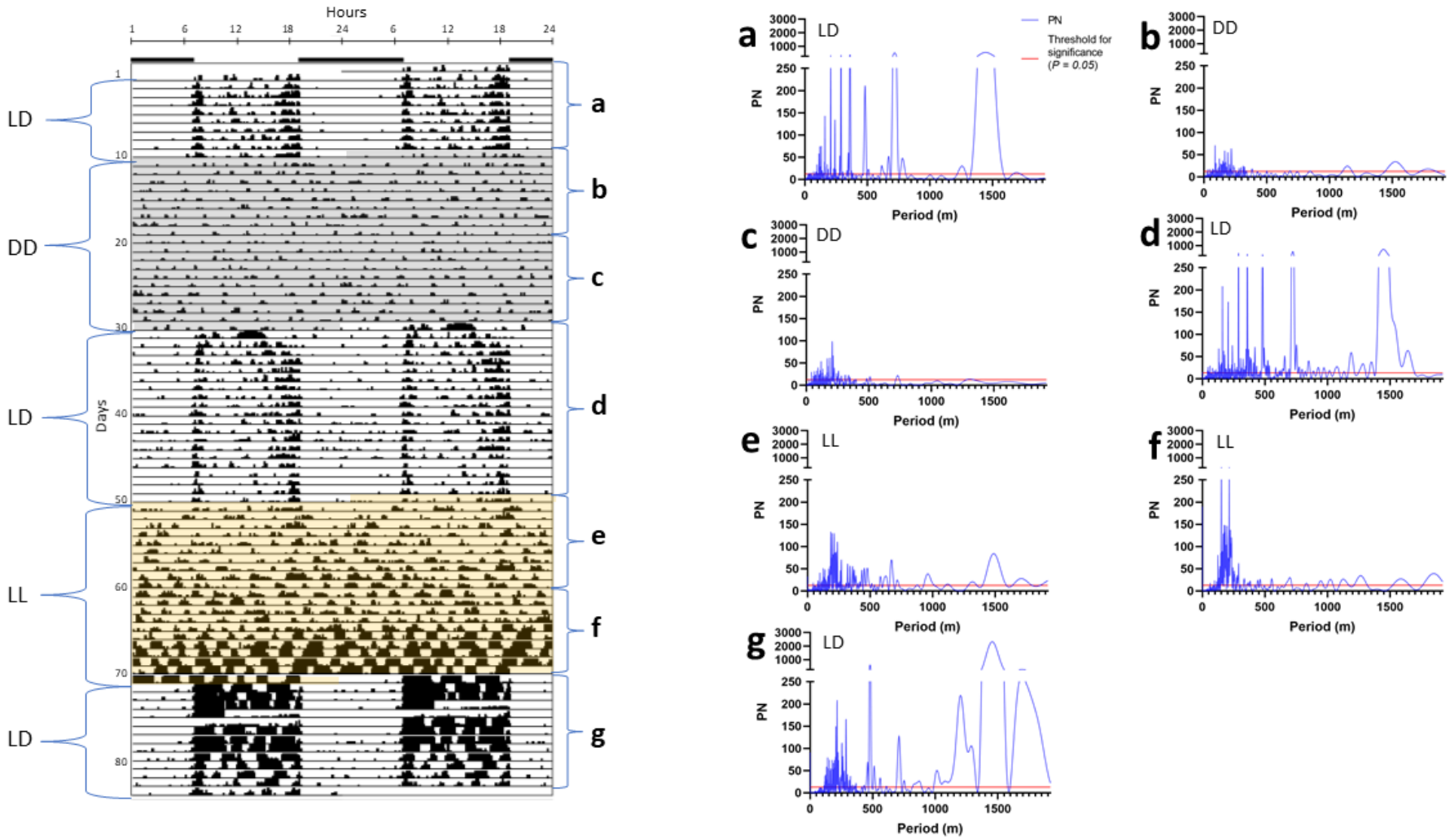

Figure A 5 Locomotor activity (ID: 041-98). Double plotted actogram (left) and corresponding periodograms (right). Each line on the actogram represents two days, and the second day is repeated in the next line. Black bars indicate activity. Data was normalized against its 99 percentiles, and the minimum value set to 0 (no activity) and the maximum value to 1 (99 percentiles). Grey shading indicates DD, yellow shading LL. Black bars above the actogram = lights off, white bars = lights on (refers to LD). The experiment was divided into segments (a-g on the right side of the actogram) and Lomb-Scargle periodograms were calculated for each segment. PN = Lomb-Scargle power

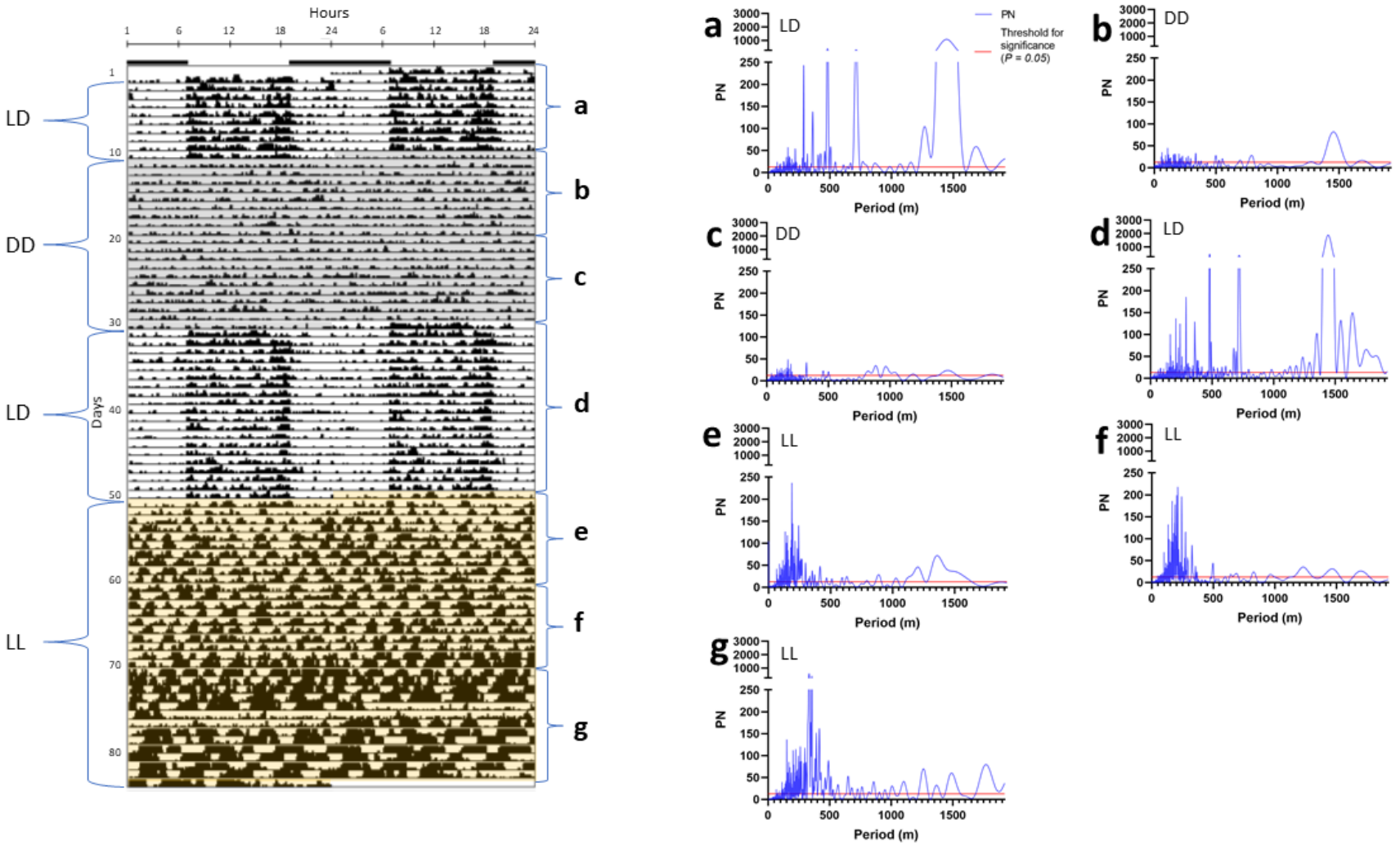

Figure A 6 Locomotor activity (ID: R35). Double plotted actogram (left) and corresponding periodograms (right). Each line on the actogram represents two days, and the second day is repeated in the next line. Black bars indicate activity. Data was normalized against its 99 percentiles, and the minimum value set to 0 (no activity) and the maximum value to 1 (99 percentiles). Grey shading indicates DD, yellow shading LL. Black bars above the actogram = lights off, white bars = lights on (refers to LD). The experiment was divided into segments (a-g on the right side of the actogram) and Lomb-Scargle periodograms were calculated for each segment. PN = Lomb-Scargle power

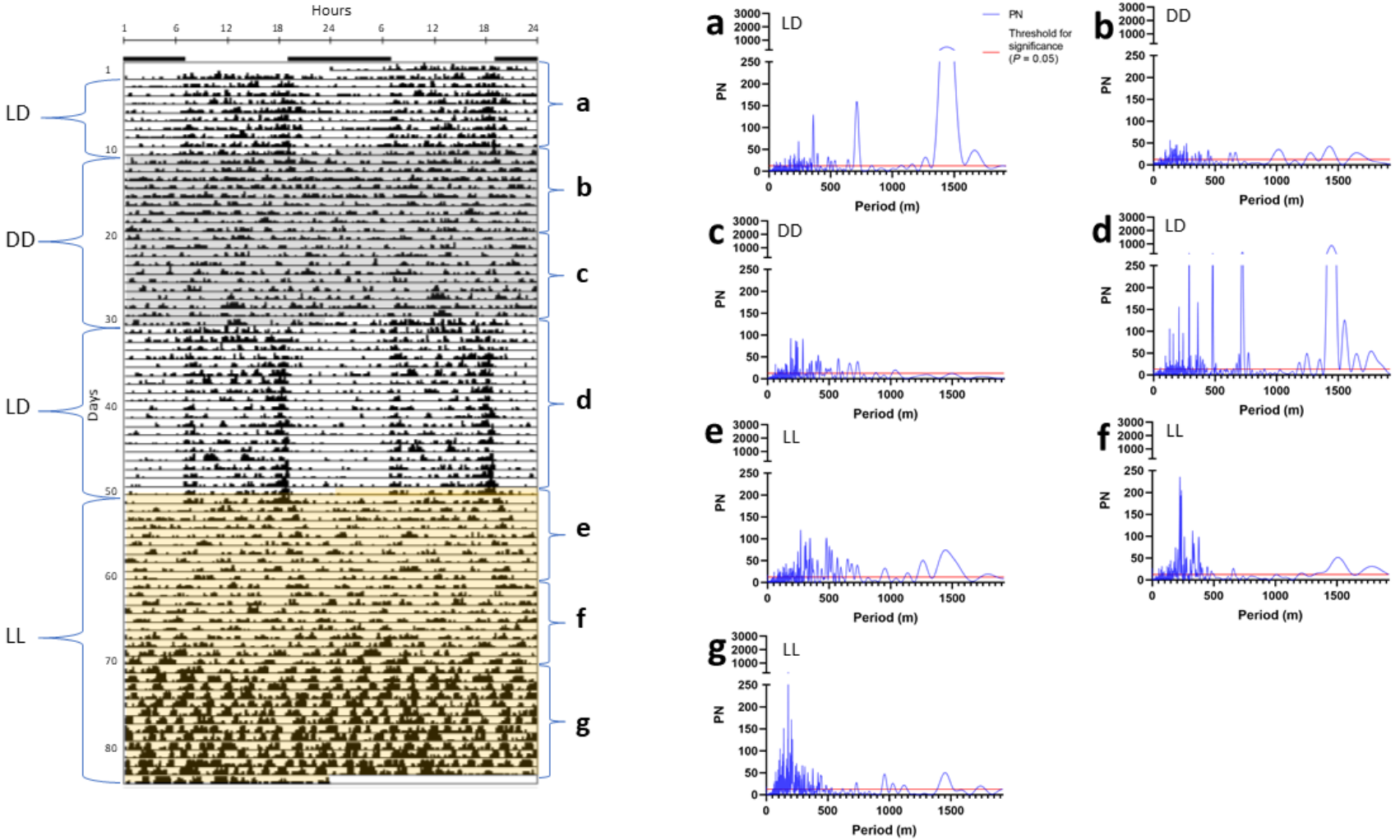

Figure A 7 Locomotor activity (ID: 047-98). Double plotted actogram (left) and corresponding periodograms (right). Each line on the actogram represents two days, and the second day is repeated in the next line. Black bars indicate activity. Data was normalized against its 99 percentiles, and the minimum value set to 0 (no activity) and the maximum value to 1 (99 percentiles). Grey shading indicates DD, yellow shading LL. Black bars above the actogram = lights off, white bars = lights on (refers to LD). The experiment was divided into segments (a-g on the right side of the actogram) and Lomb-Scargle periodograms were calculated for each segment. PN = Lomb-Scargle power

Appendix B: Feeding activity actograms and corresponding periodograms for all experimental birds

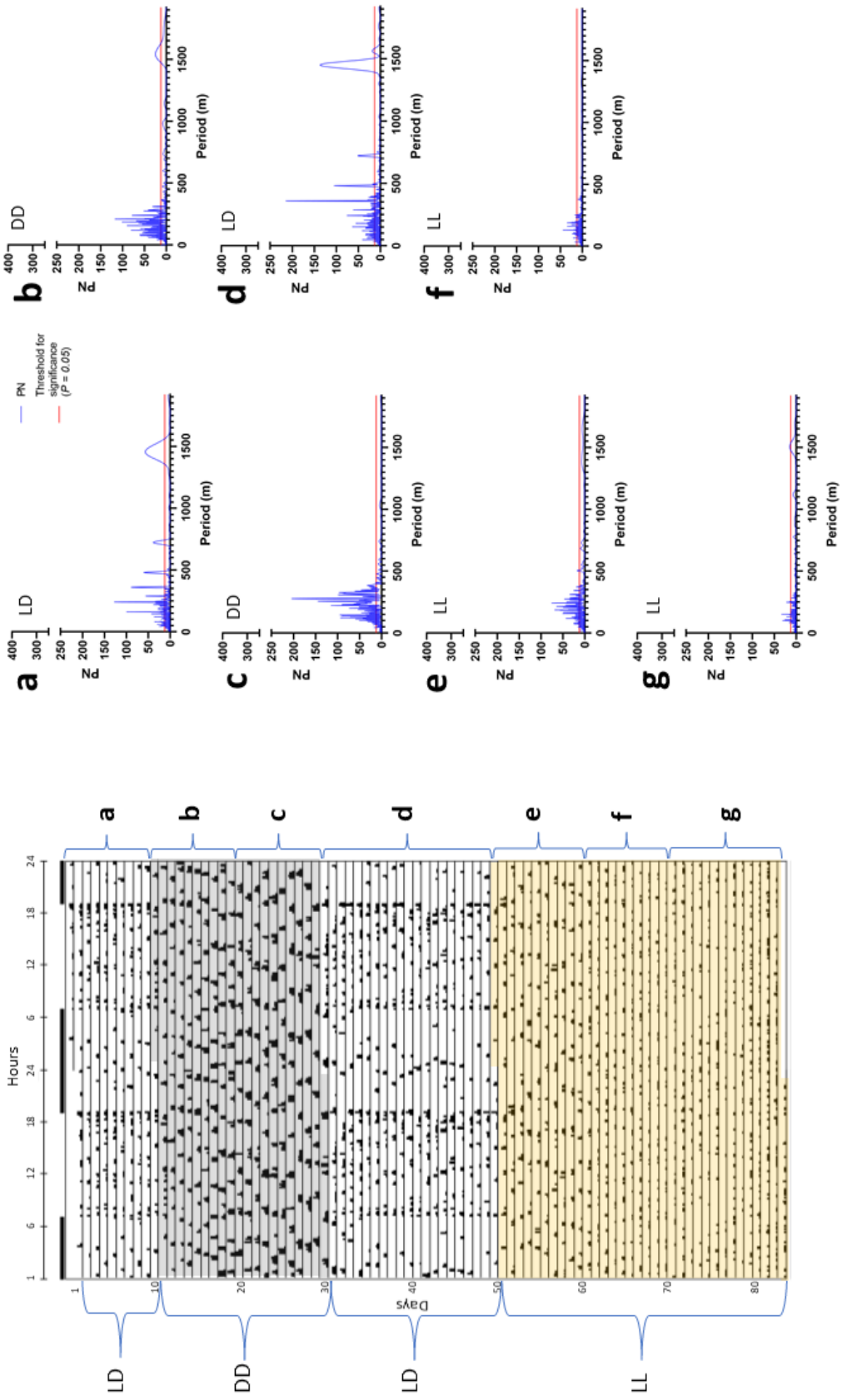

Figure A 8 Feeding activity (ID: 072-98). Double plotted actogram (left) and corresponding periodograms (right). Each line on the actogram represents two days, and the second day is repeated in the next line. Black bars indicate activity. Data was normalized against its 99 percentiles, and the minimum value set to 0 (no activity) and the maximum value to 1 (99 percentiles). Grey shading indicates DD, yellow shading LL. Black bars above the actogram = lights off, white bars = lights on (refers to LD). The experiment was divided into segments (a-g on the right side of the actogram) and Lomb-Scargle periodograms were calculated for each segment. PN = Lomb-Scargle power

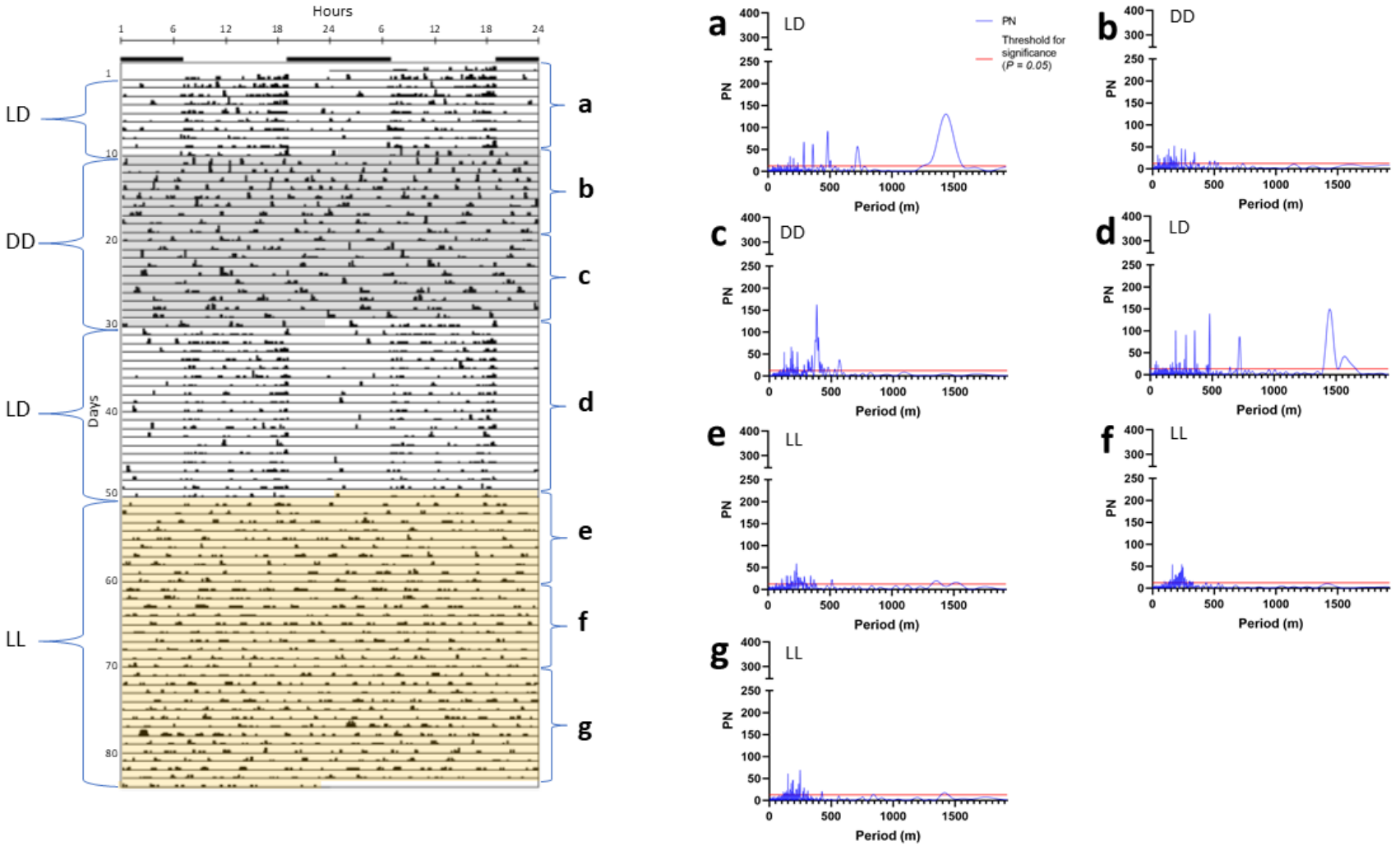

Figure A 9 Feeding activity (ID: 078-98). Double plotted actogram (left) and corresponding periodograms (right). Each line on the actogram represents two days, and the second day is repeated in the next line. Black bars indicate activity. Data was normalized against its 99 percentiles, and the minimum value set to 0 (no activity) and the maximum value to 1 (99 percentiles). Grey shading indicates DD, yellow shading LL. Black bars above the actogram = lights off, white bars = lights on (refers to LD). The experiment was divided into segments (a-g on the right side of the actogram) and Lomb-Scargle periodograms were calculated for each segment. PN = Lomb-Scargle power

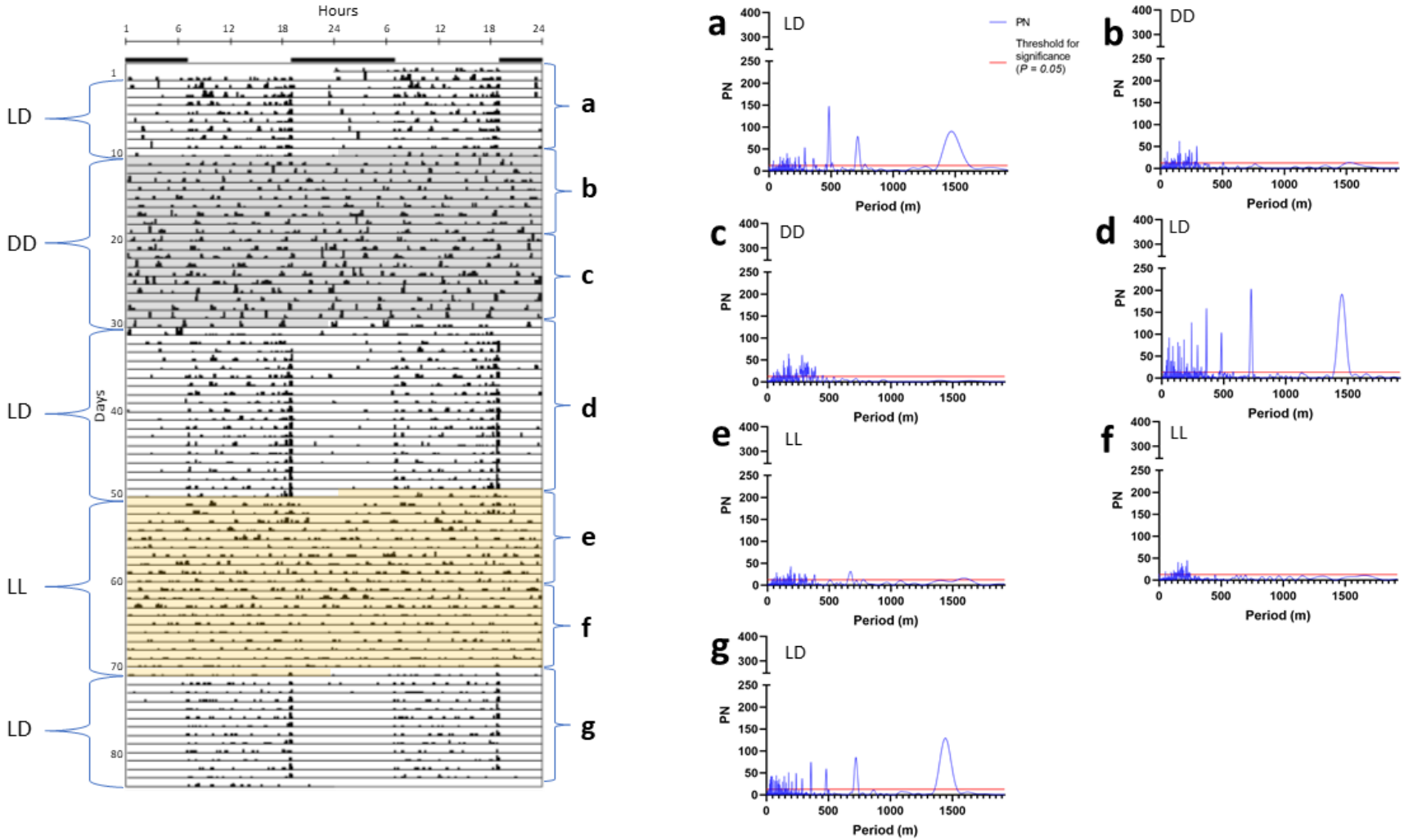

Figure A 10 Feeding activity (ID: 269-98). Double plotted actogram (left) and corresponding periodograms (right). Each line on the actogram represents two days, and the second day is repeated in the next line. Black bars indicate activity. Data was normalized against its 99 percentiles, and the minimum value set to 0 (no activity) and the maximum value to 1 (99 percentiles). Grey shading indicates DD, yellow shading LL. Black bars above the actogram = lights off, white bars = lights on (refers to LD). The experiment was divided into segments (a-g on the right side of the actogram) and Lomb-Scargle periodograms were calculated for each segment. PN = Lomb-Scargle power

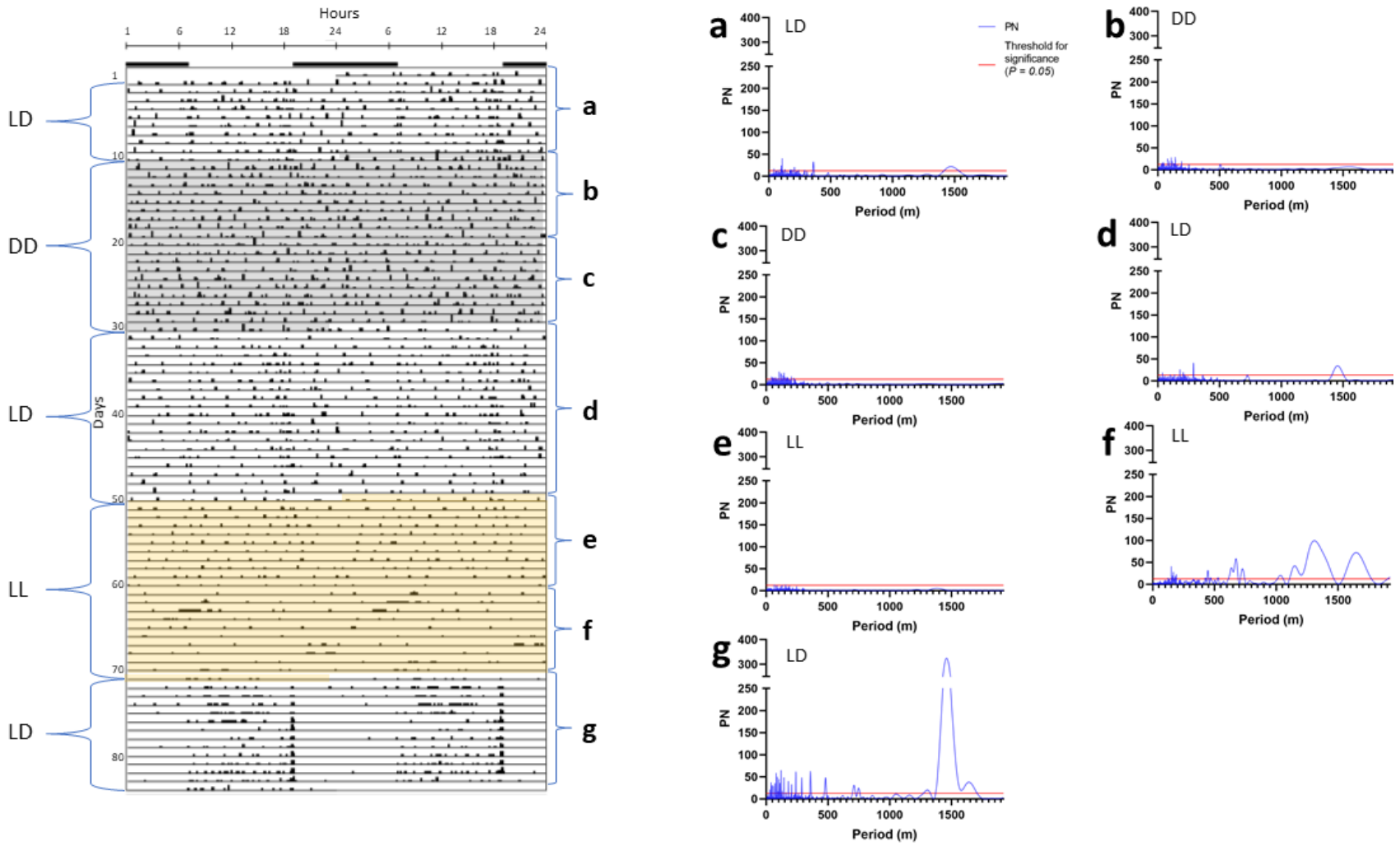

Figure A 11 Feeding activity (ID: 079-98). Double plotted actogram (left) and corresponding periodograms (right). Each line on the actogram represents two days, and the second day is repeated in the next line. Black bars indicate activity. Data was normalized against its 99 percentiles, and the minimum value set to 0 (no activity) and the maximum value to 1 (99 percentiles). Grey shading indicates DD, yellow shading LL. Black bars above the actogram = lights off, white bars = lights on (refers to LD). The experiment was divided into segments (a-g on the right side of the actogram) and Lomb-Scargle periodograms were calculated for each segment. PN = Lomb-Scargle power

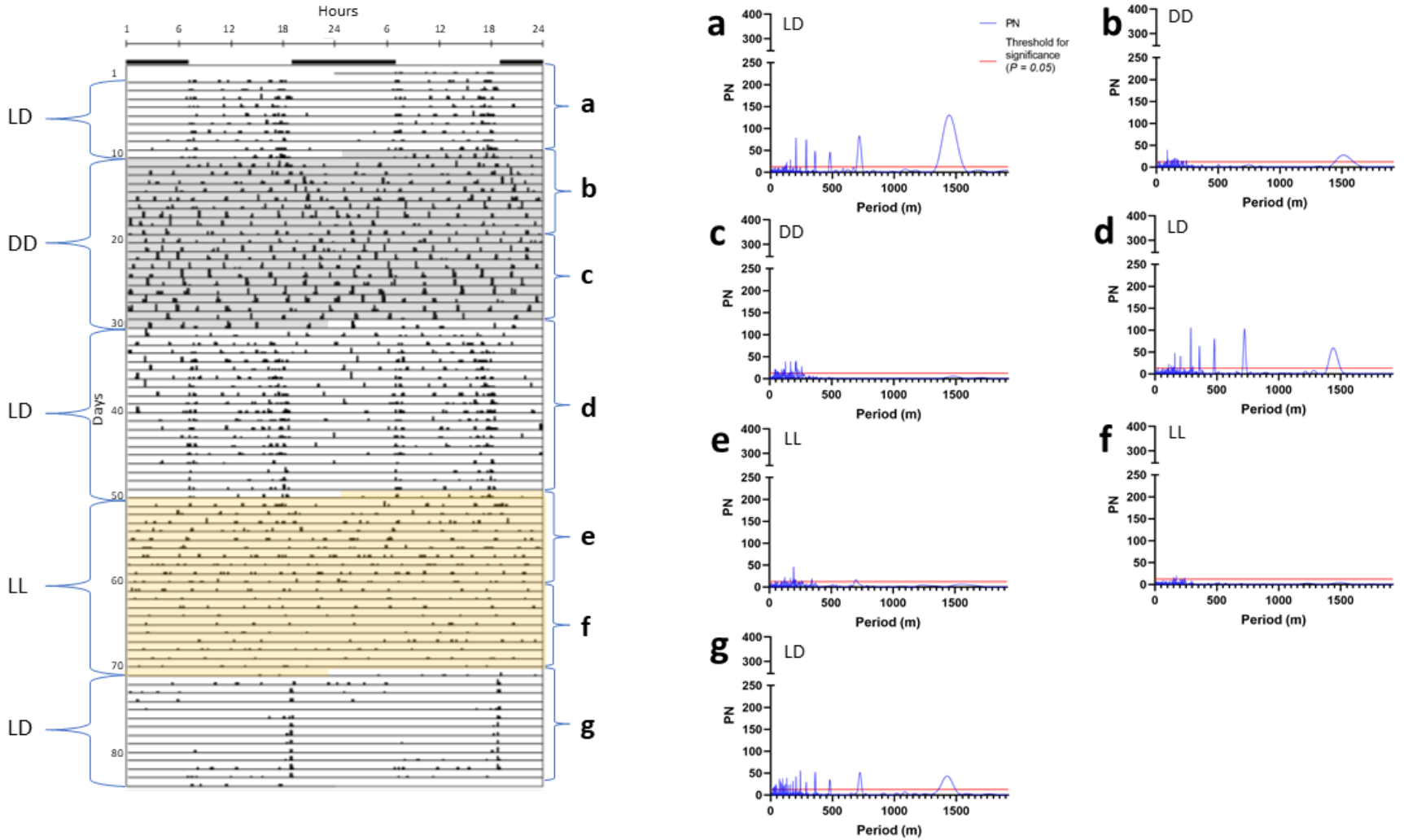

Figure A 12 Feeding activity (ID: 041-98). Double plotted actogram (left) and corresponding periodograms (right). Each line on the actogram represents two days, and the second day is repeated in the next line. Black bars indicate activity. Data was normalized against its 99 percentiles, and the minimum value set to 0 (no activity) and the maximum value to 1 (99 percentiles). Grey shading indicates DD, yellow shading LL. Black bars above the actogram = lights off, white bars = lights on (refers to LD). The experiment was divided into segments (a-g on the right side of the actogram) and Lomb-Scargle periodograms were calculated for each segment. PN = Lomb-Scargle power

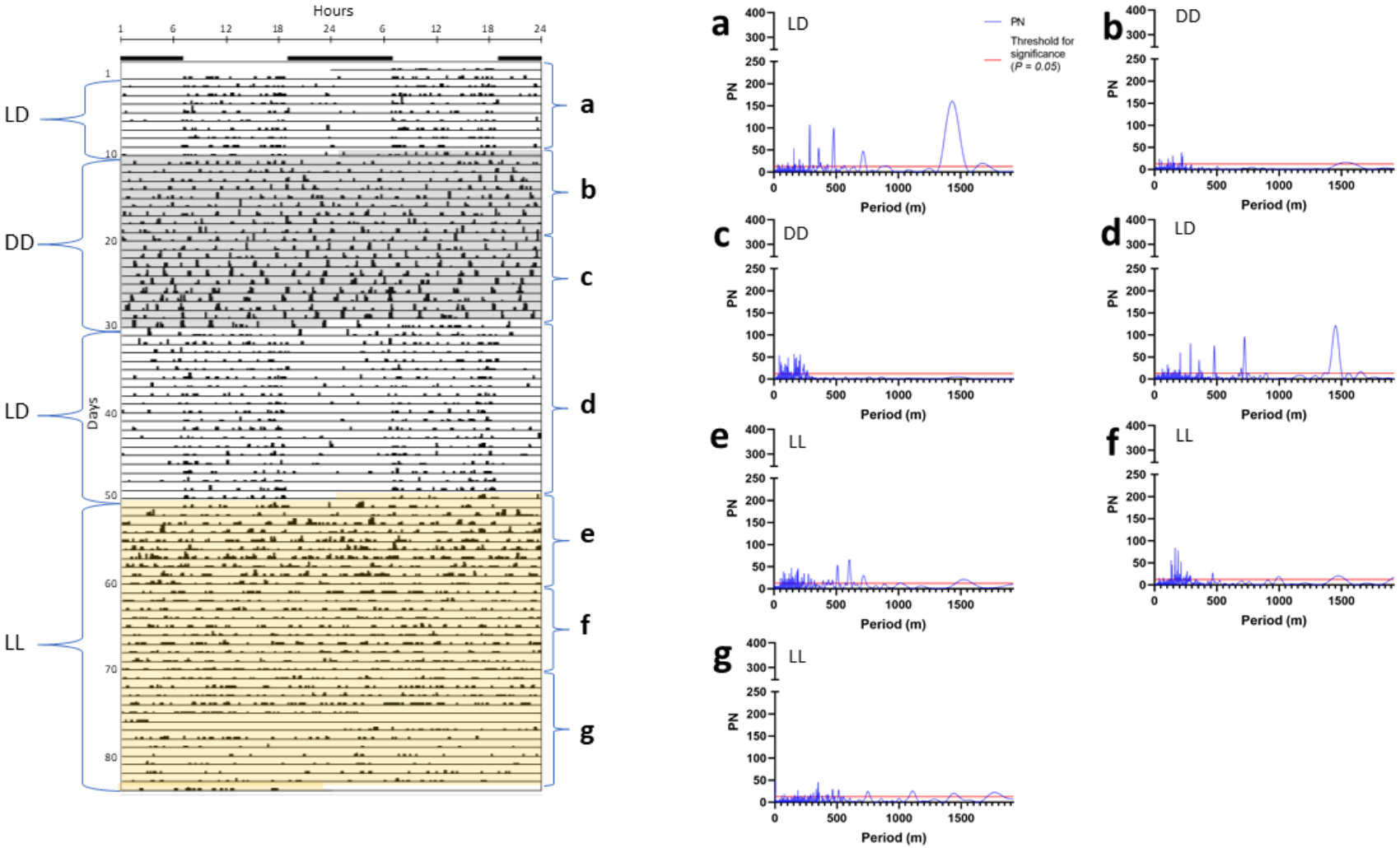

Figure A 13 Feeding activity (ID: R35). Double plotted actogram (left) and corresponding periodograms (right). Each line on the actogram represents two days, and the second day is repeated in the next line. Black bars indicate activity. Data was normalized against its 99 percentiles, and the minimum value set to 0 (no activity) and the maximum value to 1 (99 percentiles). Grey shading indicates DD, yellow shading LL. Black bars above the actogram = lights off, white bars = lights on (refers to LD). The experiment was divided into segments (a-g on the right side of the actogram) and Lomb-Scargle periodograms were calculated for each segment. PN = Lomb-Scargle power

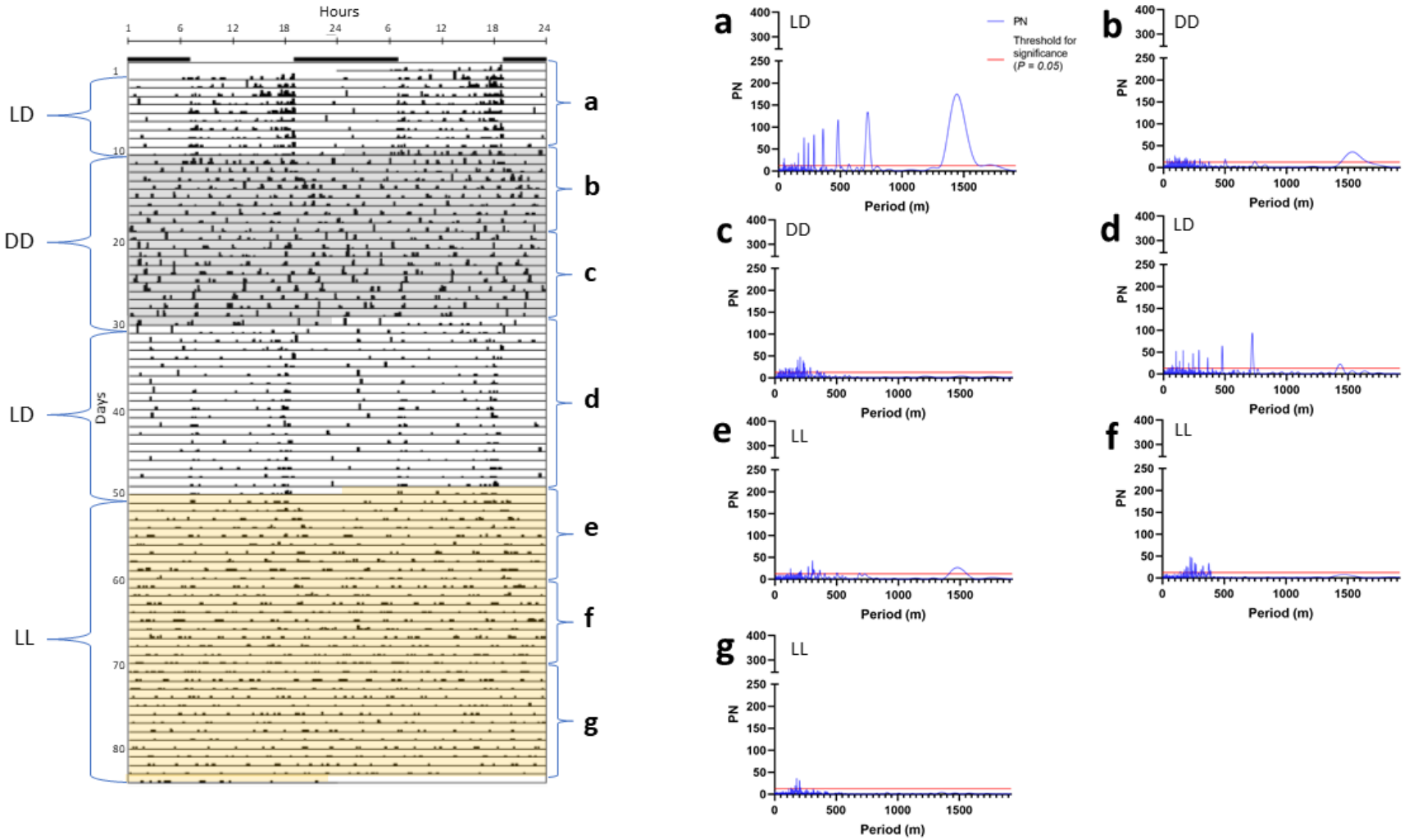

Figure A 14 Feeding activity (ID: 047-98). Double plotted actogram (left) and corresponding periodograms (right). Each line on the actogram represents two days, and the second day is repeated in the next line. Black bars indicate activity. Data was normalized against its 99 percentiles, and the minimum value set to 0 (no activity) and the maximum value to 1 (99 percentiles). Grey shading indicates DD, yellow shading LL. Black bars above the actogram = lights off, white bars = lights on (refers to LD). The experiment was divided into segments (a-g on the right side of the actogram) and Lomb-Scargle periodograms were calculated for each segment. PN = Lomb-Scargle power

Appendix C: Body temperature actograms and corresponding periodograms for all experimental birds

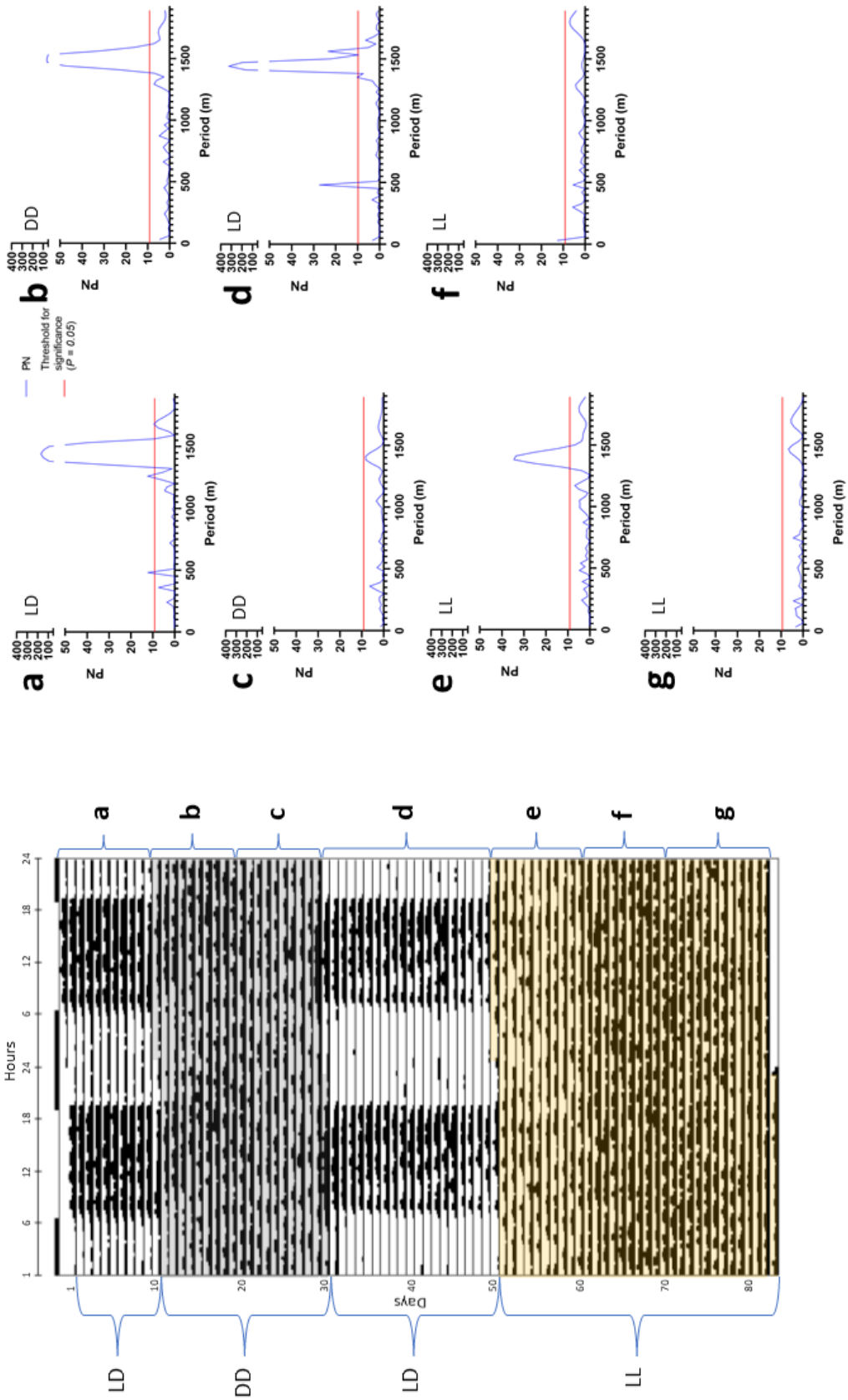

Figure A 15 T_b (ID: 072-98). Double plotted actogram (left) and corresponding periodograms (right). Each line on the actogram represents two days, and the second day is repeated in the next line. Black bars indicate increased T_b. The minimum value was set to 39 and the maximum value to 42. Grey shading indicates DD, yellow shading LL. Black bars above actogram = lights off, white bars = lights on (refers to LD). The experiment was divided into segments (a-g on the right side of the actogram) and Lomb-Scargle periodograms were calculated for each segment. PN = Lomb-Scargle power

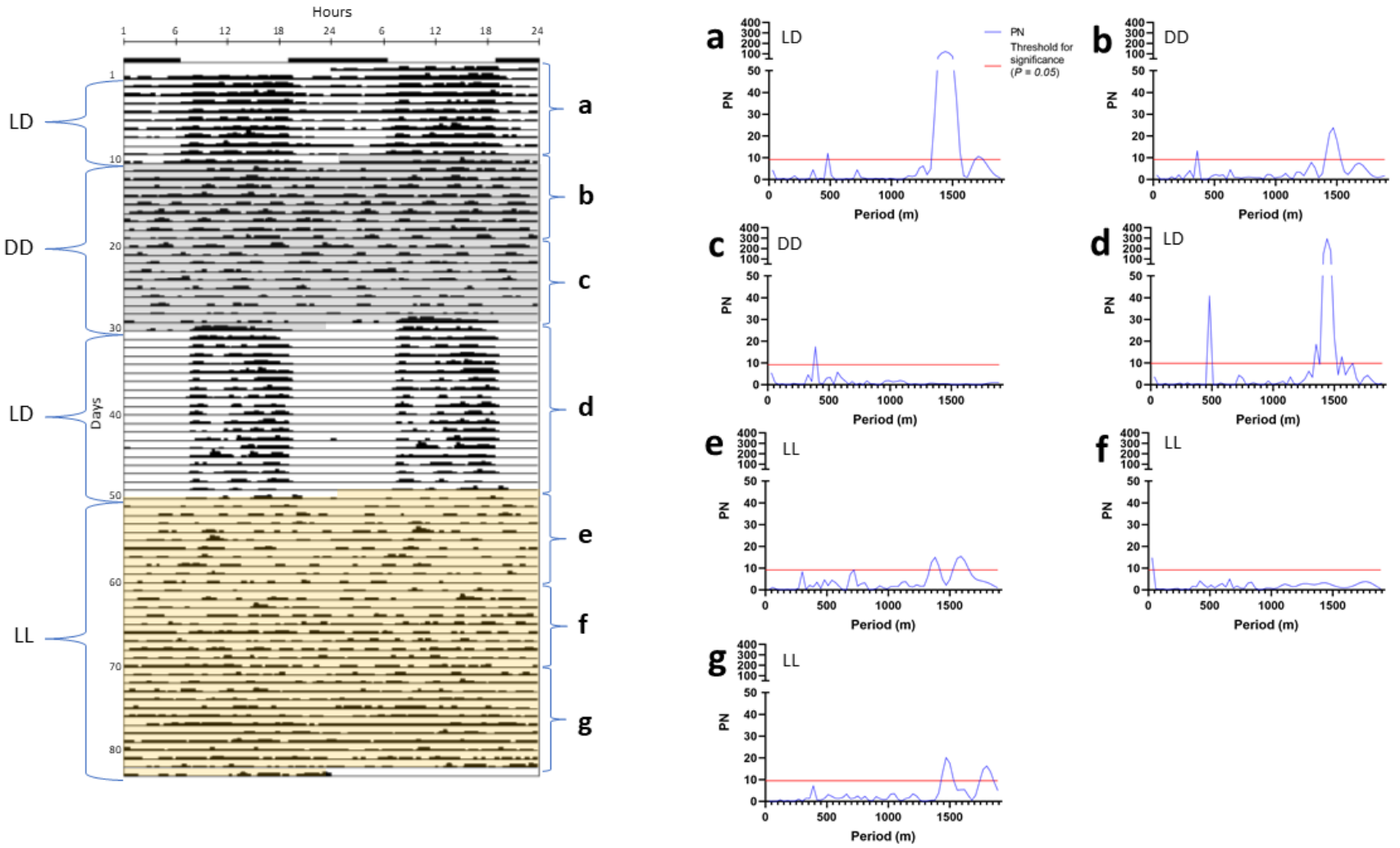

Figure A 16 T_b (ID: 078-98). Double plotted actogram (left) and corresponding periodograms (right). Each line on the actogram represents two days, and the second day is repeated in the next line. Black bars indicate increased T_b. The minimum value was set to 39 and the maximum value to 42. Grey shading indicates DD, yellow shading LL. Black bars above actogram = lights off, white bars = lights on (refers to LD). The experiment was divided into segments (a-g on the right side of the actogram) and Lomb-Scargle periodograms were calculated for each segment. PN = Lomb-Scargle power

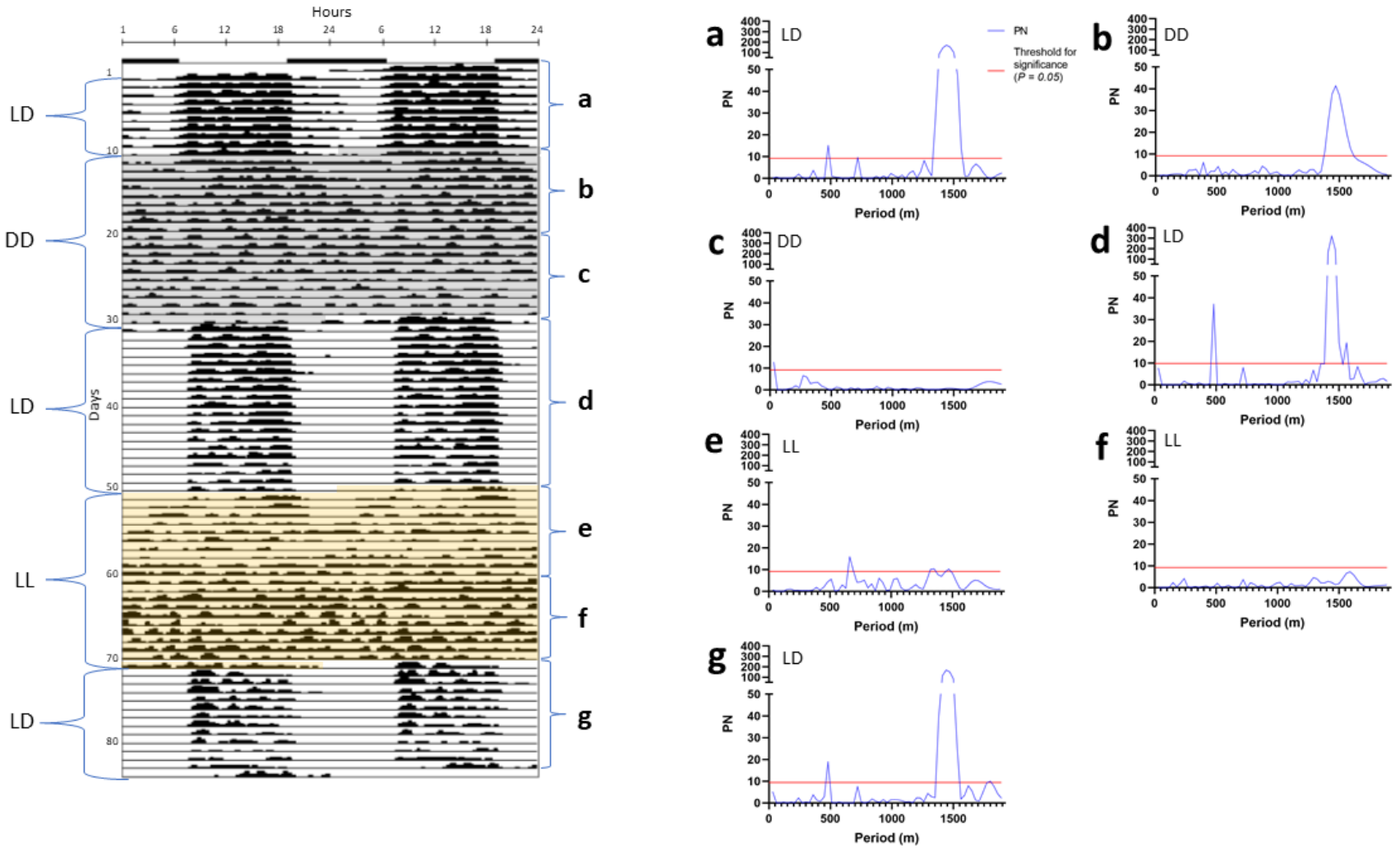

Figure A 17 T_b (ID: 269-98). Double plotted actogram (left) and corresponding periodograms (right). Each line on the actogram represents two days, and the second day is repeated in the next line. Black bars indicate increased T_b. The minimum value was set to 39 and the maximum value to 42. Grey shading indicates DD, yellow shading LL. Black bars above actogram = lights off, white bars = lights on (refers to LD). The experiment was divided into segments (a-g on the right side of the actogram) and Lomb-Scargle periodograms were calculated for each segment. PN = Lomb-Scargle power

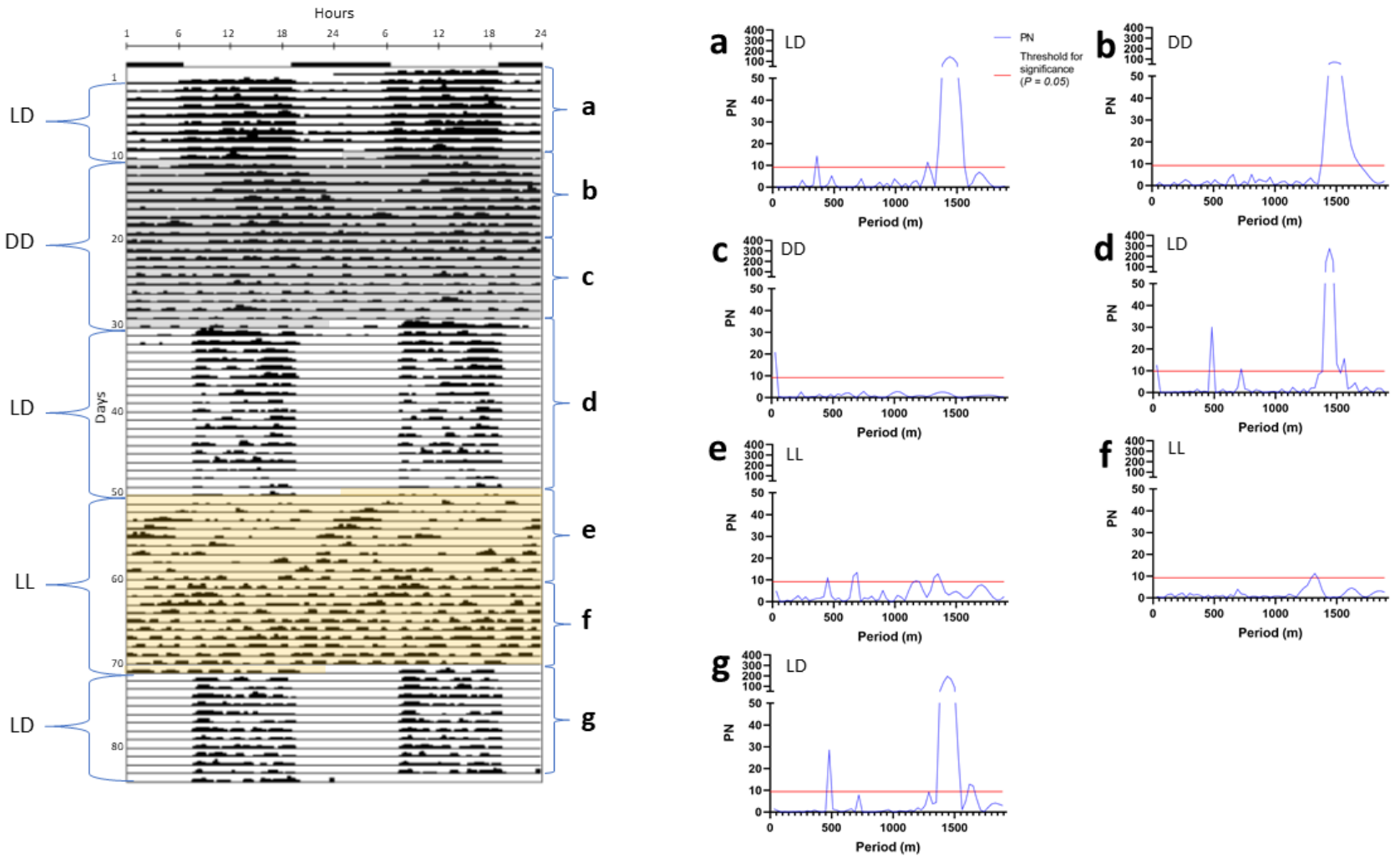

Figure A 18 T_b (ID: 079-98). Double plotted actogram (left) and corresponding periodograms (right). Each line on the actogram represents two days, and the second day is repeated in the next line. Black bars indicate increased T_b. The minimum value was set to 39 and the maximum value to 42. Grey shading indicates DD, yellow shading LL. Black bars above actogram = lights off, white bars = lights on (refers to LD). The experiment was divided into segments (a-g on the right side of the actogram) and Lomb-Scargle periodograms were calculated for each segment. PN = Lomb-Scargle power

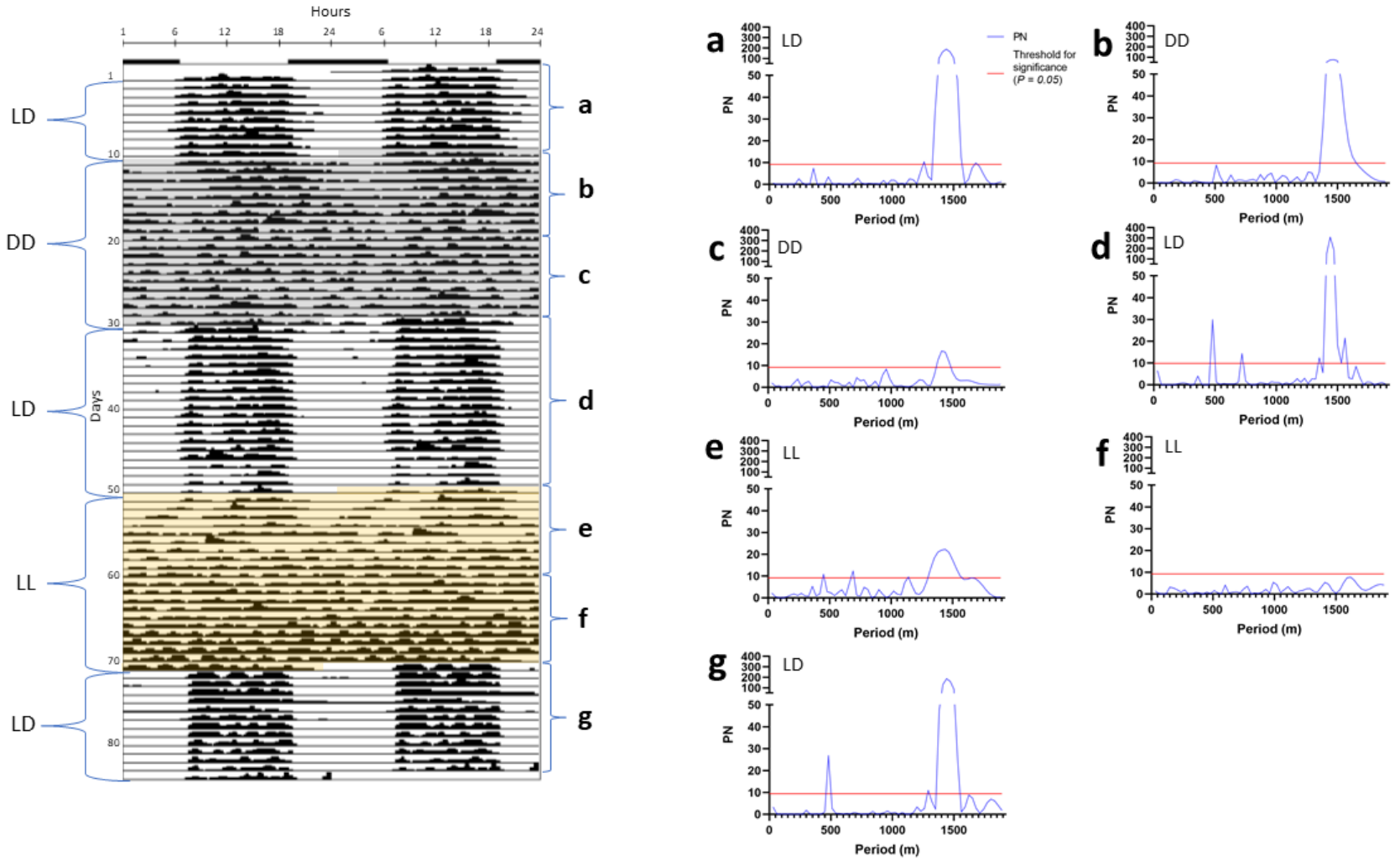

Figure A 19 T_b (ID: 041-98). Double plotted actogram (left) and corresponding periodograms (right). Each line on the actogram represents two days, and the second day is repeated in the next line. Black bars indicate increased T_b. The minimum value was set to 39 and the maximum value to 42. Grey shading indicates DD, yellow shading LL. Black bars above actogram = lights off, white bars = lights on (refers to LD). The experiment was divided into segments (a-g on the right side of the actogram) and Lomb-Scargle periodograms were calculated for each segment. PN = Lomb-Scargle power

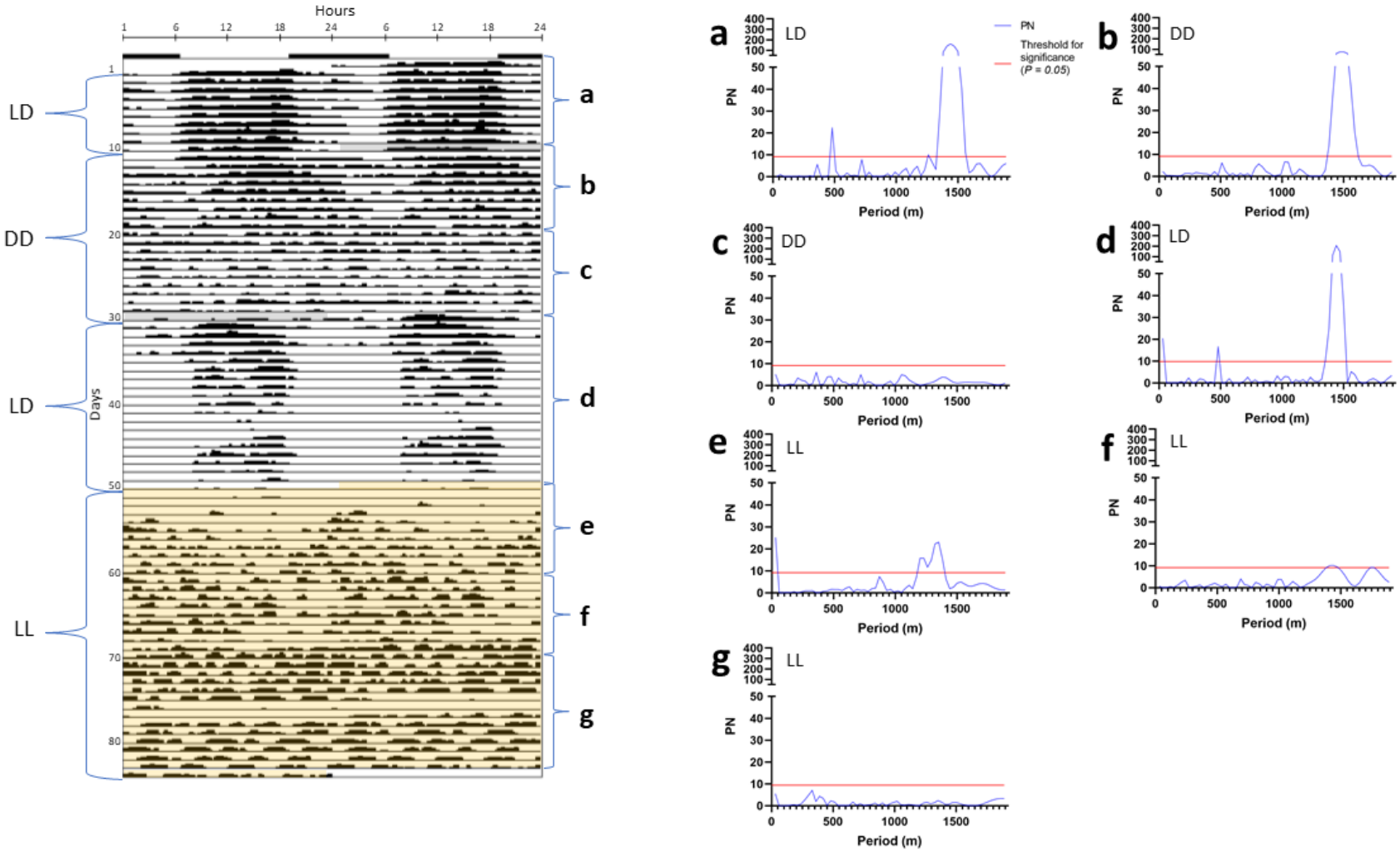

Figure A 20 T_b (ID: R35). Double plotted actogram (left) and corresponding periodograms (right). Each line on the actogram represents two days, and the second day is repeated in the next line. Black bars indicate increased T_b. The minimum value was set to 39 and the maximum value to 42. Grey shading indicates DD, yellow shading LL. Black bars above actogram = lights off, white bars = lights on (refers to LD). The experiment was divided into segments (a-g on the right side of the actogram) and Lomb-Scargle periodograms were calculated for each segment. PN = Lomb-Scargle power

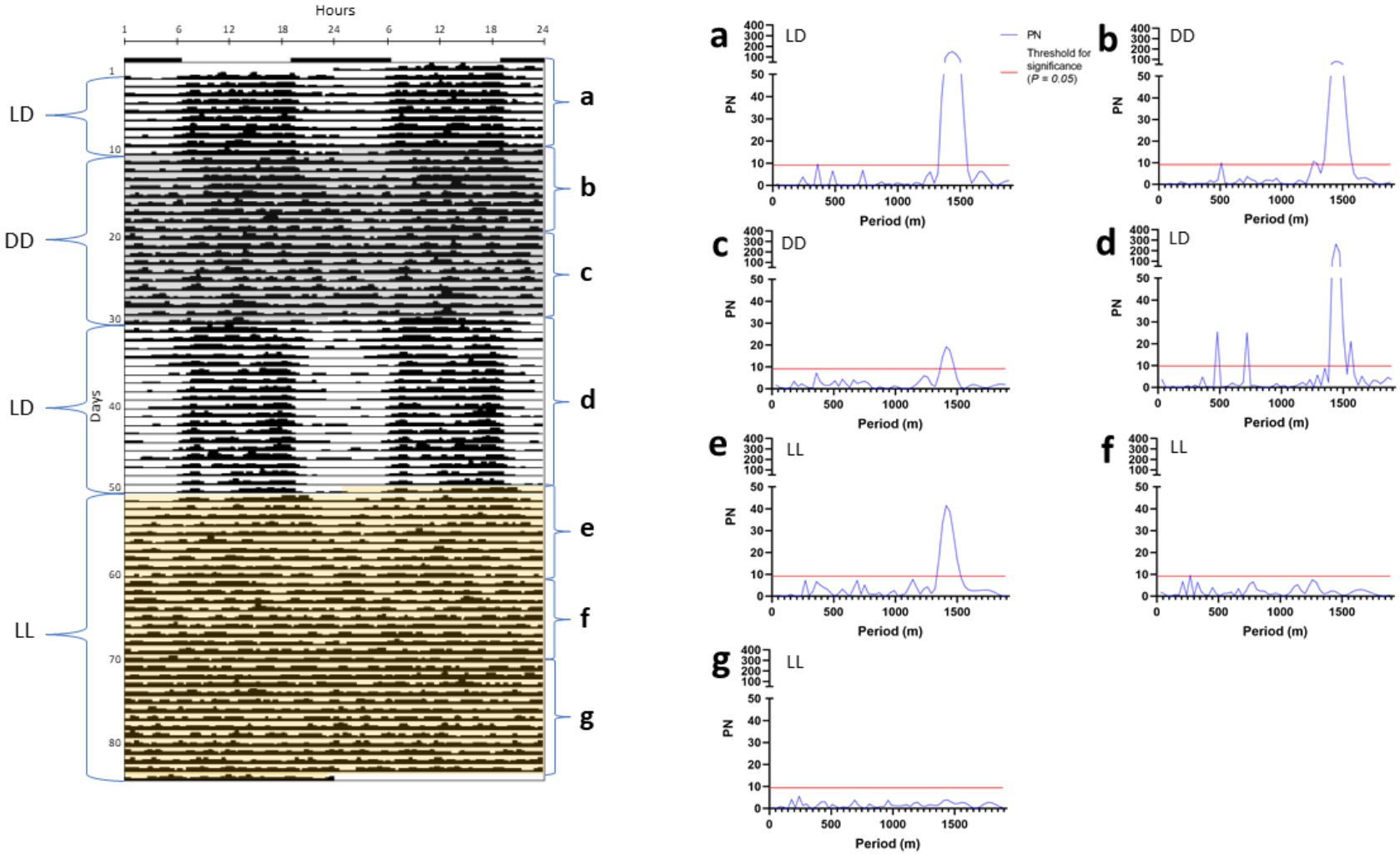

Figure A 21 T_b (ID: 047-98). Double plotted actogram (left) and corresponding periodograms (right). Each line on the actogram represents two days, and the second day is repeated in the next line. Black bars indicate increased T_b. The minimum value was set to 39 and the maximum value to 42. Grey shading indicates DD, yellow shading LL. Black bars above actogram = lights off, white bars = lights on (refers to LD). The experiment was divided into segments (a-g on the right side of the actogram) and Lomb-Scargle periodograms were calculated for each segment. PN = Lomb-Scargle power

Appendix D: Body temperature amplitude LD to DD/LL for all experimental birds

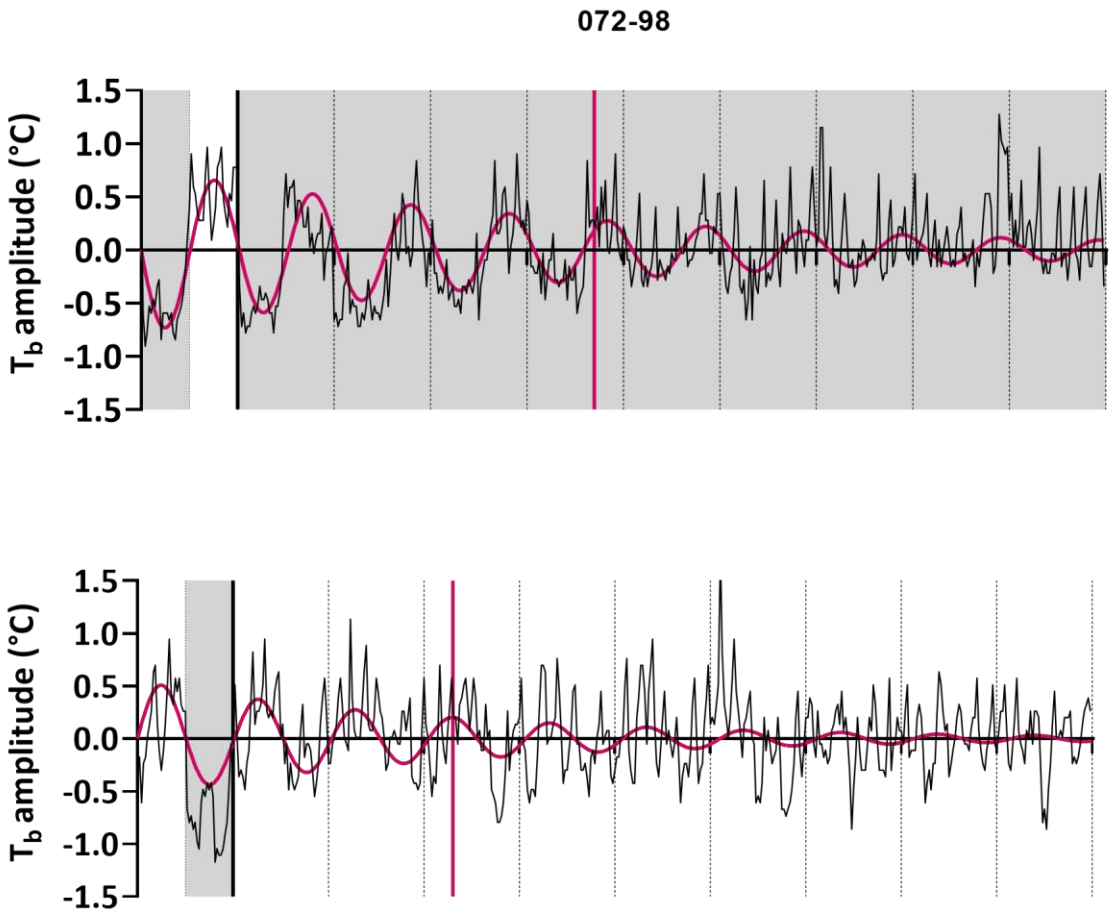

Figure A 22 T_b amplitude (ID: 072-98) for 10 days. (a) Last day under LD and following nine days under DD, and (b) last day under LD and following nine days under LL. Vertical dotted lines separate days, white background = lights on, grey background = ~~lights~~ off. A nonlinear regression was drawn as a dampened sine wave (red), vertical red line = half-life of dampened sine wave.

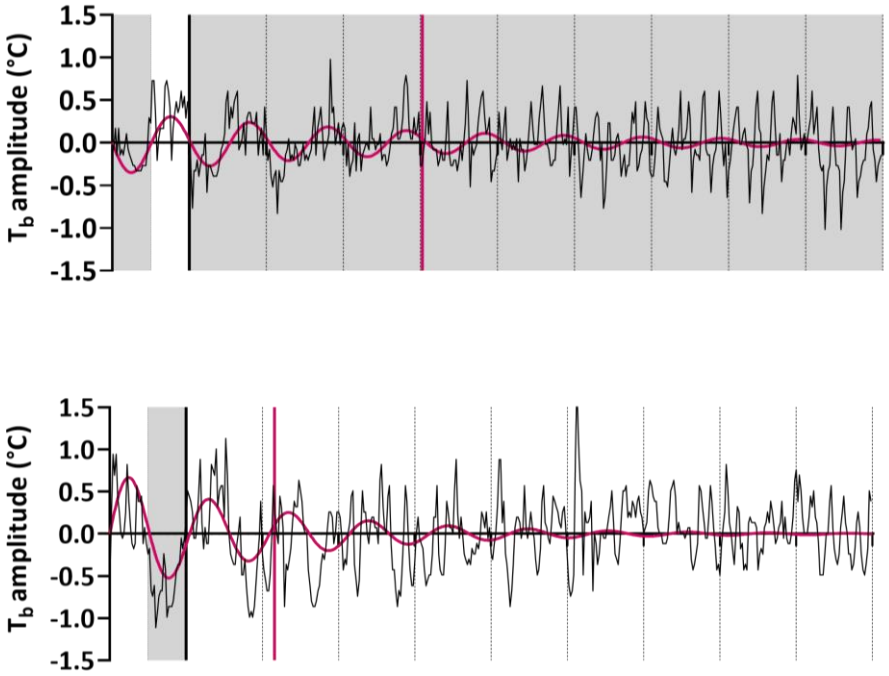

Figure A 23 T_b amplitude (ID: 078-98) for 10 days. (a) Last day under LD and following nine days under DD, and (b) last day under LD and following nine days under LL. Vertical dotted lines separate days, white background = lights on, grey background = lights off. A nonlinear regression was drawn as a dampened sine wave (red), vertical red line = half-life of dampened sine wave.

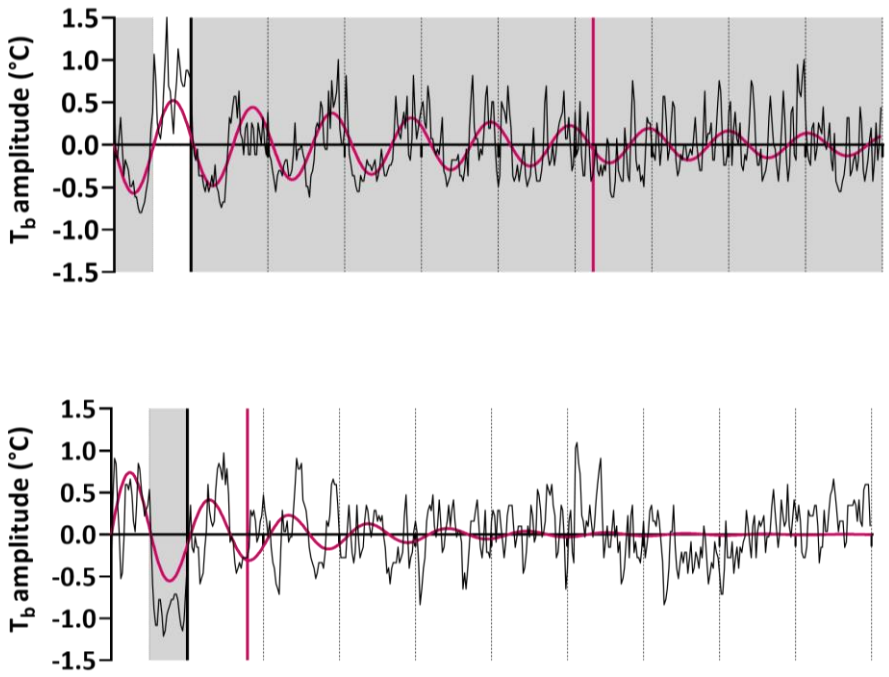

Figure A 24 T_b amplitude (ID: 269-98) for 10 days. (a) Last day under LD and following nine days under DD, and (b) last day under LD and following nine days under LL. Vertical dotted lines separate days, white background = lights on, grey background = lights off. A nonlinear regression was drawn as a dampened sine wave (red), vertical red line = half-life of dampened sine wave.

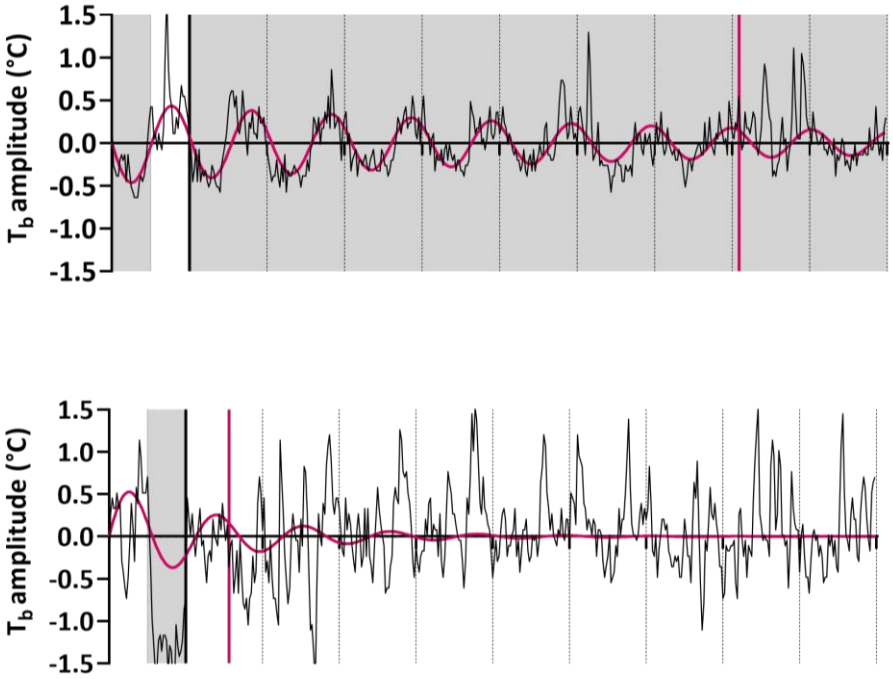

Figure A 25 T_b amplitude (ID: 079-98) for 10 days. (a) Last day under LD and following nine days under DD, and (b) last day under LD and following nine days under LL. Vertical dotted lines separate days, white background = lights on, grey background = lights off. A nonlinear regression was drawn as a dampened sine wave (red), vertical red line = half-life of dampened sine wave.

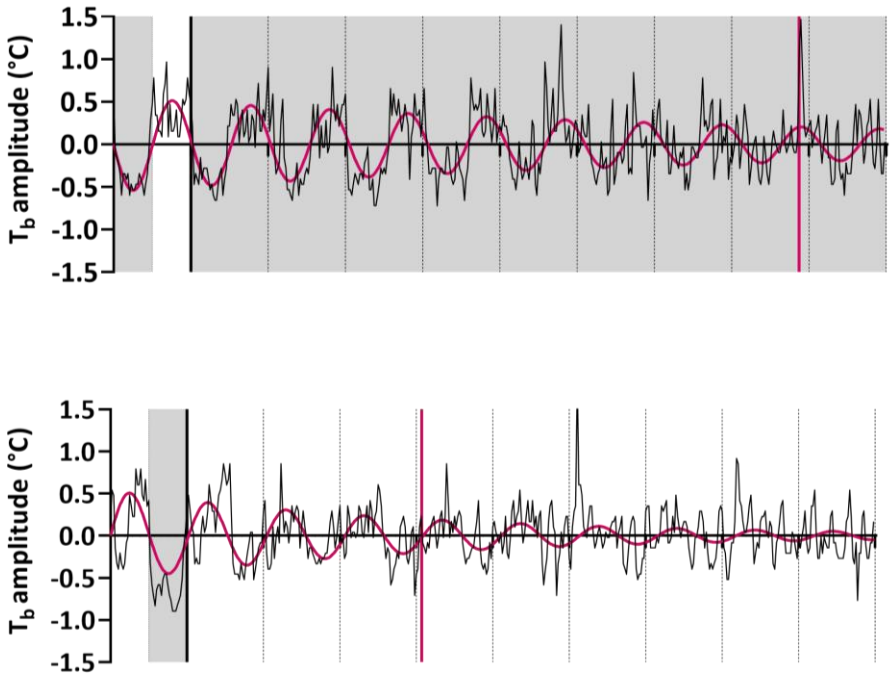

Figure A 26 T_b amplitude (ID: 041-98) for 10 days. (a) Last day under LD and following nine days under DD, and (b) last day under LD and following nine days under LL. Vertical dotted lines separate days, white background = lights on, grey background = lights off. A nonlinear regression was drawn as a dampened sine wave (red), vertical red line = half-life of dampened sine wave.

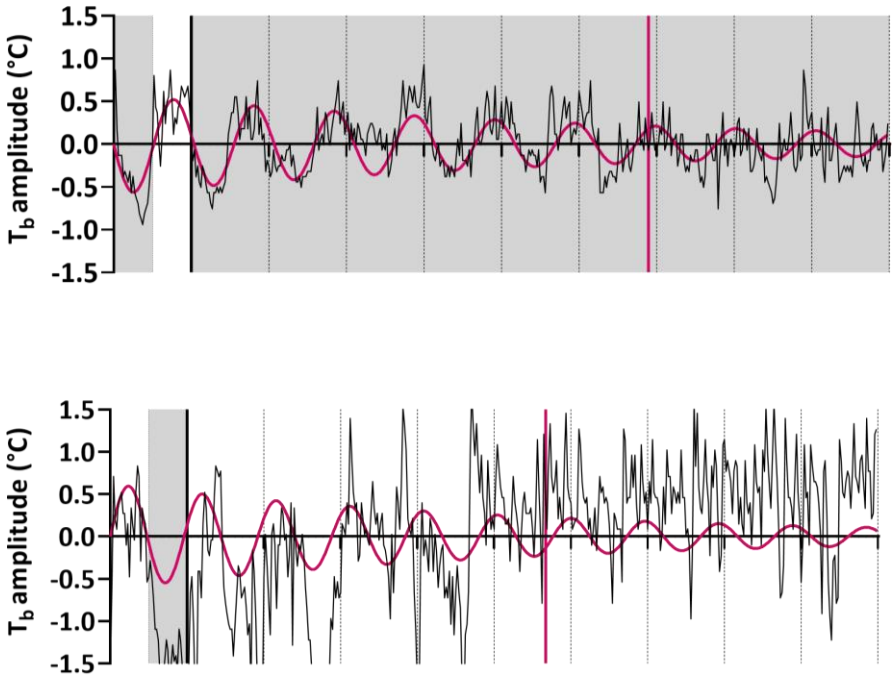

Figure A 28 T_b amplitude (ID: R35) for 10 days. (a) Last day under LD and following nine days under DD, and (b) last day under LD and following nine days under LL. Vertical dotted lines separate days, white background = lights on, grey background = lights off. A nonlinear regression was drawn as a dampened sine wave (red), vertical red line = half-life of dampened sine wave.

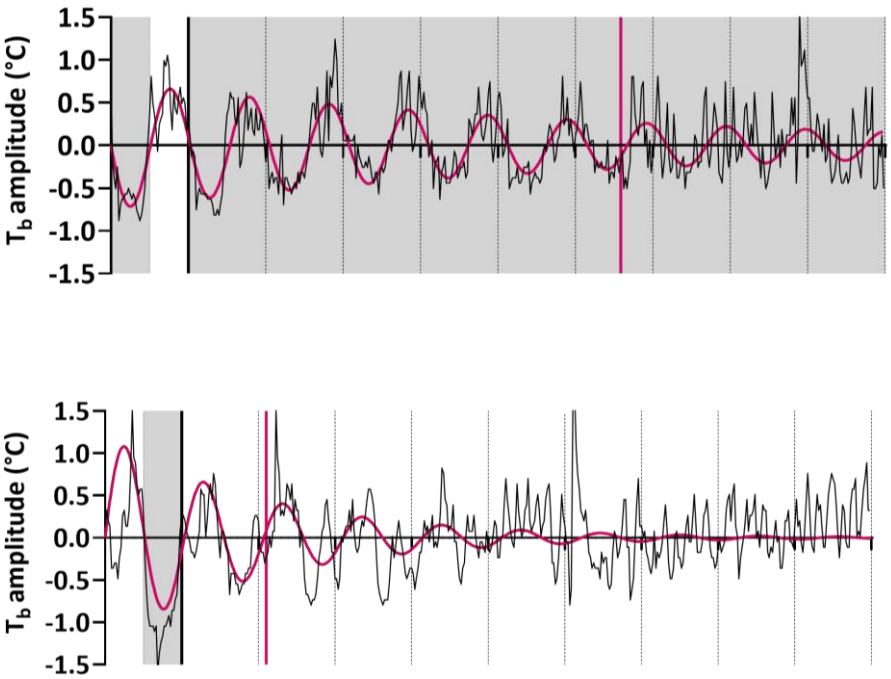

Figure A 27 T_b amplitude (ID: 047-98) for 10 days. (a) Last day under LD and following nine days under DD, and (b) last day under LD and following nine days under LL. Vertical dotted lines separate days, white background = lights on, grey background = lights off. A nonlinear regression was drawn as a dampened sine wave (red), vertical red line = half-life of dampened sine wave.

Appendix E: Body temperature amplitude DD to LL for all experimental birds, and LL to LD for birds in room 1

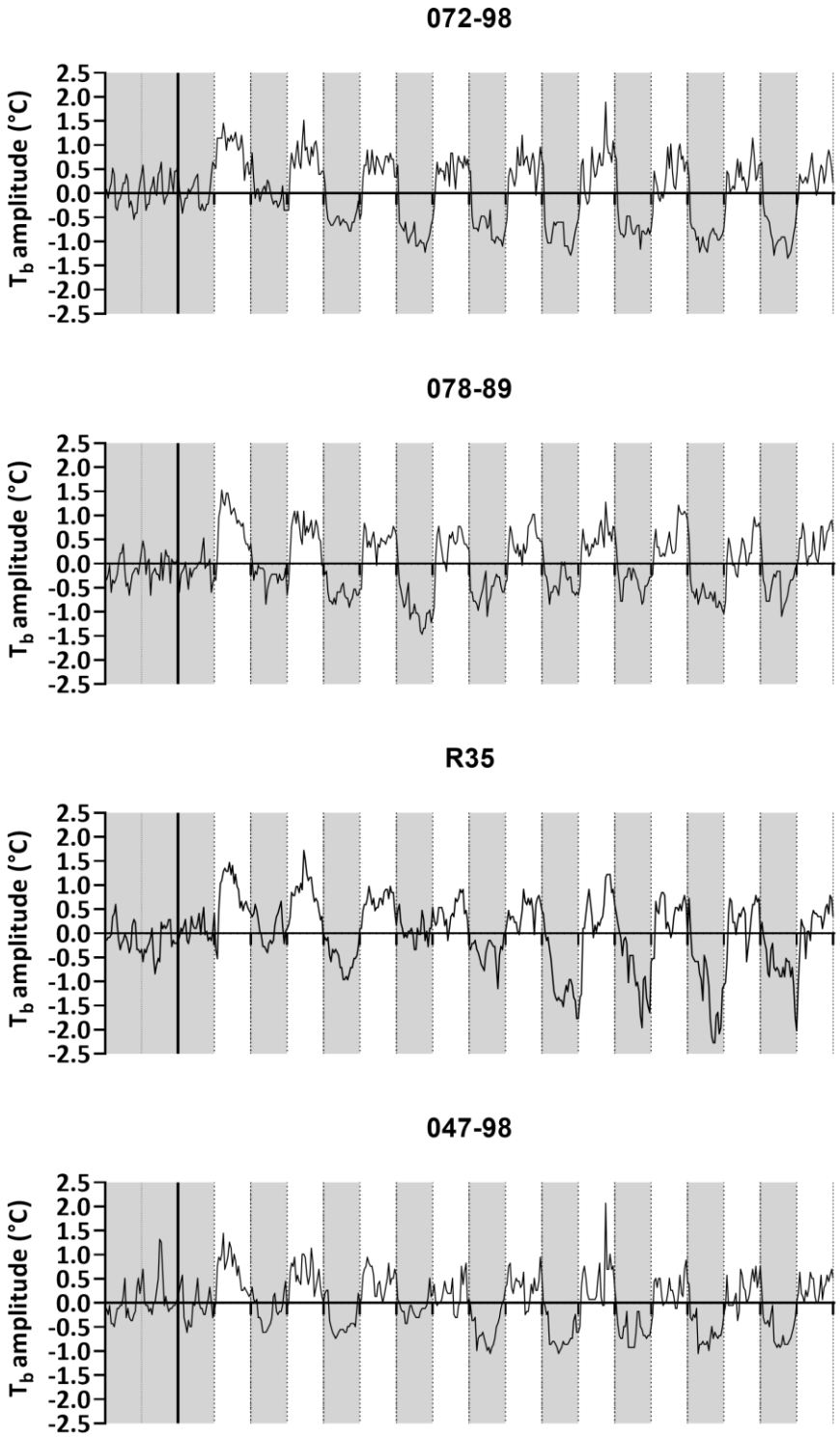

Figure A 29 T_b amplitude for four birds (titles indicate bird IDs) for 10 days. Transition from DD to LD. Vertical dotted lines separate 12 hours. White background = lights on, grey background = lights off.

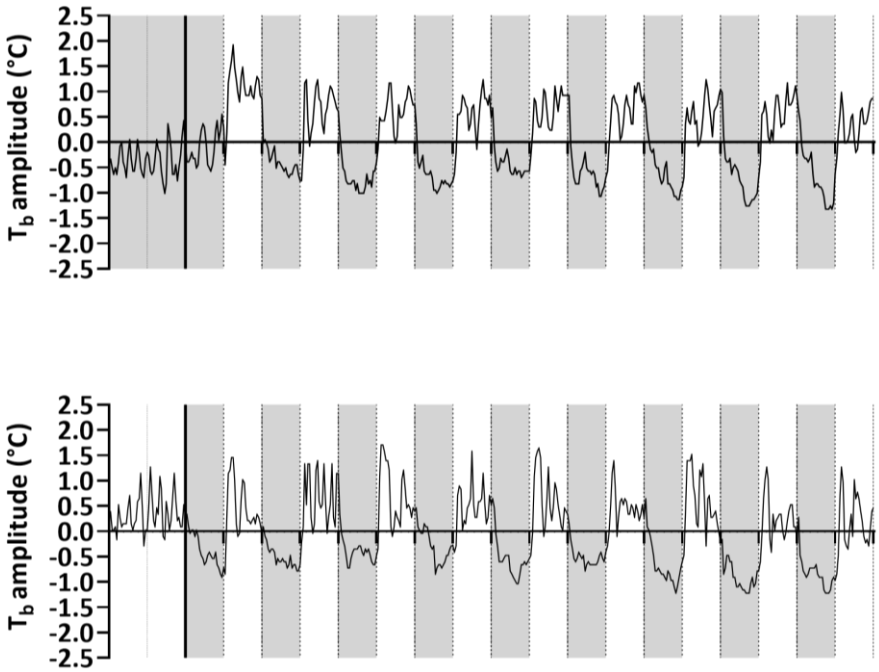

Figure A 30 T_b amplitude (ID: 269-98) for 10 days. (a) Transition from DD to LD and (b) transition from LL to LD. Vertical dotted lines separate 12 hours. White background = lights on, grey background = lights off.

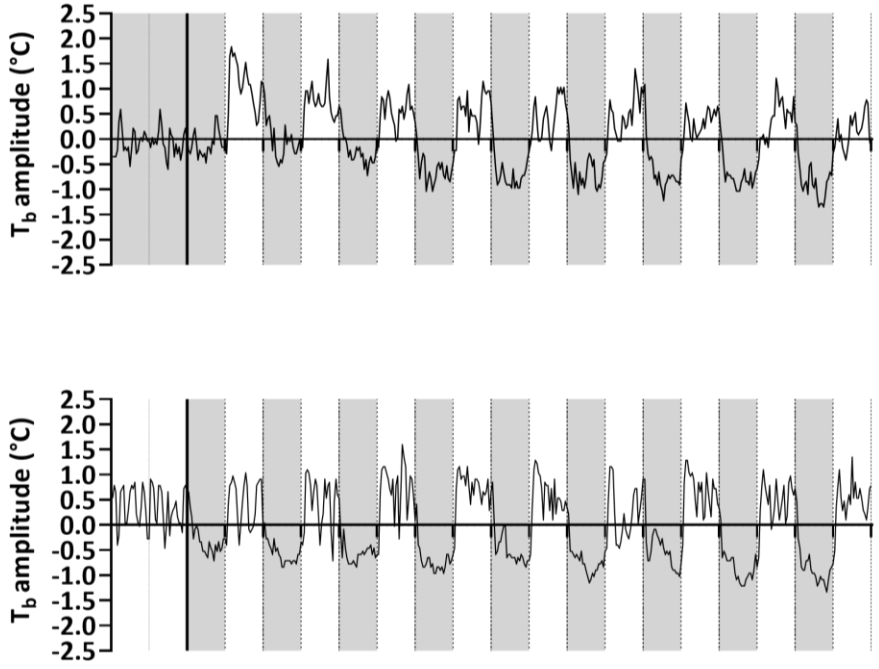

Figure A 31 T_b amplitude (ID: 079-98) for 10 days. (a) Transition from DD to LD and (b) transition from LL to LD. Vertical dotted lines separate 12 hours. White background = lights on, grey background = lights off.

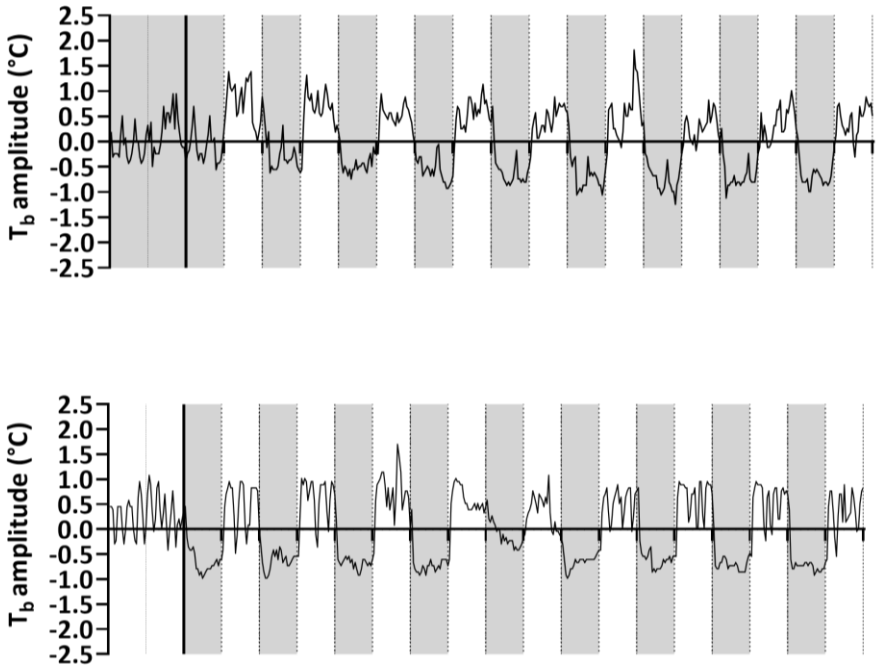

Figure A 32 T_b amplitude (ID: 241-98) for 10 days. (a) Transition from DD to LD and (b) transition from LL to LD. Vertical dotted lines separate 12 hours. White background = lights on, grey background = lights off.

Appendix F: U2OS cells synchronization and luciferase assays

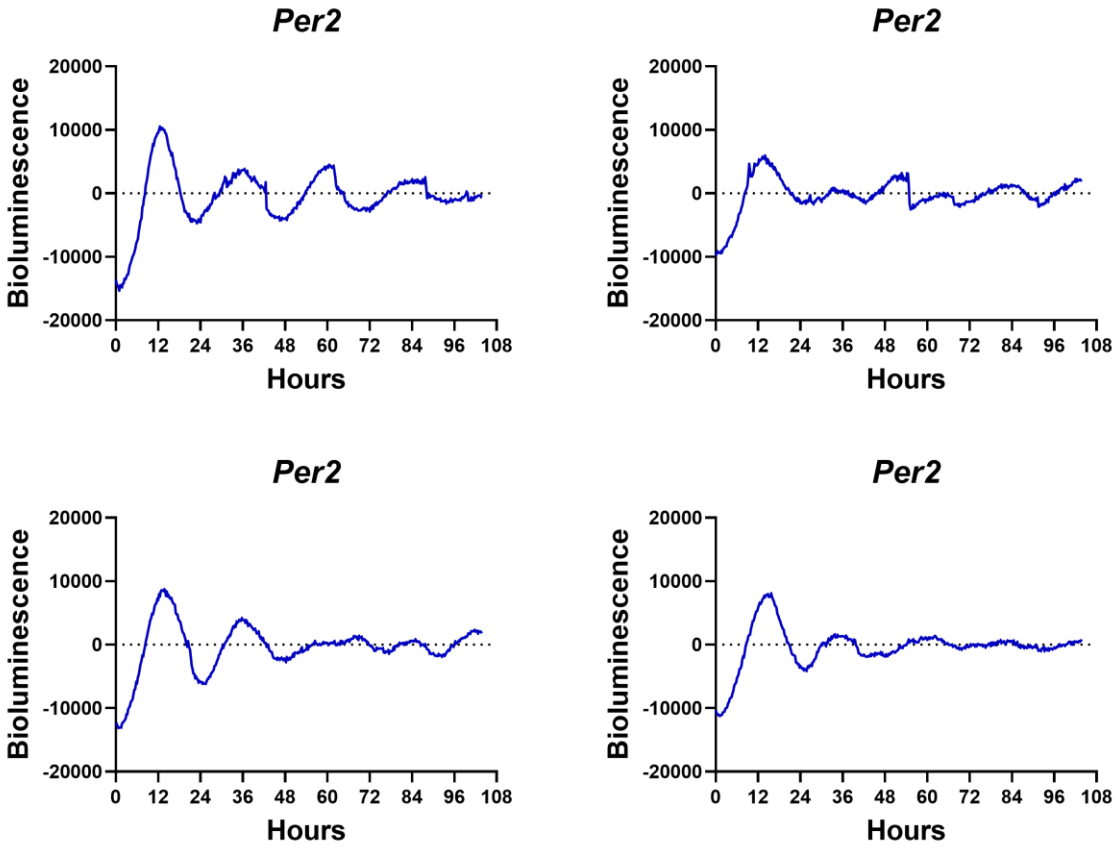

Figure A 33 Molecular rhythms in U2OS cells. Cells were transiently transfected with *Per2* luciferase reporters, synchronized with 50% FBS for one hour, then bioluminescence was recorded (photon counts per minute, one minute was measured every 15 minutes). y = baseline subtracted data, x = 0 = 12 hours after start of recording.

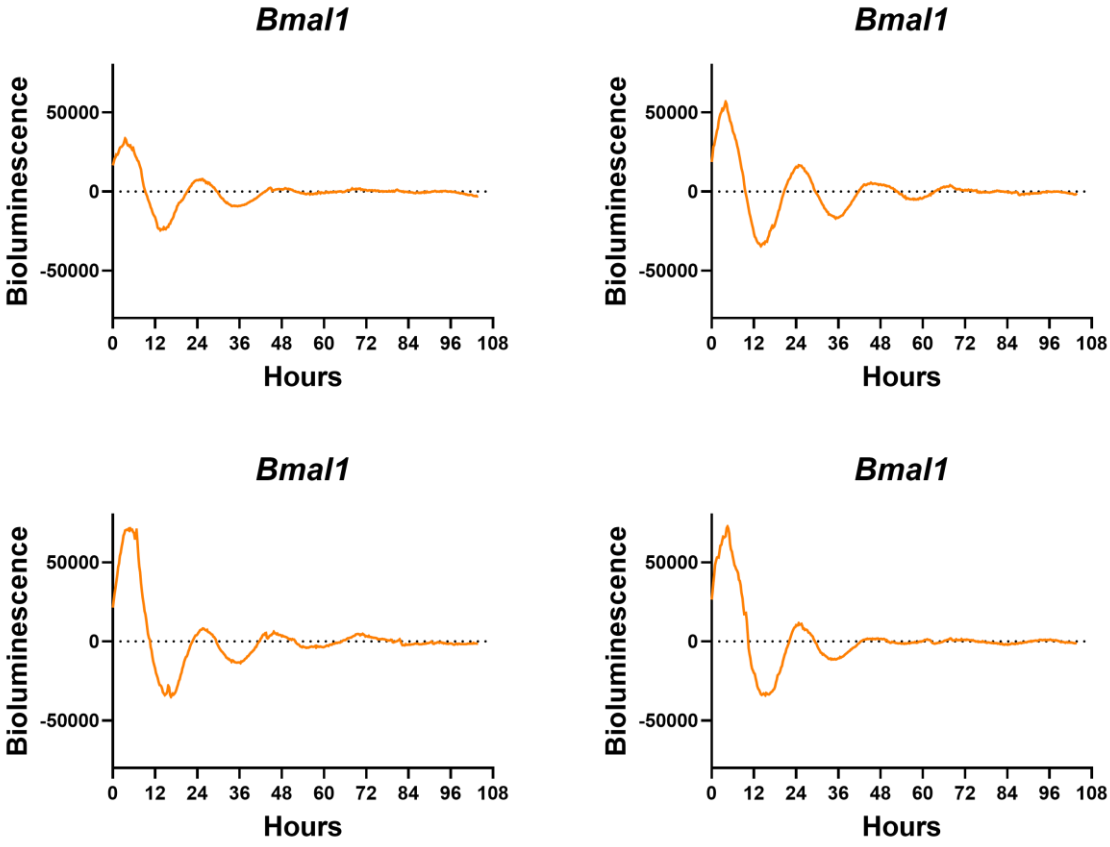

Figure A 34 Molecular rhythms in U2OS cells. Cells were transiently transfected with *Bmal1* luciferase reporters, synchronized with 50% FBS for one hour, then bioluminescence was recorded (photon counts per minute, one minute was measured every 15 minutes). y = baseline subtracted data, x = 0 = 12 hours after start of recording.

Appendix G: Ptarmigan fibroblasts stimulation and luciferase assays

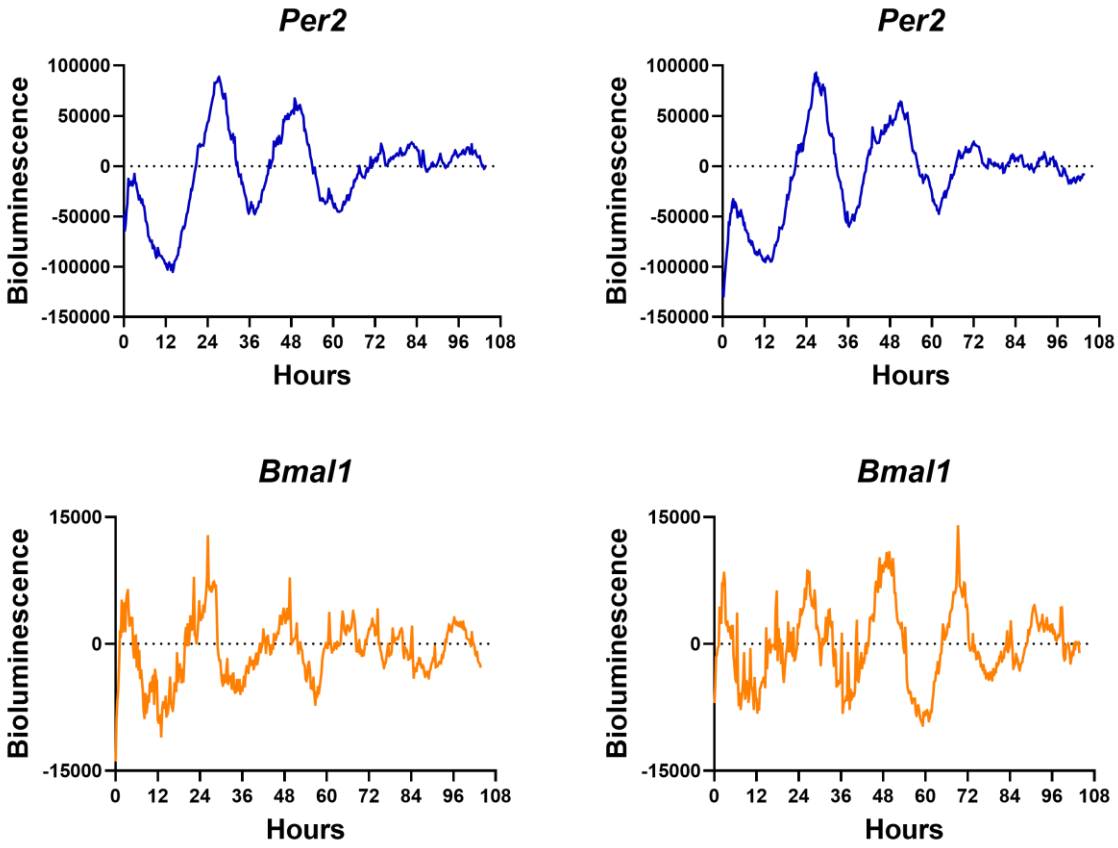

Figure A 35 Molecular rhythms in ptarmigan fibroblasts. Cells were transiently transfected with *Per2* and *Bmal1* luciferase reporters, synchronized with 50% FBS for one hour, then bioluminescence was recorded (photon counts per minute, one minute was measured every 15 minutes). y = baseline subtracted data, x = 0 = 12 hours after start of recording.

Appendix H: U2OS cells luciferase assays under simulated body temperature cycles

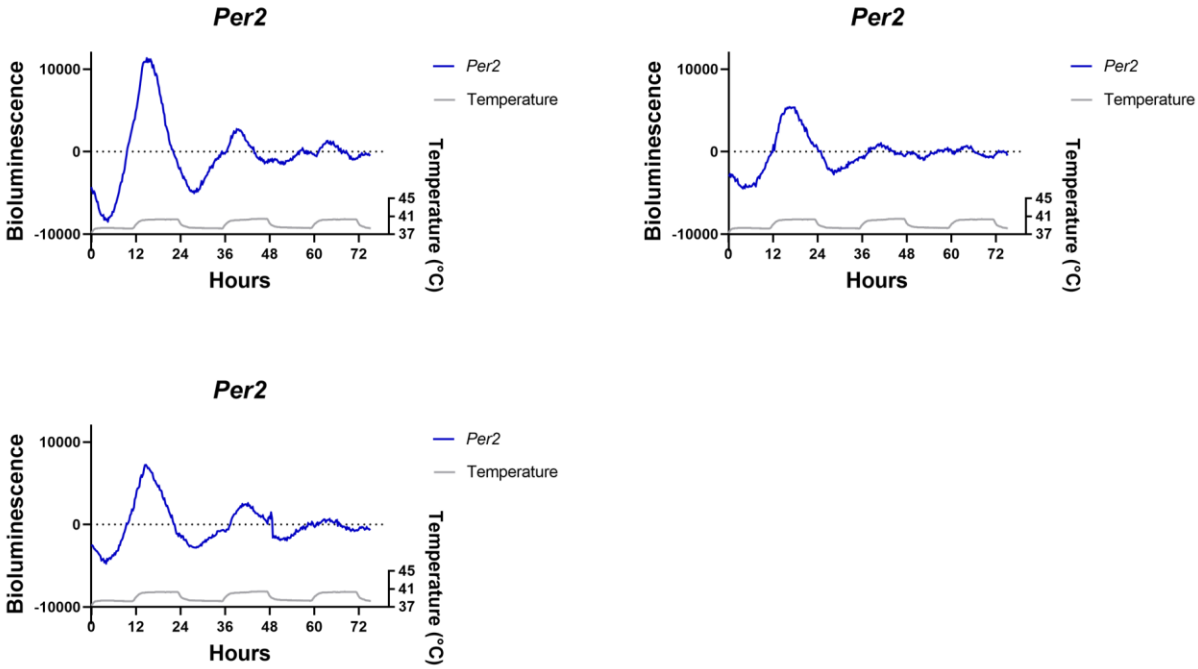

Figure A 36 Clock gene transcription under simulated body temperature cycles. U2OS cells were transiently transfected with *Per2* luciferase reporters and kept at cycling temperatures while real-time bioluminescence was measured (photon counts per minute, one minute was measured every 15 minutes). y = baseline subtracted data, x = 0 = 12 hours after start of recording.

Appendix I: Ptarmigan fibroblasts luciferase assays under simulated body temperature cycles

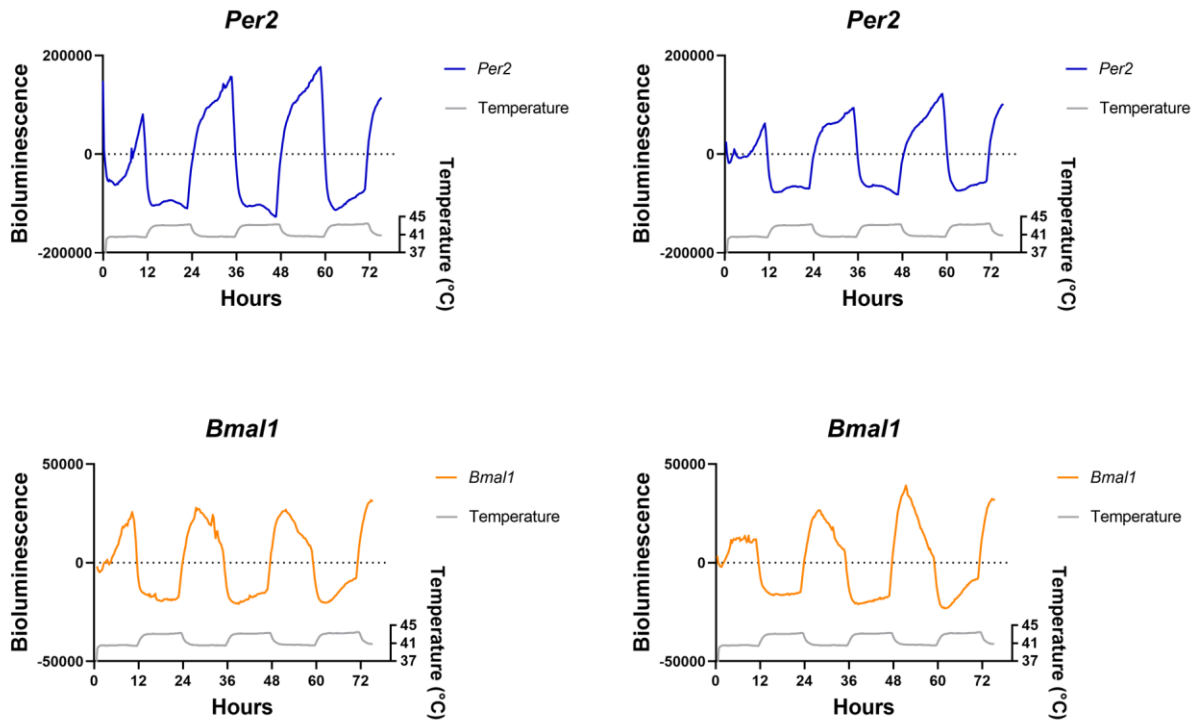

Figure A 37 Clock gene transcription under simulated body temperature cycles. Ptarmigan fibroblasts were transiently transfected with *Per2* and *Bmal1* luciferase reporters and kept at cycling temperatures while real-time bioluminescence was measured (photon counts per minute, one minute was measured every 15 minutes). y = baseline subtracted data, x = 0 = 12 hours after start of recording.